UNIVERSITY of LIVERPOOL

NONLINEAR ADAPTIVE CONTROL AND APPLICATIONS IN POWER SYSTEMS

Thesis submitted in accordance with the
requirements of the University of Liverpool
for the degree of Doctor of Philosophy

in

Electrical Engineering and Electronics

by

Lin Jiang , BSc, MSc(Eng)

March 2001

NONLINEAR ADAPTIVE CONTROL AND APPLICATIONS IN POWER SYSTEMS

by

Lin Jiang

Acknowledgements

I would like, first of all, to thank my supervisor Professor Q.H. Wu for his invaluable support and intellectual guidance, both academically and personally, for this research project. He has made a great contribution to this thesis.

Thanks is offered to Dr J. Wang for many helpful discussions and much valuable advice; also to the members of the Intelligence Engineering and Automation group, especially Mr. P. Sun for his excellent computer knowledge and Mr. D.J. Zhang for our valuable discussions.

I am grateful to the Department of Electrical Engineering and Electronics, The University of Liverpool, for providing the research facilities, making it possible for me to conduct this research. I am indebted to The University of Liverpool, both for the studentship (1997-2000) and the Committee of Vice-Chancellors and Principals for 'Overseas Research Students Awards Scheme'(1997-2000). Thanks is also extended to XJ Group Corp. China, for assistance in this research project.

Finally, I am greatly indebted to my wife Ye Yang, for her patience, understanding and support, and to our parents, for their encouragement and love, during the whole period of my postgraduate life.

Abstract

NONLINEAR ADAPTIVE CONTROL
AND APPLICATIONS IN POWER SYSTEMS

by

Lin Jiang

It is known that the feedback linearization method based on differential geometry is vulnerable to handle the presence of parameter uncertainties and external disturbances. These problems are approached conventionally by some robust or adaptive control methods. However, most robust control methods require the upper bounds of uncertainties so that it will result in an overconservative control. Nonlinear adaptive controls are always dealing with unknown constant parameters in nonlinear systems and are not suitable for handling fast time-varying and functional uncertainties. In this thesis, nonlinear adaptive control schemes based on state and perturbation observer and their applications in power system have been studied.

Nonlinear adaptive control schemes based on state and perturbation observers are studied first. The system perturbation is defined to describe the combined effect of the system nonlinearities, uncertainties and external disturbances. A *fictitious state* is introduced to represent the perturbation in the state equations. Two types of observers, high gain observer and sliding mode observer, are investigated for the estimation of states and perturbation. The on-line estimates of the states and perturbation are used to realize a nonlinear adaptive control law without requiring detailed knowledge of the system model and full state measurements. By use of the real estimate of the perturbation to replace their upper bounds, the over conservative control is avoided.

Three control schemes have been developed: (1) Nonlinear adaptive control

via high gain state and perturbation observer; (2) Nonlinear adaptive sliding mode control using sliding mode state and perturbation observer; and (3) Decentralized nonlinear adaptive control of large-scale systems. The stability of the closed-loop system including controller and observer has been analyzed with mathematical proof and numeric simulation results are presented accordingly.

The proposed control schemes are applied for control of large-scale power systems.

Nonlinear adaptive control of synchronous generators is studied in a single machine quasi-infinite bus power system model. A simple nonlinear adaptive controller based on local measurements is designed and simulation results which is compared to a conventional nonlinear state feedback linearization controller are given.

Decentralized nonlinear adaptive controllers are designed for control of synchronous generators interconnected in a multi-machine power system. The controller is developed based on a fully linearizable model and an input/output partial linearizable model, respectively. Simulation studies are carried out based on a three-machine power system and the results show that the designed controller has better performance and robustness, under variations of power system operation conditions and disturbances, in comparison with a conventional nonlinear state feedback linearization controller.

Coordinated nonlinear adaptive control of synchronous generators and Thyristor Controlled Series Compensators in the multi-machine power system is also studied. The nonlinear adaptive controllers are implemented locally, with the state and perturbation observers involved, for control of subsystems. Simulation results show that the locally installed controller can coordinate each other to improve the power system stability.

Contents

List of Figures

List of Tables

Chapter 1

Introduction

1.1 Nonlinear control systems

1.1.1 Feedback linearization

When the tasks of a control system or disturbances cause the system to cover wide regions of its state space, nonlinear effect will become dominant in the system dynamics and nonlinear control may be necessary to achieve the desired performance. The last two decades have witnessed a great deal of progress in the design and application of feedback control of nonlinear systems [1, 2, 3, 4]. The feedback linearization method based on differential geometry has been proved to be an effective means of design and analysis of nonlinear control systems as was it case for the Laplace transform, complex variable theory and linear algebra in relation to linear systems, as described in the comprehensive book of Isidori [1] and references therein.

Feedback linearization deals with techniques of transforming original system models into equivalent models of simple form. The basic idea is to transform a nonlinear system into a (fully or partially) linear system first, and then use the well-known and powerful linear design techniques to complete the control design. This methodology helps convert many previously intractable nonlinear

problems into much more simpler problems solvable by familiar linear system methods. It includes two kinds of approaches: the input/state linearization, where the full state equation is linearized; and the input/output linearization, where the linearizing the input-output map from input to output is emphasized even if the state equation is only partially linearized [3]. More detailed description of this approach is given in Appendix A.

Although feedback linearization has been used to solve a number of practical nonlinear problems, it still has some drawbacks. One of them is that it is vulnerable to handle the presence of parameter uncertainty or external disturbances. This is because its effectiveness depends on an accurate system model to cancel the system nonlinearity. However, it is unrealistic to assume the perfect knowledge of system nonlinearities or that an exact mathematical representation of them is available because there exist model approximation, imprecision or uncertainty. Another drawback is that the resulting nonlinear control law may be complex so that it can not been implemented easily in practice. In fact, such a complex nonlinear controller may not always behave better than a simple linear controller. In recent years, the problem of controlling uncertain nonlinear dynamical systems has been a topic of considerable interest. Many works in this field have been undertaken by employing robust and adaptive control method. We will review these results below.

1.1.2 Lyapunov control design and sliding mode control

In the pure model based nonlinear controller (such as feedback linearization control), the control law is designed on a nominal model of the physical system[3]. How the control law behaves in the presence of system uncertainties is not clear at the design stage. In the robust nonlinear control, on the other hand, the controller is designed on the consideration of both the exact known nominal model and some characteristics of the model uncertainties. Two main

approaches to the robust control of uncertain systems are the Lyapunov control design technique and sliding mode control technique.

A large amount of work has been undertaken on applying Lyapunov control design techniques to stabilize uncertain dynamical systems (see [5, 6, 7] and references therein). This method generally assumes that the uncertainty satisfies the so-called *matching condition* and has a known upper bound (possibly time varying and state dependent). Under these assumptions, there exists a class of continuous state feedback controllers that ensure the convergence of the state to an arbitrarily small neighborhood of the origin in finite time. Much current robust control theories concern linear systems, that is, the results are obtained under the assumption that the nominal part of the system is linear (usually finite-dimensional and time-invariant). When the actual system exhibits nonlinear behavior, its uncertainty part must be chosen large enough to encompass the nonlinear phenomena because its normal part is restricted to be linear. A disadvantage of this method is that it ignores the available information about the existing nonlinearities, and the resulted controller may be over conservative (especially when the nonlinearities are significant). A natural attempt to improve this drawback of robust linear control is to allow the nominal plant to be nonlinear and thereby pursue the nonlinear control by designing a *robust control Lyapunov function* [5].

Another robust nonlinear control technique, variable structure systems (VSS) based on sliding mode control (SMC) strategy, has also attracted many researchers [8, 9, 10, 11, 12, 13]. The theory of sliding mode in control and optimization has been well studied in the books [14, 15]. The main idea of SMC is to maintain the system *sliding* on a surface in the state space, despite the uncertainties or perturbations. This is done by means of a discontinuous control law that switches between two structures when the system passes through that surface. However, classical SMC presents several important drawbacks that severely hinders its practical application. In particular, it involves control

chattering and large control quantity. In general, chattering is highly undesirable in practice, since it implies extremely high control activity, and further may excite high frequency dynamics neglected in the course of modelling, such as resonant structural modes, actuator time-delays or sampling effects. These problems can be remedied by substituting the discontinuous control with a smooth saturation control within a boundary layer [8], or using a second-order sliding mode control [16].

SMC provides robustness of the control against perturbations (i.e., the combination of modelling uncertainties and unknown external disturbances). These perturbations are assumed to be bounded. The SMC requires the prior knowledge of these upper bounds. However, it may be difficult or sometimes impossible to obtain these upper bounds. Thus the supreme upper bound is chosen to cover the whole range of perturbations. Consequently, the control based on this knowledge becomes over conservative which may cause poor track performance and undesirable control oscillations. Sliding mode control with perturbation estimation was proposed to remedy this problem with an online perturbation estimation [17, 18, 10, 19, 20, 21]. The perturbation is estimated by the derivative of the state and control input. Replacing the upper bounds of the perturbation with its estimates yields desirable level of control activity for a given precision of trajectory tracking. The original idea of the perturbation estimation stems from Time Delay Control (TDC) [22], in which the time-delayed values of derivatives of state variables and control inputs are used to cancel the unknown nonlinear dynamics and uncertainties. In the TDC, unknown dynamics and disturbances can be easily removed without parameter estimation. TDC has been applied to input/output linearization [23], linear systems [24], DC servo motor [25, 26] and robot control [27]. A similar method, named Disturbance Auto-Rejected Control [28, 29], has also been proposed and applied to power system coordinated control [30].

Recently, representing the time-varying uncertainties in finite-term Fourier

series and updating the Fourier coefficients were proposed to estimate the unknown uncertainties and applied to sliding mode control of nonlinear systems [31]. In this method, an updated law for the constant coefficients is derived from the Lyapunov design method. Slotine and Coetsee [32] proposed the adaptive sliding mode control to reduce uncertainties in the system for further improving performance by on-line parameter estimation algorithms. In their design, the bounds of the unknown parameters do not need to be available. This method suffers the same restriction of the conventional adaptive laws derived from the Lyapunov theory, in which the unknown parameters to be estimated should be constant.

1.1.3 Nonlinear adaptive control

Adaptive control is another important approach to deal with uncertain and/or time-varying systems. One of the reasons for the rapid growth and continuing popularity of adaptive control is its clearly defined goal: to control the plants with known structure, but unknown parameters or slowly time-varying parameters. Adaptive control has been most successful for the plant models in which the unknown parameters appear linearly. Systematic theories have been developed for the adaptive control of linear systems. The existing adaptive control techniques can also treat important classes of nonlinear systems, with measurable states and linearly parameterizable dynamics[3].

Interests in adaptive control of nonlinear systems were stimulated by major advances in the differential-geometric theory of nonlinear feedback control in the middle 1980s. Nonlinear adaptive control is a research area that has been rapidly growing in the 1990s. The book of Kristić [33] gives a complete and pedagogical presentation of nonlinear adaptive control, especially the systematic adaptive *backstepping* recursive design method with unknown constant parameters.

The first adaptive backstepping design was developed in [34]. Its over-parameterization was removed by the tuning functions design [35]. Among the early estimation-based results are Sastry and Isidori [36], Pomet and Praly [37], etc. One of the first output-feedback design was proposed by Marino and Tomei [38, 39]. Kanellakopoulos, Kokotović and Morse [40] presented a solution to the partial state feedback problem. A tracking design where the regressor depends only on reference signals was given in [41]. Khalil [42] and Janković developed semi-global output feedback designs for a class which includes some systems not transformable into the output feedback form. However, most of the nonlinear adaptive work are dealing with unknown constant parameters of nonlinear systems. This adaptive control paradigm is not suitable for handling fast time-varying and functional uncertainties. It is known that problems may arise from the influence of unknown disturbances and time-varying parameters [5].

1.1.4 Output feedback control of nonlinear systems

On the state feedback linearization control of nonlinear systems, the complete accessibility of the states is a commonly invoked assumption. Nevertheless, the states are not directly available or measured economically in practice. Therefore, they must be estimated from output measurements using an adequate observer. The design of an observer for nonlinear systems has not been developed systematically as it has for linear systems. The early results of nonlinear observer methods can be found in [43, 44]. Thau [45] incorporated the nonlinearities of the plant into the dynamics of the observer design plus required that the nonlinearities be Lipschitz in the states. Thau's results were generalized by Kou et al. [46], yet the nonlinearities of the plant still appeared in the observer dynamics. Bestle and Zeitz [47] transformed the nonlinear plant into an *observable canonical form* from where the observer design is

performed. However, finding an appropriate nonlinear, time variable, one-to-one transformation is nontrivial and often impossible by their own admission. Moreover, the knowledge of the nonlinearities of the plant must be precise since it is needed in the computation of observer dynamics. Baumann and Rugh [48] utilized an extended linearization technique to produce an observer which, when linearized about any of a family of equilibrium points, has locally invariant eigenvalues. Here again, precise knowledge of the plant nonlinearities and furthermore, the first derivatives of these nonlinearities must be known in order to calculate the gain function of the observer.

When a robust controller is designed for nonlinear systems, another difficulty is that the observer must be robust so that the closed-loop system, including the observer and the controller, is still robust. There are two types of nonlinear observer that can be robust against some model uncertainties: high gain observer and sliding mode observer. The high gain observer, which can estimate robustly the states or the derivatives of the output equivalently (under local weak observability), has acted as an important technique for the design of output feedback control of nonlinear systems [49]. The combination of globally bounded state feedback control with high gain observer allows for a separation approach in which the state feedback control is designed first to meet the design objectives, then the high gain observer is designed, fast enough, to recover the performance achieved under state feedback. This separation principle is used in much work that utilizes a high gain observer. It is proved that global stabilisability by state feedback and uniform observability imply semi-global stability by output feedback[50]. A more comprehensive separation principle is proved by Atassi and Khalil[51]. Esfandiari and Khalil [7] studied the stabilization of fully-linearizable uncertain systems using high gain observers and robust state feedback control techniques. They first gave local and global stabilization results under output feedback. Then they illustrated the peaking phenomenon and how it could lead to shrinking of the region of attraction and

even destabilization of the system. A key feature of the combination of globally bounded state feedback control and high gain observers is the recovery of the region of the attraction. This feature was made explicit in the follow-up work by Khalil and Esfandiari [52] where it was shown that their approach can achieve semiglobal stabilization. This paper is the impetus for a number of research contributions by Khalil and other authors. Some fundamental tools for semiglobal stabilization using high gain observers and saturation functions were developed by Teel and Praly [50, 53]. A key technical contribution of their work is the use of Lyapunov functions to prove asymptotic stability of the closed-loop systems under output feedback without resorting to singular perturbation arguments as in Khalil's work. High gain observers have been applied in the nonlinear servomechanism problem [54, 55, 56, 57], adaptive control of nonlinear systems [42, 58], output feedback sliding mode control [59, 60], and control of induction motors [61].

In recent years a considerable number of researchers have investigated the observer design based on the variable structure system theory, and sliding mode concept[14, 62, 63, 64, 43, 65, 66, 67]. The sliding mode observer potentially offers advantages similar to those of sliding mode controllers, in particular inherent robustness to parameter uncertainty and external disturbances. These existing methods can be classified in two categories: 1) The equivalent control based methods[14, 62, 63], and 2) sliding mode observer design based on the method of Lyapunov[64, 43, 65, 66, 67]. An early sliding mode observer for linear systems appeared as the sliding mode realization of a reduced-order asymptotic observer [14, 62]. Slotine [63] proposed a sliding mode observer for nonlinear systems. The sliding function of this observer uses the estimation error of the available measured output. The basic sliding mode observer consists of switching terms added to a conventional Luenberger observer [68]. The selection of sufficiently large gains ensures the asymptotic convergence of the error dynamics. Walcott and Żak [64, 69] studied a sliding mode observer

for certain class of nonlinear system based on the method of Lyapunov and techniques prevalent in variable structures system (VSS) theory. A systematic algorithm for the design of this kind of observer was proposed in [65]. A comparative study of the techniques mentioned above was also given in [43]. Sliding mode observer has been applied for the control of robotic manipulator [70, 71].

The combination of sliding mode observers and controllers has been studied for linear systems with matching nonlinearities[72]. By Sanchis and Nijmeijer [73], the combination of the sliding mode observer and controller was studied for affine nonlinear systems. The sliding controller(based on a feedback linearization approach) is similar to that defined by Slotine and Sastry [63], except that the sliding surface is defined in terms of the estimated states instead of the true ones. Edwards and Spurgeon [65] presented a controller/observer pair based on sliding mode ideas, that provided robust output tracking of a reference signal using only measured output information.

The integration of the perturbation estimation into the sliding mode observer structure can substantially reduce the driving terms of the state observer error dynamics and result in a sliding perturbation observer [18]. Consequently, the resulting observer is able to provide much better state estimation accuracy. The combination of sliding mode perturbation observer with sliding mode control results in a robust algorithm: sliding mode controller with sliding perturbation observer. However, it is applicable for general second-order multi-degree of freedom systems. And the perturbation term is only approximately estimated. A time delay control with a time delay observer, which is actually an observer of the linear reference model of time delay control, was proposed in [74] and applied to robot control [27] and DC servo motor [26].

1.2 Applications of nonlinear control in power systems

Power systems are complex dynamical systems which involve locally installed devices interacting with each other dynamically and operates with great nonlinearities of system components under a wide range of operation conditions and various disturbances. Modern power systems are increasingly required to operate transmission networks on high power transfer levels under economical or environmental constraints. Stability problems that arise from these requirements include potential voltage instability; e.g. *voltage collapse* phenomenon, as well as a tendency toward poorly-damped power/load angle oscillations that can threaten system stability [75, 76]. This calls for the need to conceive and design new analytical techniques for robust and reliable system operation. It is generally recognized that adequate system dynamic performance depends more and more on the proper performance of control. A proper controller is the important guarantee for reliable and stable operation of power systems.

A power system controller design based on the small-signal models of the power systems obtained around a specific operation equilibrium point, such as Power System Stabilizer (PSS)[77], linear optimal controller [75] and linear adaptive controller [78, 79, 80], have been successfully developed in the last two decades. Applying such controllers for nonlinear power systems generally provides asymptotic stability in a small region about the equilibrium and is thus appropriate for the dynamic stability problem, where the primary concern is of providing damping following small disturbances. For sudden and severe disturbances, which involves significant variations in the system parameters and thus the operation point varies far from the pre-fault equilibrium point. Under these conditions, linear controllers are generally unable to maintain transient stability and the system will lose its stability in the first swing, unless severe

countermeasures of discrete-type control devices, such as dynamic resistance braking, fast valves, and load-shedding, etc., are put into effect.

There are more control devices available with the introduction of Flexible Alternative Currents Transmission Systems (FACTS) technology into modern power systems[81]. FACTS technology provides new opportunities to control the interrelated parameters that govern the operation of transmission systems including series impedance, shunt impedance, current, voltage, phase angle, and the damping of oscillations at various frequencies below the rated frequency. Thus, for controller design, the power system models described by nonlinear differential equations must be used to achieve a better performance. For the case of transient problems, the nonlinear controller is more suitable. Many nonlinear controllers have already been developed for this purpose in the past two decades, such as, Feedback Linearization Control(FLC), variable structure control, Lyapunov control design, nonlinear adaptive control and nonlinear predictive control. These works have been reviewed in our work [82] and will be given briefly in the following section. Most of these works concern the state feedback nonlinear controller but there are a few works which discuss the output feedback nonlinear control of power systems. The state observer of synchronous generator which requires the accurate nonlinear model was studied and applied to the nonlinear field voltage control of generators [83, 84].

1.2.1 Feedback linearization control of power systems

Among these nonlinear control methods, the feedback linearization control based on differential geometric techniques has received a much attention [85, 86, 87, 88]. Another feedback linearization approach, Direct Feedback Linearization (DFL), has also been proposed and applied to this field [89, 90, 91]. Subject to the availability of an accurate reference model and measurements of the power system, the inherent system nonlinearity of the nonlinear power

system model may be cancelled and replaced with some desired linear behaviors. Such a nonlinear controller can deal with most of the nonlinearity in the power system, such as the nonlinearity of the generator and they can provide performance better than those linear model based power system controllers and has achieved a significant progress in the power system control[85].

The excitation control of synchronous generators plays an important role of keeping the generator in synchronism with the power system during major disturbances resulting from sudden or sustained load changes, either the loss of generating or transmission facilities. Synchronous generator is a nonlinear device whose dynamics will change dramatically with the variation of power system operation conditions. There are many research works on the feedback linearization control of electrical machines, including synchronous generator and induction motor[85, 92, 93].

Nonlinear control of synchronous generator

When a synchronous generator is represented as a simplified third-order system model, it is input/state linearizable when the rotor angle is chosen as the control object [83, 94]; and it is only input/output linearizable when the terminal voltage is chosen as the control object[95, 96, 97]. Input/output linearization of synchronous generator based on more accurate models of synchronous generator, says fifth-order or seventh-order system model, have also been studied in [98, 99, 100, 101]. Among these works, [100, 101] the coordinated control of rotor angle and terminal voltage were investigated.

As power system consists of many interconnected subsystems, decentralized control of synchronous generator in a multi-machine power systems had received much research effort[102, 103, 87, 104]. When there exists an infinite bus, load is represented as a constant impedance, synchronous generator is modelled in a three-order model and the rotor angle is chosen as system out-

put, the multi-machine power system is a fully linearizable nonlinear system. By representing the interactions between machines with local electrical measurements, a decentralized control law was obtained in [102, 87]. In [105], the DFL method was employed to design a compensator to linearize the nonlinear power system partially at first and then the interactions between machines were taken as disturbances and a robust control method was applied.

Nonlinear control of FACTS controller

Nowadays, controllers using power electronics devices are researched and developed for damping power oscillation and improving transient stability. FACTS devices (or controllers) have already been operated in the real power systems. Feedback linearization methods have been used to design the FACTS controllers, such as the input/state linearization of Static Var Generator (SVG) [106] and High Voltage Direct Current (HVDC) [107], the direct feedback linearization of the coordinated control of Static Var Compensator (SVC), excitation control and Static Phase Shifter (SPS)[108], excitation control and dynamic brake control[109], super conducting coil control[110], and TCSC nonlinear control[111]. Most of these works are undertaken based on the single-machine infinite-bus power system model because the introduction of FACTS controllers increases the difficulties of modelling multi-machine power systems.

1.2.2 Robust and adaptive control of power systems

Due to unpredictable disturbances and faults, model uncertainties and load variations, it is unrealistic to have an accurate model of a power system. Consequently, with these uncertainties, the cancellation of nonlinearities in FLC controller is no longer exact so that the controller performance will degrade drastically with varying system topology [91, 112]. This motivated the application of several control methods, such as robust control theory and the

adaptive control, to improve the robustness of FLC controllers.

It was shown that FLC controller design based on the exact model can deal with some model uncertainties[4, 113]. Linear robust control, such as linear H_∞ control [114] and linear variable structure control[88, 115], had been used to design robust controller for the equivalent linear system. In [116] and [117], the nonlinear power system was modelled as a linear nominal model plus nonlinear uncertainties and then linear robust control theory had been used to design the decentralized controller of multi-machine power system. In [118], nonlinear H_∞ decentralized controller based on *Hamilton-Jacobi* inequality method was proposed to improve the inter-area damping and dynamic stability. In [119], a nonlinear excitation controller for a synchronous generator using the concept of exact stochastic feedback linearization was designed.

Nonlinear variable structure control had been applied to design robust nonlinear controller for power systems, such as, series capacitance and brake resistance control to improve the transient stability of single machine infinite power system [120], decentralized brake controller in multi-machine power systems[121], excitation and governor control of synchronous generator[122] and static phase shifter controller[123].

Lyapunov control design was also used to design the nonlinear controller of power systems, such as, Static VAr Compensator (SVC) controller [124] and synchronous generator excitation systems [125, 126] and multi-machine control [127, 128].

1.3 Major contributions of the thesis

The thesis reports the research work undertaken based on the review of current techniques for control of nonlinear systems and its application in power systems [82].

The nonlinear adaptive control of nonlinear systems via state and pertur-

bation observer has been studied. Two types of observers, high gain observer and sliding mode observer, have been investigated to obtain the estimate of states and perturbation. The following results have been obtained:

- Convergence analysis of observers have been given. It is shown that the state estimation performance has been improved as the driving term of observer error dynamics is reduced from the perturbation itself to its estimation error.

- Nonlinear adaptive control via high gain observer has been developed. The designed controller adopts the real-time estimates of states and perturbation to yield the adaptive control law. The real time estimate of system perturbation, which include nonlinearities, time-varying parameters and external disturbances, is a function estimation rather than the parameters estimation in most nonlinear adaptive control. A simple adaptive control law is obtained as the system nonlinearities is included in the perturbation and accurate system model is not required for the controller.

- Nonlinear adaptive sliding mode controller using sliding mode observer has been studied. The upper bounds of perturbation is only required in the design of observer. Moreover, as the upper bound of perturbation is replaced by the smaller bound of its estimation error, an over conservative control input is avoided and the tracking accuracy is improved.

- A decentralized nonlinear adaptive control strategy for large-scale interconnected systems has been investigated using of state and perturbation observer. Three control schemes, decentralized nonlinear adaptive controller with high gain observer, decentralized nonlinear adaptive sliding mode controller with sliding mode observer and decentralized nonlinear adaptive control using continuous feedback controller with sliding mode observer, have been developed. The interconnection between subsystems

is included in the perturbation of subsystem and can be estimated by the function estimation method which can handle with time-varying uncertainties and external disturbance.

The proposed control methods have been applied to design nonlinear adaptive controllers for power systems.

- A nonlinear adaptive controller design based on a state and perturbation observer has been applied for excitation control of synchronous generators [129]. The designed controller possesses great robustness and it can be implemented easily in practice. The simulation results show better control performance than the FLC which requires full system states and accurate system model.

- Decentralized nonlinear adaptive excitation control of synchronous generators in the multi-machine power system has been studied. The control design has been investigated based on a fully linearizable model of the multi-machine power systems [130] and an input/output partially linearizing multi-machine model [131], respectively. Simulation studies have been undertaken on a three-machine power system and the comparison with FLC controller design based on accurate model [87] have been obtained.

- Coordinated nonlinear adaptive controller (CNAC) has been developed for the excitation control of synchronous generators and TCSCs devices to improve the stability of multi-machine power systems [132, 133]. The CNAC has a simple form and adaptive nature. It does not ignore any system nonlinear dynamic mode but is able to be installed locally and implemented with a local measurement. The simulation results obtained based on a three-machine power systems show that the CNACs can coordinate each other or with PSSs, provide satisfactory control performance

and damp multi-mode oscillations of the power system effectively.

1.4 Thesis outline

The thesis is organized as follows.

Chapter 2: Nonlinear Adaptive Control Using High Gain State and Perturbation Observer

In Chapter 2, we investigate the nonlinear adaptive control of nonlinear system via high gain state and perturbation observer. Two types of observers, the high gain perturbation observer and the high gain state and perturbation observer, are discussed respectively. The estimate of the perturbation is used to realize the linearization of the original nonlinear system without requiring the exact knowledge of system model. Finally, numerical simulation results of an example are given.

Chapter 3: Nonlinear Adaptive Control using Sliding Mode State and Perturbation Observer

In this chapter, sliding mode state and perturbation observer is investigated for the nonlinear adaptive control of nonlinear system. As in the last chapter, we begin with sliding mode perturbation observer and then the sliding mode state and perturbation observer. We mainly employ the estimates of the states and perturbation to design the output feedback sliding mode controller. We also use the estimate of the perturbation to design a feedback linearization controller without the accurate system model. In this case, a linear continuous feedback controller, rather than a sliding mode controller, is designed for the equivalent linear system. In each case, the stability analysis of the combination of the controller and observer is presented for the completeness. Simulation results of the same example used in Chapter 2 are presented.

Chapter 4: Decentralized Nonlinear Adaptive Control Using State and Perturbation Observer

In this chapter, we focus on the decentralized nonlinear adaptive control of large scale interconnected systems based on the state and perturbation observer. Compared with the linear or nonlinear parametric assumption in most of the adaptive control scheme, the function estimation is employed in this chapter instead of the parameter adaption law. Two types of observers, high gain observer and sliding mode observer, are investigated respectively. The nonlinearities and uncertainties existing in each subsystems, plus the interconnection among subsystems, are included in the perturbation term and estimated by the observer. We also apply these control schemes to the input/output linearization of MIMO nonlinear systems. Finally, the design of decentralized output adaptive controller for the control of an inverted double pendulums on carts without the velocity measurements has been undertaken.

Chapter 5: Nonlinear Adaptive Control of Synchronous Generators

In this chapter, the nonlinear adaptive control(NAC) is proposed for the excitation control of the synchronous generator with an Automatic Voltage Regulator (AVR) installed for regulation of generator terminal voltage, only is generator relative rotor angle measured for feedback control. The design of NAC does not need an accurate power system model and other measurements, but it can provide better control performance, compared with the state feedback linearization controller which relies on the full system states and detailed nonlinear system model. The NAC is evaluated in a single-machine quasi-infinite bus power system. The simulation results are presented to show the merits of the novel nonlinear control method.

Chapter 6: Decentralized Nonlinear Adaptive Control of Synchronous generators in Multi-Machine Power Systems

This chapter presents a decentralized nonlinear adaptive controller (DNAC) for excitation control of synchronous generators interconnected in a multi-machine power system. The DNAC is developed based on a fully feedback linearizable multi-machine model and a partial feedback linearizable multi-

machine model. The DNAC is robust in performance as it does not require the exact knowledge of the power system. Moreover, the DNAC is easy to be implemented as only one measurement. The simulation study is carried out based on a three-machine power system. The results show that the DNAC has better performance and robustness, under variations of power system operation conditions and disturbances, in comparison with a conventional nonlinear state feedback linearization controller(FLC).

Chapter 7: Coordinated Control of Synchronous Generators and TCSCs in Multi-Machine Power Systems

This chapter investigates the coordinated nonlinear adaptive controller (CNAC) for the coordinated control of generators and Thyristor Controlled Series Compensators (TCSCs) in multi-machine power systems. The CNACs are implemented locally with the design of state and perturbation observer for subsystem, for the coordinated control of generators and TCSCs in the multi-machine power system. Simulation studies are undertaken based on a three-machine power system to evaluate the effectiveness of the CNAC. The simulation results show that the locally installed CNACs can coordinate each other to improve the power system stability.

Chapter 8: Conclusions

We conclude this thesis with a summary of the results and several suggestions for future work which are mostly unsolved problems that remain in this thesis. Several preliminary results and system parameters can be found in the appendices.

Chapter 2

Nonlinear Adaptive Control Using High Gain State and Perturbation Observer

2.1 Introduction

The high gain observer has been developed as an important technique for the design of output feedback control of nonlinear systems. The basic ingredients of this technique include [51]:

- a high gain observer that robustly estimates the derivatives of the output;
- a globally bounded state feedback control law, that is usually obtained by saturating a continuous state feedback function outside a compact region of interest, that meets the design objectives. The global bound of the control protects the state of the plant from peaking when the estimates of high gain observer are used instead of the true states.

This technique was first introduced by Elfandiari and Khalil [7] and since then it has been the impetus for many research results over the past few years.

It was used to achieve stabilization and semi-global stabilization of fully linearizable systems [7, 52], and to design robust servomechanisms for fully linearizable systems [54]. It was also used for the output adaptive control [42], variable structure control [60] and speed control of induction motors [61]. In most of these studies, the controller is designed in two steps. First, a globally bounded state feedback control is designed to meet the design objective. Secondly, a high gain observer, designed to act fast enough, recovers the performance achieved under state feedback. This recovery is shown using asymptotic analysis of a singular perturbed closed-loop system.

In this chapter, a nonlinear adaptive control via high gain state and perturbation observer has been investigated. A perturbation term is defined to describe the combined effect of the system nonlinearities, uncertainties and external disturbances. And a *fictitious state* is introduced to represent the perturbation in the state equations. Two types of observers, high gain perturbation observer and high gain state and perturbation observer, are discussed respectively. The estimate of the perturbation is used to achieve the cancellation of system nonlinearities and uncertainties, which realizes the linearization of the original nonlinear system without requiring the accurate system model. Moreover, as such a controller adopts the estimate of states and perturbation to yield the control signal, it can be easily implemented in practice. Finally, numerical simulation results of an example are given.

2.2 Model description and problem statement

A nonlinear system in a controllable canonical form is represented as follows:

$$\begin{cases} \dot{x} &= Ax + B\left(a(x) + b(x)u\right) \\ y &= x_1, \end{cases} \tag{2.2.1}$$

where x_i, $i = 1, 2, \cdots, n$ are the state variables, and $x = [x_1, x_2, \cdots, x_n]^T \in \mathcal{R}^n$ is the state vector; $u \in \mathcal{R}$ the control input; $y \in \mathcal{R}$ the system output; $a(x)$:

$\mathcal{R}^n \to \mathcal{R}$ and $b(x) : \mathcal{R}^n \to \mathcal{R}$ are C^∞ unknown smooth functions, defined on $\mathcal{R}^n$. The $n \times n$ matrix A and the $n \times 1$ matrix B are given by

$$A = \begin{bmatrix} 0 & 1 & 0 & \cdots & 0 \\ 0 & 0 & 1 & \cdots & 0 \\ \vdots & & & & \vdots \\ 0 & 0 & 0 & \cdots & 1 \\ 0 & 0 & 0 & \cdots & 0 \end{bmatrix}, \qquad B = \begin{bmatrix} 0 \\ 0 \\ \vdots \\ 0 \\ 1 \end{bmatrix}. \tag{2.2.2}$$

The main source of system (2.2.1) is the normal form of a fully linearizable nonlinear system which has a relative degree $r = n$. The details of this system is provided in Appendix A. In the design of a nonlinear controller using the feedback linearization technique, the most commonly used control structure is

$$u = [-a(x) + v]/b(x), \tag{2.2.3}$$

where v is a new control variable for the equivalent linear system. Such a controller works based on an exact cancellation of nonlinear terms $a(x)$ and $b(x)$. However, the exact cancellation is almost impossible for several reasons, such as model simplification, parameter uncertainties and computational errors. When nonlinear functions $a(x)$ and $b(x)$ are unknown or with uncertainties, many adaptive control schemes or robust control schemes have been developed.

2.2.1 Definition of perturbation and fictitious state

For system (2.2.1), after assuming the known part of nonlinear functions $a(x)$ and $b(x)$ be zero for the simplification of formulations, define the system perturbation as

$$\Psi(x, u, t) = a(x) + (b(x) - b_0)u, \tag{2.2.4}$$

then the last equation of system (2.2.1) can be rewritten as

$$\dot{x}_n = \Psi(x, u, t) + b_0 u, \tag{2.2.5}$$

where b_0 is a constant control gain which will be decided later.

If $\dot{x}_n$ can be estimated, then the perturbation can be obtained by

$$\Psi(x,u,t) = \dot{x}_n - b_0 u. \tag{2.2.6}$$

The original idea of this kind of perturbation estimation stems from the time delay control [22, 23], in which the time-delayed values of control input and the derivatives of state variables at the previous time steps are used to cancel the nominal nonlinear dynamics and uncertainties. A similar method, disturbance auto-rejected control , has also been proposed [28]. In the control scheme, the perturbation is estimated by an extended-order nonlinear observer based on the track-differentiator.

In the time delay control, the derivatives of state variables are always calculated by numeric differential method, such as backward difference algorithm. It is well known that the numerical differentiator will magnify the measurement noise. In the past years, high gain observers have played an important role in the design of a nonlinear output feedback controller for nonlinear systems. They are mainly used to estimate the derivatives of the output. In this section, an extended-order high gain observer is designed to estimate the system states and perturbation.

Define a *fictitious state* to represent the system perturbation, that is, $x_{n+1} = \Psi(x,u,t)$, the state equation of system (2.2.1) may be represented as

$$\begin{cases} \dot{x}_1 &= x_2 \\ & \cdots \\ \dot{x}_n &= x_{n+1} + b_0 u \\ \dot{x}_{n+1} &= \dot{\Psi}(\cdot) \\ y &= x_1, \end{cases} \tag{2.2.7}$$

where $\dot{\Psi}(\cdot)$ is the derivative of $\Psi(\cdot)$.

Then system (2.2.7) can be rewritten in a matrix form:

$$\begin{cases} \dot{x}_e &= A_1 x_e + B_3 u + B_1 \dot{\Psi}(\cdot) \\ y &= C_1 x_e, \end{cases} \tag{2.2.8}$$

where

$$x_e = \begin{bmatrix} x_1 \\ x_2 \\ \vdots \\ x_n \\ x_{n+1} \end{bmatrix}, \quad A_1 = \begin{bmatrix} 0 & 1 & \cdots & \cdots & 0 \\ 0 & 0 & 1 & \cdots & 0 \\ \vdots & & & & \vdots \\ 0 & 0 & 0 & \cdots & 1 \\ 0 & 0 & 0 & \cdots & 0 \end{bmatrix}_{(n+1)\times(n+1)},$$

$$B_3 = \begin{bmatrix} 0 \\ 0 \\ \vdots \\ 1 \\ 0 \end{bmatrix}_{(n+1)\times 1}, \quad B_1 = \begin{bmatrix} 0 \\ 0 \\ \vdots \\ 0 \\ 1 \end{bmatrix}_{(n+1)\times 1}, \text{ and } C_1 = \begin{bmatrix} 1 \\ 0 \\ \vdots \\ 0 \\ 0 \end{bmatrix}^T_{(n+1)\times 1}.$$

The following assumptions are made on system (2.2.1).

A2.1 b_0 is chosen to satisfy: $|b(x)/b_0 - 1| \leq \theta < 1$, where θ is a positive constant.

A2.2 The function $\Psi(x,u,t) : \mathcal{R}^n \times \mathcal{R} \times \mathcal{R}^+ \to \mathcal{R}$ and $\dot{\Psi}(x,u,t) : \mathcal{R}^n \times \mathcal{R} \times \mathcal{R}^+ \to \mathcal{R}$ are locally Lipschitz in their arguments over the domain of interest and are globally bounded in x:

$$|\Psi(x,u,t)| \leq \gamma_1, \quad |\dot{\Psi}(x,u,t)| \leq \gamma_2,$$

where γ_1 and γ_2 are positive constants. In addition, $\Psi(0,0,0) = 0$ and $\dot{\Psi}(0,0,0) = 0$.

Assumption $A2.2$ guarantees that the origin is an equilibrium point of the open-loop system.

The control problem is described as follows. Under assumptions $A2.1 \sim A2.2$, $a(x)$ and $b(x)$ are unknown continuous functions, $y = x_1$ is the only available measurement, find the output feedback control u, such that the origin of system (2.2.1) is stable.

In order to illustrate the idea of perturbation estimation, first all the system states are assumed to be available and a high gain perturbation observer is designed to track the last system state and obtain the estimate of the perturbation. Then, when only one state is measurement available , a high gain state and perturbation observer is investigated to obtain the estimate of the system states and the perturbation.

2.3 High gain perturbation observer

Assuming all states x_n, $i = 1, \cdots, n$ are available and taking x_n as a measurement, a high gain track differentiator is designed as

$$\begin{cases} \dot{\hat{x}}_n &= \hat{x}_{n+1} + h_1(x_n - \hat{x}_n) + b_0 u \\ \dot{\hat{x}}_{n+1} &= h_2(x_n - \hat{x}_n), \end{cases} \tag{2.3.1}$$

where h_1 and h_2 are gains of the high gain observer. Throughout this section, $\tilde{x}_i = x_i - \hat{x}_i$ refers to the estimation error of x_i whereas $\hat{x}_i$ symbolizes the estimated quantity of x_i. The estimation error $\tilde{x}_i = x_i - \hat{x}_i$, $i = n, n+1$, satisfies the equation

$$\begin{cases} \dot{\tilde{x}}_n &= -h_1\tilde{x}_n + \tilde{x}_{n+1} \\ \dot{\tilde{x}}_{n+1} &= -h_2\tilde{x}_n + \dot{\Psi}(\cdot). \end{cases} \tag{2.3.2}$$

The above error dynamics can be represented in a matrix form as:

$$\dot{\tilde{x}}_{\text{po}} = A_{\text{po}}\tilde{x}_{\text{po}} + B_{\text{po}}\dot{\Psi}(\cdot), \tag{2.3.3}$$

where $\tilde{x}_{\text{po}} = [\tilde{x}_n,\ \tilde{x}_{n+1}]^T$, and

$$A_{\text{po}} = \begin{bmatrix} -h_1 & 1 \\ -h_2 & 0 \end{bmatrix}, B_{\text{po}} = \begin{bmatrix} 0 \\ 1 \end{bmatrix},$$

where $A_{\rm po}$ is a Hurwitz matrix.

2.3.1 Analysis of estimation error

As in any asymptotic observer, the observer gain $H_{\rm po} = [h_1, h_2]^T$ should be chosen to achieve the asymptotical error convergence, that is,

$$\lim_{t\to\infty} \tilde{x}_{\rm po} = 0.$$

In the absence of the perturbation $\dot{\Psi}(\cdot)$, the asymptotic error convergence is achieved by choosing the observer gain such that the matrix $A_{\rm po}$ is a Hurwitz matrix, e.g., its eigenvalues have negative real parts. For this second-order system, $A_{\rm po}$ is Hurwitzian for any positive constants h_1 and h_2.

In the presence of $\Psi(\cdot)$, the observer gain is needed to be determined with the additional goal of rejecting the effect of the perturbation $\dot{\Psi}(\cdot)$ on the estimation error $\tilde{x}_{\rm po}$. This could be ideally achieved, for any perturbation $\dot{\Psi}(\cdot)$, if the transfer function from $\dot{\Psi}(\cdot)$ to $\tilde{x}_{\rm po}$

$$H_{\rm po}(s) = \frac{1}{s^2 + h_1 s + h_2} \begin{bmatrix} 1 \\ s + h_1 \end{bmatrix}$$

is identically zero.

By calculating the $\|H_{\rm po}\|_\infty$, it can be seen that the norm can be arbitrarily small by choosing $h_2 \gg h_1 \gg 1$. In particular, taking

$$h_1 = \frac{\alpha_1}{\epsilon}, \quad h_2 = \frac{\alpha_2}{\epsilon^2} \tag{2.3.4}$$

for some positive constants α_1, α_2, and ϵ, $\epsilon \ll 1$. It can be shown that

$$H_{\rm po}(s) = \frac{\epsilon}{(\epsilon s)^2 + \alpha_1 \epsilon s + \alpha_2} \begin{bmatrix} \epsilon \\ \epsilon s + \alpha_1 \end{bmatrix}.$$

Hence, $\lim_{\epsilon\to 0} H_{\rm po}(s) = 0$. While an infinite gain is not possible in practice, the observer gain can be determined such that the estimation error $\tilde{x}_{\rm po}$ will converge exponentially to a small neighbourhood which is arbitrarily close to origin. The results is summarized as the following theorem.

Theorem 2.1. *Consider system (2.2.7), and design a high gain perturbation observer (2.3.1). If assumptions A2.1 $\sim$ A2.2 hold, then given any constant $\delta_{\rm po}$, the gain $H_{\rm po}$ can be chosen such that the error $\tilde{x}_{\rm po}$ of the perturbation observer (2.3.1), from any initial value $\tilde{x}_{\rm po}(0)$, converges exponentially to the neighbourhood*

$$\|\tilde{x}_{\rm po}\| \leq \delta_{\rm po}. \tag{2.3.5}$$

Proof: For system (2.3.3), $A_{\rm po}$ is a Hurwitz matrix ; let define the Lyapunov function $V_{\rm po}(\tilde{x}_{\rm po}) = \tilde{x}_{\rm po}^T P_{\rm po} \tilde{x}_{\rm po}$ where $P_{\rm po}$ is the positive definite solution of the Lyapunov equation $P_{\rm po}A_{\rm po} + A_{\rm po}^T P_{\rm po} = -I$. Differentiating $V_{\rm po}$ along system (2.3.2) one obtains

$$\dot{V}_{\rm po} = -\|\tilde{x}_{\rm po}\|^2 + 2P_{\rm po}\tilde{x}_{\rm po}B_{\rm po}\dot{\Psi}(\cdot),$$

which, using assumption *A2.2*, can be rewritten as

$$\dot{V}_{\rm po} \leq -\|\tilde{x}_{\rm po}\|^2 + 2\|P_{\rm po}\|\|\tilde{x}_{\rm po}\|\gamma_2.$$

Take a value $0 < \alpha < 1$, it is easy to show that

$$\dot{V}_{\rm po} \leq -\alpha\|\tilde{x}_{\rm po}\|^2,$$

if

$$\|\tilde{x}_{\rm po}\| \geq \delta_{\rm po1},$$

where $\delta_{po1} = \frac{2\lambda_{\max}(P_{\rm po})\gamma_2}{1-\alpha}$ is a constant. As $\lambda_{\min}(P_{\rm po})\|\tilde{x}_{\rm po}\|^2 \leq V_{\rm po}(\tilde{x}_{\rm po}) \leq \lambda_{\max}(P_{\rm po})\|\tilde{x}_{\rm po}\|^2$, applying Corollary 5.3 of Theorem 5.1 in [4], one can conclude that if $\|\tilde{x}_{\rm po}(0)\| \geq \delta_{\rm po1}$, $\exists\, t_1$, $t_1 > 0$, such that

$$\|\tilde{x}_{\rm po}(t)\| \leq \sqrt{\frac{\lambda_{\max}(P_{\rm po})}{\lambda_{\min}(P_{\rm po})}}\|\tilde{x}_{\rm po}(0)\|e^{-\frac{\alpha}{2\lambda_{\max}(P_{\rm po})}t}, \qquad \forall t < t_1; \tag{2.3.6}$$

and

$$\|\tilde{x}_{\rm po}(t)\| \leq \sqrt{\frac{\lambda_{\max}(P_{\rm po})}{\lambda_{\min}(P_{\rm po})}}\delta_{\rm po1}, \qquad \forall t \geq t_1; \tag{2.3.7}$$

where

$$t_1 \leq \frac{2\lambda_{\max}(P_{\rm po})}{\alpha} \log\left(\frac{\|\tilde{x}_{\rm po}(0)\|}{\delta_{\rm po1}}\right). \tag{2.3.8}$$

Thus, $\exists\ \alpha$, $0 < \alpha < 1$, for any given constant $\delta_{\rm po}$, it has

$$\delta_{\rm po} = \sqrt{\frac{\lambda_{\max}(P_{\rm po})}{\lambda_{\min}(P_{\rm po})}}\delta_{\rm po1} = \sqrt{\frac{\lambda_{\max}(P_{\rm po})}{\lambda_{\min}(P_{\rm po})}}\frac{2\lambda_{\max}(P_{\rm po})\gamma_2}{1-\alpha}, \qquad \forall t \geq t_1$$

such that

$$\|\tilde{x}_{\rm po}(t)\| \leq \delta_{\rm po}, \qquad \forall t \geq t_1.$$

□

2.3.2 Perturbation observer represented in singular perturbation form

The perturbation rejection property of the high gain observer (2.3.4) can also be seen in the time domain by representing the error equation (2.3.2) in the singularly perturbed form. To that end, define the scaled estimation errors

$$\eta_1 = \frac{\tilde{x}_n}{\epsilon}, \quad \eta_2 = \tilde{x}_{n+1}. \tag{2.3.9}$$

The newly defined variables satisfy the singularly perturbed equation

$$\epsilon\dot{\eta} = A_2\eta + \epsilon B_2\dot{\Psi}(\cdot), \tag{2.3.10}$$

where

$$A_2 = \begin{bmatrix} -\alpha_1 & 1 \\ -\alpha_2 & 0 \end{bmatrix}, \qquad B_2 = \begin{bmatrix} 0 \\ 1 \end{bmatrix},$$

and the positive constants α_1 and α_2 are chosen such that A_2 is a Hurwitz matrix.

This equation shows clearly that reducing ϵ diminishes the effect of the perturbation $\dot{\Psi}(\cdot)$. It also shows that, for small ϵ, the dynamics of the estimation error will be much faster than that of x. Notice, however, that the

change of variables (2.3.9) may cause the initial condition $\eta_1(0)$ to be of order $O(1/\epsilon)$ even when $\tilde{x}_n(0)$ is of order of $O(1)$. With this initial condition, equation (2.3.10) will contain a term of the form $(1/\epsilon)e^{-at/\epsilon}$ for some constant $a > 0$. While this exponential mode decays rapidly, it exhibits an impulse-like behaviour where the transient peaks to $O(1/\epsilon)$ value before it decays rapidly towards zero. In fact, the function $(1/\epsilon)e^{-at/\epsilon}$ approaches an impulse function as ϵ tends to zero. This behaviour is known as the *peaking phenomenon.* It is important to realize that the peaking phenomenon is not a consequence of using the change of variables (2.3.9) to represent the error dynamics in the singularly perturbed form. It is an intrinsic feature for any high gain observer design that rejects the effect of the perturbation $\dot{\Psi}$ in (2.3.2); e.g., any design with $h_2 \gg h_1 \gg 1$.

System (2.3.1) is basically an approximate differentiator. This can be easily seen in the special case when the perturbation $\dot{\Psi}(\cdot)$ and control u are chosen to be zero and thus the observer is linear. For system (2.3.1) the transfer function from $y = x_n$ to $\hat{x}_{\text{po}}$ is given by

$$\frac{\alpha_2}{(\epsilon s)^2 + \alpha_1 \epsilon s + \alpha_2} \begin{bmatrix} 1 + (\epsilon\alpha_1/\alpha_2)s \\ s \end{bmatrix} \rightarrow \begin{bmatrix} 1 \\ s \end{bmatrix} \quad \text{as } \epsilon \rightarrow 0.$$

Thus, on a compact frequency internal, the high gain observer approximates $x_{n+1} = \dot{x}_n$ for sufficiently small ϵ.

2.3.3 Nonlinear adaptive control design via high gain perturbation observer

The estimate of perturbation $\hat{x}_{n+1}$ is used to realize the feedback linearization of the nonlinear system (2.2.1). After the unknown system nonlinearities and uncertainties are cancelled by the perturbation estimate, a linear state feedback controller is designed for the equivalent linear system. The complete

control is designed as follows:

$$u = v/b_0 - \hat{x}_{n+1}/b_0, \tag{2.3.11}$$

$$v = -Kx, \tag{2.3.12}$$

where $K = [k_1, k_2, \cdots, k_n]^T$ is the linear feedback controller gains, which make the matrix $A_0 = A - BK$ be Hurwitzian.

The analysis of the closed-loop system under the perturbation observer and the controller is given as follows. The system is represented in the singularly perturbed form:

$$\dot{x} = A_0 x + B\eta_2, \tag{2.3.13}$$

$$\epsilon\dot{\eta} = A_2\eta + \epsilon B_2\dot{\Psi}(\cdot). \tag{2.3.14}$$

The system represented by equations (2.3.13) and (2.3.14) is a standard singular perturbed system, and $\eta = 0$ is the unique solution of equation (2.3.14) when $\epsilon = 0$. The reduced system, obtained by substituting $\eta = 0$ in equation (2.3.13), is as:

$$\dot{x} = A_0 x. \tag{2.3.15}$$

The boundary-layer system, obtained by applying the change of time variable $\tau = t/\epsilon$ to equation (2.3.14) and setting $\epsilon = 0$, is given by

$$\frac{d\eta}{d\tau} = A_2\eta. \tag{2.3.16}$$

For the proof of next theorem, the following corollary, which is a special case of *Young's inequality*, will be used.

Corollary 2.1: $\forall a, b \in R^+$, $\forall p > 1$, $\epsilon_0 \in R^+$ we have

$$ab \leq \frac{1}{\epsilon_0}a^p + (\epsilon_0)^{1/(p-1)}b^{p/(p-1)}.$$

Theorem 2.2. *Let assumptions A2.1 and A2.2 hold, design perturbation observer (2.3.1) and control law (2.3.11) and (2.3.12); then, there exists* ϵ_1^*, $\epsilon_1^* > 0$ *such that,* $\forall\epsilon$, $0 < \epsilon < \epsilon_1^*$, *the origin of system (2.3.13) and (2.3.14) is exponentially stable.*

Proof: It is known that the origin of system (2.3.15) is exponentially stable in a region $\mathcal{R}$ which includes the origin, and system(2.3.16) is also exponentially stable in a region Ω which includes the origin, as both A_0 and A_2 are Hurwitzian.

For the reduced system (2.3.15), let define the Lyapunov function

$$V_0(x) = x^T P_0 x, \tag{2.3.17}$$

over a ball $B(0,r) \subset \mathcal{R}^n$, for some $r > 0$, and P_0 is the positive definite solution of the Lyapunov equation $P_0 A_0 + A_0^T P_0 = -I$. $\forall x \in B(0,r)$, we have

$$\lambda_{\min}(P_0)\|x\|^2 \leq V_0(x) \leq \lambda_{\max}(P_0)\|x\|^2, \tag{2.3.18}$$

$$\frac{\partial V_0}{\partial x} A_0 x \leq -\|x\|^2, \tag{2.3.19}$$

$$\|\frac{\partial V_0}{\partial x}\| \leq 2\lambda_{\max}(P_0)\|x\|. \tag{2.3.20}$$

For the boundary-layer system (2.3.16), we define the Lyapunov function $W_2(\eta) = \eta^T P_2 \eta$, where P_2 is the positive definite solution of the Lyapunov equation $P_2 A_2 + A_2^T P_2 = -I$. This function satisfies

$$\lambda_{\min}(P_2)\|\eta\|^2 \leq W_2(\eta) \leq \lambda_{\max}(P_2)\|\eta\|^2, \tag{2.3.21}$$

$$\frac{\partial W_2}{\partial \eta} A_2 \eta \leq -\|\eta\|^2, \tag{2.3.22}$$

$$\|\frac{\partial W_2}{\partial \eta}\| \leq 2\lambda_{\max}(P_2)\|\eta\|. \tag{2.3.23}$$

Let us consider $V(x,\eta) = V_0(x) + \beta W(\eta)$, where $\beta > 0$ is to be determined, as a Lyapunov function candidate for system (2.3.13) and (2.3.14). Choose $\xi < r$; then, given Assumptions $A2.1 \sim A2.2$, we have, for all $(x,\eta) \in B(0,\xi) \times \{\|\eta\| \leq \xi\} = \Lambda$

$$|\dot{\Psi}(x, u(x,\eta), t)| = |\dot{\Psi}(x,\eta,t)| \leq L_1\|x\| + L_2\|\eta\|, \tag{2.3.24}$$

where $B(\|\eta\|, \xi) \in \Omega$, ξ is a positive constant, L_1 and L_2 are Lipschitz constants.

Using equations (2.3.18) $\sim$ (2.3.23) and Young's inequality, it can be shown that, $\forall\ (x,\eta) \in \Lambda$, we have

$$\begin{aligned}
\dot{V} &= \tfrac{\partial V_0(x)}{\partial x}(A_0 x + B_0\eta_2) + \beta\tfrac{\partial W_2(\eta)}{\partial \eta}(\tfrac{A_2\eta}{\epsilon} + B_2\dot{\Psi}(\cdot)) \\
&\leq -\|x\|^2 - \tfrac{\beta}{\epsilon}\|\eta\|^2 + 2\beta L_2\|P_2\|\|\eta\|^2 \\
&\quad +(2\|P_0\| + 2\beta L_1\|P_2\|)\|x\|\|\eta\| \\
&\leq -\|x\|^2 - \tfrac{\beta}{\epsilon}\|\eta\|^2 + 2\beta L_2\|P_2\|\|\eta\|^2 \\
&\quad +(2\|P_0\| + 2\beta L_1\|P_2\|)(\tfrac{1}{\epsilon_0}\|x\|^2 + \epsilon_0\|\eta\|^2) \\
&\leq -\tfrac{1}{2}\|x\|^2 - \tfrac{\beta}{2\epsilon}\|\eta\|^2 - b_1\|x\|^2 - b_2\|\eta\|^2,
\end{aligned} \tag{2.3.25}$$

where $b_1 = \frac{1}{2} - \frac{2}{\epsilon_0}(\|P_0\| + \beta L_1\|P_2\|)$, $b_2 = \frac{\beta}{2\epsilon} - 2\beta(\epsilon_0 * L_1 + L_2)\|P_2\| - 2\epsilon_0\|P_0\|$, and $\epsilon_0 > 0$. Now choose $\epsilon_0 \geq \epsilon_0^* = 4\|P_0\| + 4\beta L_1\|P_2\|($ where $\beta > 0$ is a constant) such that $b_1 > 0$, and then it can be shown that there exists $\epsilon_1^* = 1/(\epsilon_0^{*2}/\beta + 4L_2\|P_2\|)$, such that, for every $0 < \epsilon \leq \epsilon_1^*$, we have

$$\dot{V} \leq -\min(1/2, \beta/(2\epsilon))[\|x\|^2 + \|\eta\|^2]. \tag{2.3.26}$$

Thus it can conclude that the origin of system (2.3.13) and (2.3.14) is exponentially stable. □

2.4 High gain state and perturbation observer

In this section, the output is chosen as $y = x_1$ and a $(n+1)$th-order state observer is designed to estimate the system states and perturbation. The state estimate $\hat{x}_1$ of system (2.2.8) is obtained using the observer as

$$\dot{\hat{x}}_e = A_1\hat{x}_e + B_3 u + H(y - C_1\hat{x}_e). \tag{2.4.1}$$

The observer gain H is chosen as:

$$H = \begin{bmatrix} \alpha_1/\epsilon \\ \alpha_2/\epsilon^2 \\ \vdots \\ \alpha_n/\epsilon^n \\ \alpha_{n+1}/\epsilon^{n+1} \end{bmatrix}, \tag{2.4.2}$$

where ϵ is a positive constant, $0 < \epsilon < 1$, to be specified and the positive constants α_i, $i = 1, 2, \cdots, n+1$, are chosen such that the roots of

$$s^{n+1} + \alpha_1 s^n + \cdots + \alpha_n s + \alpha_{n+1} = 0$$

are in the open left-half complex plan, where s is the Laplace operator.

Defining the estimation error as $\tilde{x}_e = x_e - \hat{x}_e$, the error dynamics of observer (2.4.1) becomes

$$\dot{\tilde{x}}_e = (A_1 - HC_1)\tilde{x}_e + B_1\dot{\Psi}(\cdot). \tag{2.4.3}$$

For the purpose of analysis, replace the observer error dynamics by the equivalent dynamics of the scaled estimation error

$$\eta_i = \frac{\tilde{x}_i}{\epsilon^{n+1-i}}, \qquad 1 \le i \le n+1.$$

Hence, we have $\hat{x}_e = x_e - D(\epsilon)\eta$, where

$$\begin{aligned} \eta &= [\eta_1, \eta_2, \cdots, \eta_{n+1}]^T, \\ D(\epsilon) &= \text{diag}[\epsilon^{n}, \cdots, 1]_{(n+1)\times(n+1)}. \end{aligned}$$

Then the error dynamics of observer (2.4.3) can be represented as

$$\begin{aligned} \dot{\eta} &= D^{-1}(\epsilon)(A_1 - HC_1)D(\epsilon)\eta + D^{-1}(\eta)B_1\dot{\Psi}(\cdot) \\ &= \tfrac{1}{\epsilon}A_{10}\eta + B_1\dot{\Psi}(\cdot), \end{aligned} \tag{2.4.4}$$

where

$$A_{10} = \begin{bmatrix} -\alpha_1 & 1 & \cdots & \cdots & 0 \\ -\alpha_2 & 0 & 1 & \cdots & 0 \\ \vdots & & & & \vdots \\ -\alpha_n & 0 & 0 & \cdots & 1 \\ -\alpha_{n+1} & 0 & 0 & \cdots & 0 \end{bmatrix}$$

is Hurwitzian.

2.4.1 Observer error dynamics analysis

To achieve fast enough tracking of the system states and perturbation, the observer gains can be chosen such that the estimation error $\tilde{x}_1$ will converge exponentially to a small neighbourhood which is arbitrarily close to origin. The analysis result is summarized as the following theorem.

Theorem 2.3. *Consider system (2.2.7), design a high gain state and perturbation observer (2.4.1) and choose the gain H as described in equation (2.4.2). If assumptions A2.1 and A2.2 hold, then given any positive constant $\delta_{\text{spo}} > 0$, there exits a positive constant ϵ^*_{spo}, such that $\forall \epsilon$, $0 < \epsilon < \epsilon^*_{\text{spo}}$, the observer error $\tilde{x}_e$, from any initial value $\tilde{x}_e(0)$, converges exponentially to the neighborhood*

$$\|\tilde{x}_e\| \leq \delta_{\text{spo}}.$$

Proof: For system (2.4.4), A_{10} is a Hurwitz matrix ; thus we can define the Lyapunov function

$$W_{10}(\eta) = \eta^T P_{10} \eta, \tag{2.4.5}$$

where P_{10} is the positive definite solution of the Lyapunov equation $P_{10}A_{10} + A_{10}^T P_{10} = -I$. This function satisfies

$$\lambda_{\min}(P_{10})\|\eta\|^2 \leq W_{10}(\eta) \leq \lambda_{\max}(P_{10})\|\eta\|^2, \tag{2.4.6}$$

$$\frac{\partial W_{10}}{\partial \eta} A_{10}\eta \leq -\|\eta\|^2, \tag{2.4.7}$$

$$\|\frac{\partial W_{10}}{\partial \eta}\| \leq 2\lambda_{\max}(P_{10})\|\eta\|. \tag{2.4.8}$$

Differentiating W_{10} along system (2.4.4) one obtains

$$\dot{W}_{10} = -\frac{1}{\epsilon}\|\eta\|^2 + 2P_{10}\eta B_1 \dot{\Psi}(\cdot), \tag{2.4.9}$$

that, using assumption $A2.2$, can be rewritten as

$$\dot{W}_{10} \leq -\frac{1}{\epsilon}\|\eta\|^2 + 2\lambda_{\max}(P_{10})\|\eta\|\gamma_2. \tag{2.4.10}$$

Take a value of α, $0 < \alpha < 1$, it is easy to show that

$$\dot{W}_{10} \leq -\alpha\|\eta\|^2, \tag{2.4.11}$$

if

$$\|\eta\| \geq = \delta'_{\text{spo}}, \tag{2.4.12}$$

where $\delta'_{\text{spo}} = \frac{2\lambda_{\max}(P_{10})\gamma_2}{\frac{1}{\epsilon}-\alpha}$ is a positive constant. As $\lambda_{\min}(P_{10})\|\eta\|^2 \leq W_{10}(\eta) \leq \lambda_{\max}(P_{10})\|\eta\|^2$, applying Corollary 5.3 of Theorem 5.1 of [4], one can conclude that if $\|\eta(0)\| \geq \delta_{\text{spo1}}$, $\exists\, t_1$, $t_1 > 0$, such that

$$\|\eta(t)\| \leq \sqrt{\frac{\lambda_{\max}(P_{10})}{\lambda_{\min}(P_{10})}}\|\eta(0)\|e^{-(\alpha/(2\lambda_{\max}(P_{10})))t}, \qquad \forall t < t_1; \tag{2.4.13}$$

and

$$\|\eta(t)\| \leq \sqrt{\frac{\lambda_{\max}(P_{10})}{\lambda_{\min}(P_{10})}}\delta'_{\text{spo}}, \qquad \forall t \geq t_1; \tag{2.4.14}$$

where

$$t_1 \leq \frac{2\lambda_{\max}(P_{10})}{\alpha}\log\left(\frac{\|\eta\|}{\delta_{\text{spo1}}}\right). \tag{2.4.15}$$

Based on $\tilde{x}_i = \eta_i\epsilon^{n+1-i}$ and $0 < \epsilon < 1$, we have $\|\tilde{x}_e\| \leq \|\eta\|$. Thus, for any given constant δ_{spo}, $\exists\, \epsilon^*_{\text{spo}}$, $0 < \epsilon^*_{\text{spo}} < 1$

$$\epsilon^*_{\text{spo}} = \left(\sqrt{\frac{\lambda_{\max}(P_{10})}{\lambda_{\min}(P_{10})}}\frac{2\lambda_{\max}(P_{10})\gamma_2}{\delta_{\text{spo}}} + \alpha\right)^{-1},$$

such that, $\forall\, \epsilon\ 0 < \epsilon < \epsilon^*_{\text{spo}}$,

$$\|\tilde{x}_e(t)\| \leq \delta_{\text{spo}}, \qquad \forall t \geq t_1.$$

□

2.4.2 Closed-loop stability analysis

Using the estimates of states and perturbation, an output feedback linearization control law is designed for the nonlinear system (2.2.1). The complete control is designed the same as that represented by equations (2.3.11) and (2.3.12) except that the true states are replaced with the estimated states:

$$u = v/b_0 - \hat{x}_{n+1}/b_0, \tag{2.4.16}$$

$$v = -K\hat{x}, \tag{2.4.17}$$

where $K = [k_1, k_2, \cdots, k_n]^T$ are the linear feedback controller gains, which makes matrix $A_0 = A - BK$ Hurwitzian.

Note that $\hat{x} = x - D'(\eta)\eta'$, $\hat{x}_{n+1} = x_{n+1} - \eta_{n+1}$, where

$$D'(\epsilon) = \text{diag}[\epsilon^{n+1}, \cdots, \epsilon]_{(n)\times(n)},$$

and

$$\eta' = [\eta_1, \eta_2, \cdots, \eta_n]^T.$$

Control (2.4.16) can be represented as:

$$u = \frac{1}{b_0}(-x_{n+1} - Kx - K_1 D(\epsilon)\eta), \tag{2.4.18}$$

where $K_1 = [K, 1]^T$.

Applying control (2.4.18) to system (2.2.7), the closed-loop system can be represented by

$$\dot{x} = A_0 x + BK_1 D(\epsilon)\eta \tag{2.4.19}$$

$$\epsilon\dot{\eta} = A_{10}\eta + \epsilon B_4 \dot{\Psi}(x, D(\epsilon)\eta). \tag{2.4.20}$$

System (2.4.19) and (2.4.20) is a standard singular perturbed system, and $\eta = 0$ is the unique solution of system (2.4.20) when $\epsilon = 0$. The reduced system, obtained by substituting $\eta = 0$ in system (2.4.19), is obtained as follows:

$$\dot{x} = A_0 x. \tag{2.4.21}$$

The boundary-layer system, obtained by applying the change of time variable $\tau = t/\epsilon$ to (2.4.20) and then setting $\epsilon = 0$, is given by

$$\frac{d\eta}{d\tau} = A_{10}\eta. \tag{2.4.22}$$

Theorem 2.4. *Consider system (2.2.8) and high gain state and perturbation observer (2.4.1), choose the observer gain as described in equation (2.4.2), and let assumptions A2.1 and A2.2 hold; then, $\exists\epsilon_2^*$, $\epsilon_2^* > 0$ such that, $\forall\epsilon$, $0 < \epsilon < \epsilon_2^*$, the origin of system (2.4.19) and (2.4.20) is exponentially stable.*

Proof: For the reduced system (2.4.21), we define the same Lyapunov function as function (2.3.17). For the boundary-layer system (2.4.22), we define the Lyapunov function $W_{10}(\eta)$ according to equation (2.4.5).

Let us consider $V_2(x,\eta) = V_0(x)+\beta W_{10}(\eta)$, where $\beta > 0$ is to be determined, as a Lyapunov function candidate for system (2.4.19) and (2.4.20). Choose $\xi < r$; then, given Assumptions $A2.1 \sim A2.2$, $\forall\ (x,\eta)$, $(x,\eta) \in B(0,\xi) \times \|\eta\| \leq \xi = \Lambda$, we have

$$|\dot{\Psi}(x, D(\epsilon)\eta)| \leq L_3\|x\| + L_4\|\eta\|. \tag{2.4.23}$$

Using equations (2.3.18) $\sim$ (2.3.23) and Young's inequality, it can be shown that, for all $(x,\eta) \in \Lambda$, we have

$$\begin{aligned}
\dot{V}_2 &= \tfrac{\partial V_0(x)}{\partial x}(A_0x + BK_1D(\epsilon)\eta) + \beta\tfrac{\partial W_2(\eta)}{\partial \eta}(\tfrac{A_{10}\eta}{\epsilon} + B_4\dot{\Psi}(\cdot)) \\
&\leq -\|x\|^2 - \tfrac{\beta}{\epsilon}\|\eta\|^2 \\
&\quad +2\beta L_4\|P_4\|\|\eta\|^2 + (2\|P_0\|\|K_1\|\|D(\epsilon)\| + 2\beta L_3\|P_{10}\|)\|x\|\|\eta\| \\
&\leq -\|x\|^2 - \tfrac{\beta}{\epsilon}\|\eta\|^2 + 2\beta L_4\|P_{10}\|\|\eta\|^2 \\
&\quad +(2\|P_0\|\|K_1\| + 2\beta L_3\|P_{10}\|)\|x\|\|\eta\| \\
&\leq -\|x\|^2 - \tfrac{\beta}{\epsilon}\|\eta\|^2 + 2\beta L_4\|P_{10}\|\|\eta\|^2 \\
&\quad +(2\|P_0\|\|K_1\| + 2\beta L_3\|P_{10}\|)(\tfrac{1}{\epsilon_0}\|x\|^2 + \epsilon_0\|\eta\|^2) \\
&\leq -\tfrac{1}{2}\|x\|^2 - \tfrac{\beta}{2\epsilon}\|\eta\|^2 - b_3\|x\|^2 - b_4\|\eta\|^2,
\end{aligned} \tag{2.4.24}$$

where $b_3 = \frac{1}{2} - \frac{2}{\epsilon_0}(\|K_1\|\|P_0\| + \beta L_3\|P_{10}\|)$, $b_4 = \frac{\beta}{2\epsilon} - 2\beta(\epsilon_0 * L_3 + L_4)\|P_{10}\| - 2\epsilon_0\|P_0\|\|K_1\|$, and $\epsilon_0 > 0$.

Now choose $\epsilon_0^* = 4\|K_1\|\|P_0\| + 4\beta L_3\|P_{10}\|$ (where $\beta > 0$ is a constant), $\epsilon_0 \geq \epsilon_0^*$, such that $b_3 > 0$, and then let $\epsilon_2^* = \beta/(\epsilon_0^{*2} + 4\beta L_4\|P_{10}\|)$, $\forall\ \epsilon$, $\epsilon \leq \epsilon_2^*$, $b_4 > 0$. Then, it can be shown that

$$\dot{V} \leq -\min(1/2, \beta/(2\epsilon))[\|x\|^2 + \|\eta\|^2]. \tag{2.4.25}$$

Thus it can conclude that the origin of system (2.4.19) and (2.4.20) is exponentially stable. □

Remark 2.1 The designed state and perturbation observer can be regarded as a functional estimation method, in contrast to the parameter estimation method used in most nonlinear adaptive control. It can deal with fast varying unknown parameters, unknown nonlinear dynamics and external disturbances. When there does not exist uncertainties and external disturbances and the exact system nonlinearities are obtainable, such a controller provides the same performance as the state exact feedback linearization controller. But when there exists uncertainties, such controller performs much better.

Remark 2.2 The proposed controller uses the estimates of states and perturbation to realize the whole controller, it needs only one measurable output and can be easily implemented in practice.

Remark 2.3 We mainly focus on the nonlinear adaptive control design based on the nonlinear canonical system. The proposed control schemes can be extended easily to the input/output linearization of minimum phase nonlinear system.

2.5 Example

In this section, simulation of the control of a nonlinear system without a known system model is performed using the proposed adaptive output feedback control scheme. Consider a second order nonlinear system in the form of

equation (2.2.1) as

$$\begin{cases} \dot{x}_1 &= x_2 \\ \dot{x}_2 &= f(x) + (b(x) - b_0)u + b_0 u \\ y &= x_1 \end{cases} \tag{2.5.1}$$

where $x = (x_1, x_2)^T$, $f(x) = -(2 + \sin(x_1))x_1^3 - 5(3 + \cos(\pi x_1))\sin(x_2)$, and $b(x) = 1 + 0.5\sin(x_1)$. The system, initially at the state of $x_1(0) = 5$ and $x_2(0) = 0$, is required to track the desired trajectory $y_r(t) = 5\sin(t)$. By defining new states $e_1 = y - y_r$ and $e_2 = y^{(1)} - y_r^{(1)}$, the track problem of system can be converted to the stabilization of system around the origin. As $0.5 \leq |b(x)| \leq 1.5$, choose $b_0 = 2$ to satisfy Assumption A2.1. For system (2.5.1), we have perturbation

$$\begin{aligned} \Psi(x, u, t) &= f(x) + (b(x) - b_0)u \\ &= -(2 + \sin(\pi x_1))x_1^3 - 5(3 + \cos(\pi x_1))\sin(x_2) \\ &\quad (-1 + 0.5\sin(x_1))u \\ &\leq 3|x_1|^3 + 1.5|u|. \end{aligned}$$

Parameters of a HGSPO (2.4.1) are selected to be $\alpha_1 = 300$, $\alpha_2 = 3 \times 10^4$, $\alpha_3 = 1 \times 10^6$, and $\epsilon = 0.01$. Parameters of the controller described in equations (2.4.16) and (2.4.17) are chosen as $k_1 = 100$ and $k_2 = 20$. The system responses are shown in Figure 2.1. The estimation error of states x_1 and x_2, and perturbation Ψ are shown in Figures 2.2 and 2.3.

2.6 Conclusion

In this chapter, the nonlinear adaptive control via the high gain state and perturbation observer has been studied. Two types of observers, the high gain perturbation observer and the high gain state and perturbation observer, have been discussed respectively. The designed controller adopts the real time estimates of states and perturbation to yield the adaptive, output feedback control

law. It can deal with the fast varying unknown parameters, unknown nonlinear dynamics and external disturbances. Moreover, the proposed controller needs only one measurable state and does not require the detailed system model. It can be implemented easily in practice. Finally, the numerical simulation results of an example have been given.

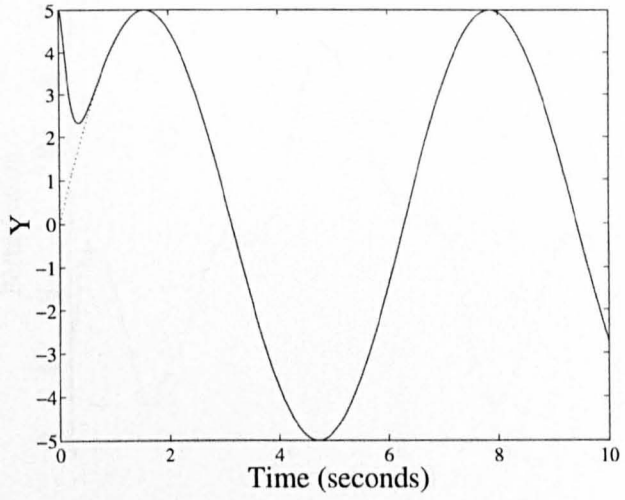

(a) Output – $y(t), \cdots y_r(t)$

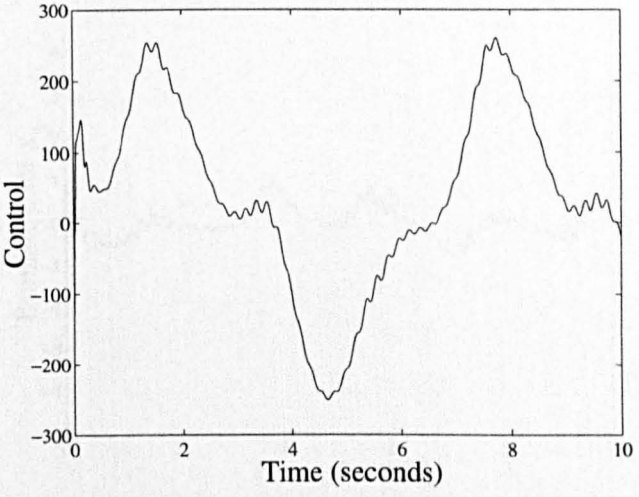

(b) Control u

Figure 2.1: System response of NAC with HGSPO

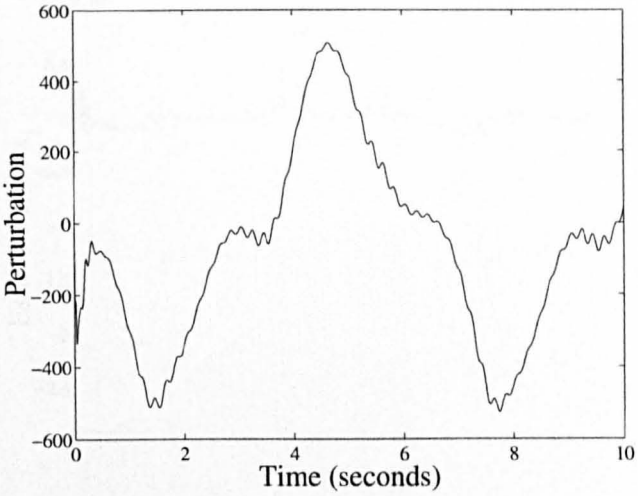

(a) Perturbation and its estimate – Ψ, $\cdots$ $\hat{\Psi}$

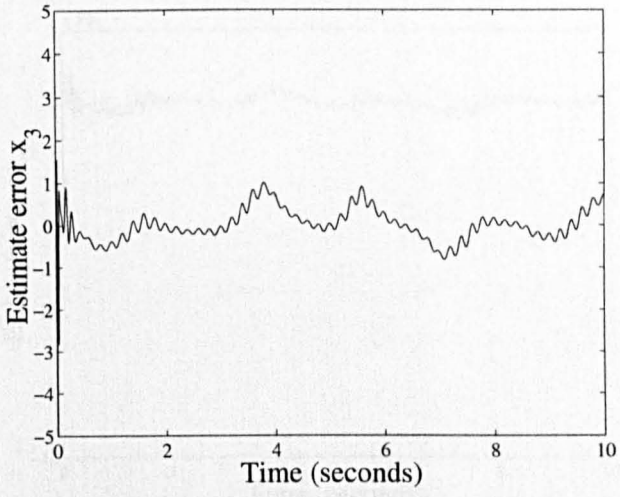

(b) Perturbation estimate error $\tilde{\Psi}$

Figure 2.2: Perturbation estimation of NAC with HGSPO

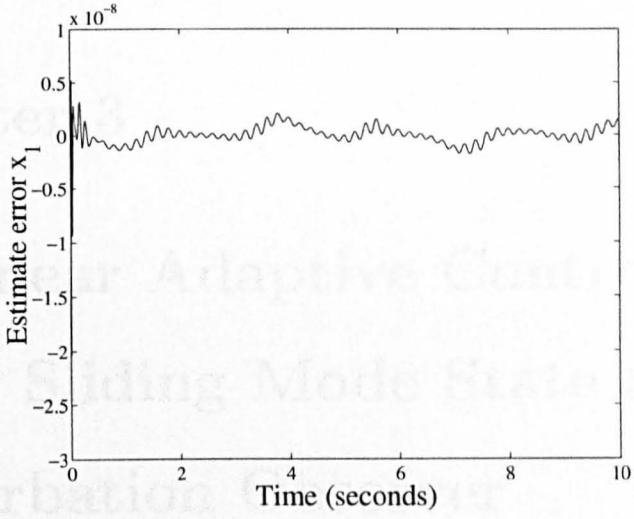

(a) Estimate error of $\tilde{x}_1$

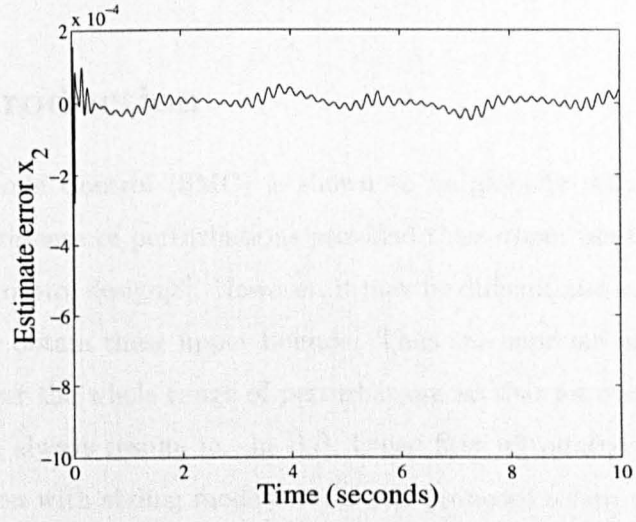

Estimate error of $\tilde{x}_2$

Figure 2.3: Performance of high gain state and perturbation observer

Chapter 3

Nonlinear Adaptive Control Using Sliding Mode State and Perturbation Observer

3.1 Introduction

Sliding Mode Control (SMC) is shown to be globally stable and robust despite the presence of perturbations provided their upper bounds are known priori to the control design[8]. However, it may be difficult and even sometimes impossible to obtain these upper bounds. Thus the supreme upper bound is chosen to cover the whole range of perturbations so that an over conservative control input always results in. In [17], Olgac first introduced the perturbation estimation with sliding mode control and proposed a new scheme named as Sliding Mode Control with Perturbation Estimation (SMCPE). The upper bounds of the perturbations is replaced with its estimate so that a desirable level of control activity is yielded for a given precision of trajectory tracking. In this scheme, the perturbation estimation is implemented by a numerical differentiation algorithm. However, it is well known that the numeric differen-

tiation algorithm is very sensitive to measurement noise. Moreover, a kind of Sliding Mode State and Perturbation Observer (SMSPO) is proposed as a tool to eliminate the requirement of full state feedback, reducing the implementation costs [18]. Consequently, the resulting observer is able to provide much better state estimation accuracy. The combination of this kind of SMSPO with SMC results in a control algorithm that is robust against perturbations, utilizes only partial state feedback and outperforms conventional SMC with full state feedback and perfect measurements. However, the perturbation is only approximately estimated by using a variable transformation and the analysis is mainly for general second-order multi-degree of freedom nonlinear systems [18].

In this chapter, a new kind of Sliding Mode State and Perturbation Observer (SMSPO) is investigated for the output feedback control of nonlinear systems. In SMSPO, the perturbation is defined to describe the combined effect of the system nonlinearities, uncertainties and external disturbances. And a *fictitious state* is introduced to represent the perturbation in the state equations. As in the last chapter, the chapter begins with sliding mode perturbation observer to illustrate the perturbation estimation method, and then move to study the sliding mode state and perturbation observer. During the design of the observer, the sliding condition is first examined, and then the sliding mode dynamics on the sliding surface has been investigated with the Lyapunov analysis method.

In this chapter, the estimates of the states and perturbation are employed to design the nonlinear adaptive, output feedback sliding mode controller. The upper bounds of perturbation is not included in the controller loop. It is only needed in the design of the observer. Moreover, as the real estimate of perturbation is used to compensate the system perturbation, the upper bound of perturbation is replaced with the relatively smaller bound of its estimation error, an over conservative control input is avoided such that the tracking accuracy is improved. The nonlinear adaptive control using continuous output

feedback and the sliding mode observer has also been studied. In this case, the linearization of the original nonlinear system is realized without requiring the accurate system model. And a linear continuous feedback controller, rather than a sliding mode controller, is designed for the equivalent linear system. In each case, the stability analysis of the combined of the controller and observer has been given. Numerical simulation results are provided to demonstrate the effectiveness of the proposed control schemes. Finally, conclusion is drawn in the last section.

3.2 Problem formulation

Consider the sliding mode control of the nonlinear systems which has the following canonical form:

$$\begin{cases} \dot{x} &= Ax + B\left(a(x) + b(x)u + d(t)\right) \\ y &= x_1, \end{cases} \tag{3.2.1}$$

where $x = [x_1, x_2, \cdots, x_n]^T \in \mathcal{R}^n$ is the state variable vector; $u \in \mathcal{R}$ the control input; $y \in \mathcal{R}$ the system output; $a(x) : \mathcal{R}^n \to \mathcal{R}$ and $b(x) : \mathcal{R}^n \to \mathcal{R}$ C^∞ smooth functions; $d(t) : [0, \infty] \to \mathcal{R}$ the external disturbance. The $n \times n$ matrix A and the $n \times 1$ matrix B are given by

$$A = \begin{bmatrix} 0 & 1 & 0 & \cdots & 0 \\ 0 & 0 & 1 & \cdots & 0 \\ \vdots & & & & \vdots \\ 0 & 0 & 0 & \cdots & 1 \\ 0 & 0 & 0 & \cdots & 0 \end{bmatrix}, \qquad B = \begin{bmatrix} 0 \\ 0 \\ \vdots \\ 0 \\ 1 \end{bmatrix}. \tag{3.2.2}$$

For system (3.2.1), define the system perturbation as

$$\Psi(x, u, t) = a(x) + (b(x) - b_0)u + d(t), \tag{3.2.3}$$

then the last equation of system (3.2.1) can be rewritten as

$$\dot{x}_n = \Psi(x, u, t) + b_0 u, \tag{3.2.4}$$

where b_0 is a constant control gain which will be decided later.

Define a *fictitious state* to represent the perturbation: $x_{n+1} = \Psi(x, u, t)$, system (3.2.1) may be represented as

$$\begin{cases} \dot{x}_1 &= x_2 \\ & \cdots \\ \dot{x}_n &= x_{n+1} + b_0 u \\ \dot{x}_{n+1} &= \dot{\Psi}(\cdot) \\ y &= x_1, \end{cases} \tag{3.2.5}$$

where $\dot{\Psi}(\cdot)$ is the derivative of $\Psi(\cdot)$. The state vector is defined as $x_e = \begin{bmatrix} x_1 & x_2 & \cdots & x_n & x_{n+1} \end{bmatrix}^T$.

The following assumptions are made on system (3.2.1).

A3.1 b_0 is chosen to satisfy: $|b(x)/b_0 - 1| \leq \theta < 1$, where θ is a positive constant.

A3.2 The function $\Psi(x, u, t) : \mathcal{R}^n \times \mathcal{R} \times \mathcal{R}^+ \to \mathcal{R}$ and $\dot{\Psi}(x, u, t) : \mathcal{R}^n \times \mathcal{R} \times \mathcal{R}^+ \to \mathcal{R}$ are globally bounded:

$$|\Psi(x, u, t)| \leq \gamma_1, \quad |\dot{\Psi}(x, u, t)| \leq \gamma_2,$$

where γ_1 and γ_2 are positive constants. In addition, $\Psi(0, 0, 0) = 0$ and $\dot{\Psi}(0, 0, 0) = 0$.

A3.3 The desired trajectory $y_d(t)$ and its up to nth-order derivative are continuous and bounded.

The control problem is to study the sliding mode control of system (3.2.1) in the presence of model imprecision $a(x)$, $b(x)$ and external disturbance $d(t)$. There are two cases: one is to design a sliding mode perturbation observer with all states available; the other is to design a sliding mode state and perturbation observer with only one state $y = x_1$ available. The control object is to get the system state x to track the desired state $x_d = \begin{bmatrix} y_d & y_d^{(1)} & \cdots & y_d^{(n-1)} \end{bmatrix}^T$.

3.3 Sliding mode perturbation observer

In this section, all states are assumed to be available and a sliding mode perturbation observer is designed to estimate system perturbation. The slide mode controller utilize the estimate of system perturbation to compensate the real perturbation has been investigated. The upper bound of system perturbation is not required in the controller design and an over conservative control is avoided. A classical state feedback sliding mode control is designed for comparison.

3.3.1 Design of sliding mode perturbation observer

Taking x_n as the available measurement, a Sliding Mode Perturbation Observer (SMPO) is designed for system (3.2.5) as:

$$\begin{cases} \dot{\hat{x}}_n &= \hat{x}_{n+1} + \alpha_1 \tilde{x}_n + k_1 \operatorname{sgn}(\tilde{x}_n) + b_0 u \\ \dot{\hat{x}}_{n+1} &= \alpha_2 \tilde{x}_n + k_2 \operatorname{sgn}(\tilde{x}_n) \end{cases}, \tag{3.3.1}$$

where $\tilde{x}_n = x_n - \hat{x}_n$, α_i and $k_i = 0$, $i = 1, 2$ are positive gains. The signum function is defined as:

$$\operatorname{sgn}(\chi) = \begin{cases} 1 & \text{if } |\chi| > 0; \\ 0 & \text{if } |\chi| = 0; \\ -1 & \text{if } |\chi| < 0. \end{cases} \tag{3.3.2}$$

The error dynamics satisfies the equation:

$$\begin{cases} \dot{\tilde{x}}_n &= -\alpha_1 \tilde{x}_n - k_1 \operatorname{sgn}(\tilde{x}_n) + \tilde{x}_{n+1} \\ \dot{\tilde{x}}_{n+1} &= -\alpha_2 \tilde{x}_n - k_2 \operatorname{sgn}(\tilde{x}_n) + \dot{\Psi}(\cdot). \end{cases} \tag{3.3.3}$$

The sliding surface is defined as $S_{\text{po}}(\tilde{x}) = \tilde{x}_n = 0$. Introducing function $V_{\text{po}} = \frac{1}{2} S_{\text{po}}^2$, the sliding surface is attractive if $\dot{V}_{\text{po}} < 0$, $\forall\ \tilde{x}_i \notin S_{\text{po}}$. The condition for the existence of sliding mode is:

$$\begin{cases} \tilde{x}_{n+1} - k_1 - \alpha_1 \tilde{x}_n \leq 0, & \text{if } \tilde{x}_n > 0; \\ \tilde{x}_{n+1} + k_1 - \alpha_1 \tilde{x}_n \geq 0, & \text{if } \tilde{x}_n < 0. \end{cases} \tag{3.3.4}$$

The value of the gain k_1 must be chosen to satisfy the sliding condition of the sliding surface $S_{\text{po}} = 0$ is satisfied, i.e.

$$k_1 + \alpha_1|\tilde{x}_n| \geq |\tilde{x}_{n+1}|_{\max}, \qquad \forall t > 0. \tag{3.3.5}$$

Hence, the choice of k_1 depends upon the estimated error of $\tilde{x}_{n+1}$. If above condition is satisfied, it is guaranteed that the system will reach the sliding surface at time t_s and thereafter remain inside the sliding surface after $t \geq t_s$. It follows that the switch function satisfies $S_{\text{po}}(\tilde{x}) = x_n - \hat{x}_n = 0$, $\forall t > t_s$, which in turn implies that $\dot{S}_{\text{po}}(\tilde{x}) = x_n - \hat{x}_n = 0$, $\forall t \geq t_s$.

Considering the designed sliding mode observer (3.3.1), the $\text{sgn}(\tilde{x}_n)$ term is a discontinuous input which enforces sliding mode to stay on sliding surface. The discontinuous input can be considered as the combination of a low frequency equivalent control term and a high frequency switching term. Therefore, *equivalent control* is defined as the *average* value of the discontinuous control which maintains the sliding motion on sliding surface [14, 15]. The equivalent control is not the actual control signal applied to the system but it may be thought of as the control signal which is applied 'on average'. In fact, it is the low frequency components of the real control signal[15]. Thus, by solving the first equation of system (3.3.3) with replacing $S_{\text{po}}(\tilde{x})$ and $\dot{S}_{\text{po}}(\tilde{x})$ by zero, the equivalent control of the $\text{sgn}(\tilde{x}_n)$ term can be obtained as follows:

$$u_{\text{eq}} = \frac{1}{k_1}\tilde{x}_{n+1}. \tag{3.3.6}$$

Substituting $\text{sgn}(\tilde{x}_n)$ term in system (3.3.3) with equivalent control (3.3.6), the resulting error dynamics on sliding surface is

$$\dot{\tilde{x}}_{n+1} = -\frac{k_2}{k_1}\tilde{x}_{n+1} + \dot{\Psi}(\cdot). \tag{3.3.7}$$

Note that equation (3.3.7) is a filter between $\dot{\Psi}$ and $\tilde{x}_{n+1}$ with a cut-off frequency k_2/k_1. It is desirable to place the break point k_2/k_1 as high as possible in order to maximize the attenuation from $\dot{\Psi}(\cdot)$ to $\tilde{x}_{n+1}$, and consequently improve the estimation accuracy of x_{n+1}.

As $|\dot{\Psi}(x,u,t)| \leq \gamma_2$, the stability of the sliding observer is guaranteed by setting $k_2 \geq \gamma_2$ and the sliding condition is fulfilled by setting

$$k_1 \geq |\tilde{x}_{n+1}(0)|.$$

It is also assumed that γ_2 is an upper bound of $\dot{\Psi}(\hat{x},t)$, meaning that the error due to state estimation are negligible compared to the modelling uncertainties and external disturbances. This is a reasonable assumption since the estimation errors can be reduced by increasing k_2/k_1 independently from $\dot{\Psi}(\cdot)$.

To avoid the chatter of observer output, it is necessary to smooth the discontinuous function $\mathrm{sgn}(\cdot)$ with a saturation function $\mathrm{sat}(\chi,\epsilon_o)$, where ϵ_o is the thickness of the boundary layer. This will eliminate another source of the control input chatter. The saturation function $\mathrm{sat}(\chi,\epsilon)$ is defined as

$$\mathrm{sat}(\chi,\epsilon) = \begin{cases} \frac{\chi}{\|\chi\|}, & \text{if } |\chi| \geq \epsilon \\ \frac{\chi}{\epsilon}, & \text{if } |\chi| \leq \epsilon. \end{cases} \tag{3.3.8}$$

where ϵ, $0 < \epsilon < 1$, is the thickness of the boundary layer.

Without loss of generality, it can assume that at time $t = 0$ states x_n and x_{n+1} are perfectly known so that $\tilde{x}_n = 0$ and $\tilde{x}_{n+1} = 0$. That means that the observer starts on the sliding surface and will always remain in the boundary layer provided that the gain k_2 is high enough. Thus, all the $\mathrm{sgn}(\tilde{x}_n)$ terms of (3.3.3) can be replaced by $\mathrm{sat}(\tilde{x}_n,\epsilon_o)$ and becomes

$$\begin{cases} \dot{\tilde{x}}_n &= (-\alpha_1 + \frac{k_1}{\epsilon_o})\tilde{x}_n + \tilde{x}_{n+1} \\ \dot{\tilde{x}}_{n+1} &= (-\alpha_2 + \frac{k_2}{\epsilon_o})\tilde{x}_n + \dot{\Psi}(\cdot) \end{cases}. \tag{3.3.9}$$

Above error dynamics on boundary layer can be analyzed by the same method as a high gain observer described in Theorem 2.2. It shows that after the system states have entered the boundary layer $|\tilde{x}_n| \leq \epsilon_o$, $\tilde{x}_n$ and $\tilde{x}_{n+1}$ will converge exponentially to a neighbourhood around the origin in a limited time and remain in the boundary layer with the chosen gains k_i and α_i, $i = 1,2$.

3.3.2 Sliding mode control via perturbation observer

In this section, a sliding mode controller with perturbation observer (SMCPO) is designed for the tracking control of the nonlinear system (3.2.1). A classical sliding mode controller is designed at first and then the design of SMCPO is investigated. Let $e_1 = x_1 - y_d$ be the tracking error of the output y, and let F

$$E = x - x_d = [\ e_1 \quad \dot{e}_1 \quad \cdots \quad e^{(n-1)}\ ]^T$$

be the tracking error vector. Furthermore, define a sliding surface as

$$S_{\text{smcpo}}(x,t) = \sum_{i=1}^{n} \rho_i \left(x_i - y_d^{(i-1)}\right), \tag{3.3.10}$$

where $\rho_n = 1$ and ρ_i, $i = 2, \cdots, n-1$ are gains for a stable polynomial. If all poles of the polynomial are equal to real and negative constant $-\lambda_c$, gains ρ_i can be chosen as:

$$\rho_i = C_{n-1}^{i-1} \lambda_c^{n-i}, \qquad i = 1, 2, \cdots, n, \tag{3.3.11}$$

where $C_{n-1}^{i} = \frac{(n-1)!}{i!(n-1-i)!}$.

Here some basic results about SMC design is given briefly [3]. For the tracking task to be achievable using a finite control, the initial desired state $x_d(0)$ must be:

$$x_d(0) = x(0). \tag{3.3.12}$$

Otherwise, tracking can only be achieved after a transient. Given the initial condition (3.3.12), the problem of tracking $x = x_d$ is equivalent to that of remaining on the surface $S_{\text{smcpo}}(t)$ for all $t > 0$; indeed $S_{\text{smcpo}} = 0$ represents a linear differential equation whose unique solution is $x = 0$, given initial conditions (3.3.12). Thus the problem of tracking the n-dimensional vector x_d can be reduced to that of keeping the scalar quantity S_{smcpo} at zero. More precisely, the problem of tracking the n-dimensional vector x_d (i.e., the original nth-order tracking problem in x) can in effect be replaced by a 1st-order

stabilization problem in S_{smcpo}. Furthermore, bounds of S_{smcpo} can be translated into bounds on the tracking error vector $x - x_d$, and therefore the scalar represents a true measure of tracking performance. Specially, assuming that $x_1(0) - x_{d1}(0) = 0$ (the effect of non-zero initial conditions in error can be added separately), we have:

$$\begin{aligned} \forall t \geq 0,\ |S_{smcpo}(t)| &< \epsilon_c \Rightarrow \\ \forall t \geq 0,\ |e^{(i)}(t)| &\leq (2\lambda_c)^i \frac{\epsilon_c}{\lambda_c^{n-1}},\ i = 0, 1, \cdots, n-1. \end{aligned} \tag{3.3.13}$$

Classical sliding mode controller design

Assuming that system nonlinearities are unknown and all states are available, a sliding mode controller is designed as

$$u = \frac{1}{b_0}\left[y_d^{(n)} - \sum_{i=1}^{n-1} \rho_i (x_{i+1} - y_d^{(i)}) - \zeta S_{\text{smcpo}} - \varphi\ \text{sgn}(S_{\text{smcpo}}) \right], \tag{3.3.14}$$

where ζ and φ are control gains and determined to fulfill the attractive condition of the sliding surface S_{smcpo}.

Differentiating (3.3.10) along system (3.2.1) and using control (3.3.14), one obtains

$$\begin{aligned} \dot{S}_{\text{smcpo}} &= y_d^{(n)} + \textstyle\sum_{i=1}^{n-1} \rho_i (x_{i+1} - y_d^{(i)}) + \Psi(\cdot) + b_0 u \\ &= -\zeta S_{\text{smcpo}} - \varphi\ \text{sgn}(S_{\text{smcpo}}) + \Psi(\cdot). \end{aligned} \tag{3.3.15}$$

Therefore, the attractiveness condition is

$$\zeta |S_{\text{smcpo}}| + \varphi > |\Psi(\cdot)|_{\max}. \tag{3.3.16}$$

As $|\Psi(\cdot)|_{\max} \leq \gamma_1$, the above condition is obviously satisfied if the gain φ is chosen as

$$\varphi \geq \gamma_1. \tag{3.3.17}$$

The discontinuity in control (due to the signum function) should be smoothed to eliminate the control chatter. A replacement of the signum function with the unit saturation function was proposed first by Slotine and Sastry

[8]. This operation removes the fundamental cause of control chatter by utilizing a continuous control law. The saturation function used for SMC design is defined same as equation (3.3.8), i.e., $\text{sat}(\chi, \epsilon_c)$, where ϵ_c is the thickness of the boundary layer of sliding mode controller.

Moreover, the corresponding sliding mode dynamics with the saturation function type controller is not desired to exhibit high frequency oscillation either. Therefore the S_{smcpo} dynamics should be enforced into a low-pass filter mode to get rid of the effects of high-frequency components of perturbations. This control design method will eliminate another source of control chatter [17]. With the unit saturation type control function, the dynamics of S_{smcpo} within the boundary layer

$$|S_{\text{smcpo}}| \leq \epsilon_c, \tag{3.3.18}$$

take the form:

$$\dot{S}_{\text{smcpo}} + (\zeta + \frac{\varphi}{\epsilon_c}) S_{\text{smcpo}} = \Psi(\cdot). \tag{3.3.19}$$

This equation acts as a low-pass filter against the perturbations and

$$\omega = \zeta + \frac{\varphi}{\epsilon_c} \tag{3.3.20}$$

is the tuneable break frequency. In order to eliminate the influence of the perturbations, this frequency is bounded by an $\omega_{\max}$. This can be achieved by choosing a boundary layer ϵ_c as:

$$\epsilon_c = \frac{\varphi}{\omega_{\max} - \zeta}. \tag{3.3.21}$$

It is desired to keep ϵ_c as small as possible for tracking precision. However, for a given the bandwidth bound $\omega_{\max}$, it can easily shown from equation (3.3.21) that when φ increases due to the increase of perturbations, so does ϵ_c. Therefore, this choice of ϵ_c introduces a trade-off between robustness and tracking accuracy. Note that the actual S_{smcpo} variations are expected to be limited to a small fraction of the boundary layer thickness ϵ_c due to the conservative selections of φ.

Design of sliding mode controller with perturbation observer

As shown in equation (3.3.17), the upper bound on the perturbation is employed to decide the control gain. The resulting gain is conservative and high for practical applications. In fact, most often the worst conditions in which the perturbation takes its upper bound does not occur. Therefore, this conservative control is not necessary. In this section, the perturbation estimation is utilized to design the sliding mode control and a low and reasonable control gain will be obtained. It should be pointed out that, when SMPO is used to estimate the perturbation, the upper bound of the derivative of perturbation is required to guarantee the estimation accuracy. And such a upper bound will cause a conservative observer gain. However, the conservative gain is only included in the observer-loop, not in the controller loop. Such properties will be illustrated as follows.

Using the estimated perturbation, a sliding mode control law is designed as

$$u = \frac{1}{b_0}\left[y_d^{(n)} - \sum_{i=1}^{n-1}\rho_i(x_{i+1} - y_d^{(i)}) - \zeta S_{\text{smcpo}} - \varphi\ \text{sgn}(S_{\text{smcpo}}) - \hat{\Psi}(\cdot)\right], \tag{3.3.22}$$

where $\hat{\Psi}(\cdot) = \hat{x}_{n+1}$ is obtained from sliding mode track-differentiator (3.3.1).

The corresponding S_{smcpo} dynamics are:

$$\dot{S}_{\text{smcpo}} = -\zeta S_{\text{smcpo}} - \varphi\ \text{sgn}(S_{\text{smcpo}}) + \tilde{\Psi}(\cdot). \tag{3.3.23}$$

where $\tilde{\Psi}(\cdot) = \Psi(\cdot) - \hat{\Psi}(\cdot)$ is the estimation error in the perturbation. Therefore, the attractive condition is

$$\zeta\,|S_{\text{smcpo}}| + \varphi > |\tilde{\Psi}(\cdot)|_{\max}. \tag{3.3.24}$$

The above condition is obviously satisfied if the gain φ is chosen as

$$\varphi \geq |\tilde{\Psi}(\cdot)|_{\max}.$$

Considering $k_1 \geq |\tilde{\Psi}(\cdot)|_{\max}$, we have

$$\varphi \geq k_1. \tag{3.3.25}$$

Note that in comparison with the conservative control gain in equation (3.3.17), φ is rather small. This reduction is because of the driving term of the S_{smcpo} dynamics decreasing from upper bound of the perturbation $\Psi(\cdot)$ to its estimation error $\tilde{\Psi}(\cdot)$.

Using the saturation function $\text{sat}(\xi, \epsilon_c)$ to smooth the signum function $\text{sgn}(\xi)$, the dynamics of S_{smcpo} in the boundary layer act as

$$\dot{S}_{\text{smcpo}} + (\zeta + \frac{\varphi}{\epsilon_c}) S_{\text{smcpo}} = \tilde{\Psi}(\cdot). \tag{3.3.26}$$

The sliding mode dynamics is similar to equation (3.3.19) except for a much smaller driving term. Thus, smaller boundary thickness ϵ_c is obtained for the same break frequency bound ω_{max}. Moreover, the desired low-pass filter behaviour of S_{smcpo} is obtained by limiting its maximum break frequency to ω_{max}, which can be designed by choosing the boundary layer thickness as:

$$\epsilon_c = \frac{\varphi}{\omega_{\text{max}} - \zeta}. \tag{3.3.27}$$

It can be seen that, for the same break frequency frequency ω_{max}, the boundary layer thickness in equation (3.3.27) is much smaller than SMC application in equation (3.3.21) as φ becomes smaller. Thus a better tracking performance results. An identical trade-off between robustness and the tracking accuracy appears again.

3.4 Sliding mode state and perturbation observer

In this section, only one state of the system, x_1, is measurable and a Sliding Mode State and Perturbation Observer (SMSPO) is designed. The design of a Sliding Mode State Observer(SMSO) is presented for comparison. The SMSPO is employed to design two kinds of controller. One is a sliding mode controller

with output feedback and perturbation compensation. The other is an adaptive output feedback linearization controller which uses the estimated perturbation to cancel system nonlinearities and disturbances and the estimated states to design a linear output feedback control law for the equivalent linear system.

3.4.1 Design of a sliding mode state and perturbation observer

Taking x_1 as the measured system output, a sliding mode observer for system (3.2.5) is designed as follows:

$$\begin{cases} \dot{\hat{x}}_1 &= \hat{x}_2 + \alpha_1 \tilde{x}_1 + k_1 \operatorname{sgn}(\tilde{x}_1) \\ &\vdots \\ \dot{\hat{x}}_n &= \hat{x}_{n+1} + \alpha_n \tilde{x}_1 + k_n \operatorname{sgn}(\tilde{x}_1) + b_0 u \\ \dot{\hat{x}}_{n+1} &= \alpha_{n+1} \tilde{x}_1 + k_{n+1} \operatorname{sgn}(\tilde{x}_1), \end{cases} \tag{3.4.1}$$

where $\tilde{x}_1 = x_1 - \hat{x}_1$, k_i and α_i, $i = 1, \cdots, n+1$, are positive coefficients. The estimate and estimation error of the state vector are defined as $\hat{x}_e = \begin{bmatrix} \hat{x}_1 & \hat{x}_2 & \cdots & \hat{x}_n & \hat{x}_{n+1} \end{bmatrix}^T$ and $\tilde{x}_e = x_e - \hat{x}_e = \begin{bmatrix} \tilde{x}_1 & \tilde{x}_2 & \cdots & \tilde{x}_n & \tilde{x}_{n+1} \end{bmatrix}^T$, respectively.

The constants α_i are chosen as in a Luenberger observer (which corresponds to $k_i = 0$, $i = 1, \cdots, n+1$) so as to place the poles of the Luenberger observer at desired locations in the open left plane of the complex plane.

From equations (3.2.5) and (3.4.1), the error dynamics of the observer can be obtained as:

$$\begin{cases} \dot{\tilde{x}}_1 &= \tilde{x}_2 - \alpha_1 \tilde{x}_1 - k_1 \operatorname{sgn}(\tilde{x}_1) \\ &\vdots \\ \dot{\tilde{x}}_n &= \tilde{x}_{n+1} - \alpha_n \tilde{x}_1 - k_n \operatorname{sgn}(\tilde{x}_1) \\ \dot{\tilde{x}}_{n+1} &= -\alpha_{n+1} \tilde{x}_1 - k_{n+1} \operatorname{sgn}(\tilde{x}_1) + \dot{\Psi}. \end{cases} \tag{3.4.2}$$

The sliding surface is defined as $S_{\text{spo}}(\tilde{x}) = \tilde{x}_1 = 0$. Introducing the function $V_{\text{spo}} = \frac{1}{2} S_{\text{spo}}^2$, the sliding surface is attractive if $\dot{V}_{\text{spo}} < 0$ for $\tilde{x} \notin S_{\text{spo}}$. The

condition for the existence of sliding mode is:

$$\begin{cases} \tilde{x}_2 \leq k_1 + \alpha_1 \tilde{x}_1, & \text{if } \tilde{x}_1 > 0; \\ \tilde{x}_2 \geq -k_1 + \alpha_1 \tilde{x}_1, & \text{if } \tilde{x}_1 < 0. \end{cases} \tag{3.4.3}$$

Such a condition can be guaranteed by choosing k_1 as:

$$k_1 \geq \mid \tilde{x}_2 \mid_{\max} . \tag{3.4.4}$$

It can be seen that the choice of gain k_1 depends upon the estimation error of $\tilde{x}_2$. Under the above condition, it is guaranteed that the system will enter into the sliding surface at $t > t_s$ and thereafter remain $S_{\text{spo}} = 0$, $\forall t \geq t_s$. Actually, the dynamic of observer can start in the sliding mode, if $\hat{x}_1(t = 0)$ can be taken as $x_1(t = 0)$.

It follows that the switch function satisfies $S_{\text{spo}}(\tilde{x}) = 0$, $\forall t > t_s$, which in turn implies that $\dot{S}_{\text{spo}}(\tilde{x}) = 0$, $\forall t \geq t_s$. Thus, from the first equation of (3.4.2), the equivalent control which maintains the sliding mode motion on $S_{\text{spo}}(\tilde{x}) = 0$ is

$$u_{\text{eq}} = \frac{1}{k_1} \tilde{x}_2. \tag{3.4.5}$$

Substituting $\text{sgn}(\tilde{x}_n)$ term in system (3.4.2) with equivalent control (3.4.5), the resulting error dynamics on the sliding mode take the form :

$$\begin{cases} \dot{\tilde{x}}_2 &= -\frac{k_2}{k_1} \tilde{x}_2 + \tilde{x}_3 \\ \dot{\tilde{x}}_3 &= -\frac{k_3}{k_1} \tilde{x}_2 + \tilde{x}_4 \\ &\vdots \\ \dot{\tilde{x}}_n &= -\frac{k_n}{k_1} \tilde{x}_2 + \tilde{x}_n \\ \dot{\tilde{x}}_{n+1} &= -\frac{k_{n+1}}{k_1} \tilde{x}_2 + \dot{\Psi}(\cdot), \end{cases} \tag{3.4.6}$$

or

$$\dot{\tilde{x}}_{e1} = A_1 \tilde{x}_{e1} + B_1 \dot{\Psi}, \tag{3.4.7}$$

where $\tilde{x}_{e1} = \begin{bmatrix} \tilde{x}_2 & \cdots & \tilde{x}_{n+1} \end{bmatrix}^T$, and $n \times n$ matrix A_1 and $n \times 1$ matrix B_1

$$A_1 = \begin{bmatrix} -\frac{k_2}{k_1} & 1 & \cdots & \cdots & 0 \\ -\frac{k_3}{k_1} & 0 & 1 & \cdots & 0 \\ \vdots & & & & \vdots \\ -\frac{k_n}{k_1} & 0 & 0 & \cdots & 1 \\ -\frac{k_{n+1}}{k_1} & 0 & 0 & \cdots & 0 \end{bmatrix}, \qquad B_1 = \begin{bmatrix} 0 \\ \vdots \\ 0 \\ 1 \end{bmatrix}.$$

The following theorem states the observer convergence.

Theorem 3.1. *Consider system (3.2.5), and design a sliding mode state and perturbation observer (3.4.1). If assumption A3.2 holds for some value γ_2, then given any constant δ, the gains k_1, k_2, $\cdots$, k_n and k_{n+1} can be chosen such that, from an initial estimation error $\tilde{x}_e(0)$, the observer error $\tilde{x}_e$ converges exponentially into the neighborhood*

$$\|\tilde{x}_e\| \leq \delta.$$

Proof: Assume that a value of k_1 is taken such that the sliding condition (3.4.4) holds for all t. Then the observer stays in the sliding surface $\tilde{x}_1 = 0$, $\dot{\tilde{x}}_1 = 0$. Applying the equivalent dynamics of the discontinues term during the sliding mode, the observation error during sliding is reduced to system (3.4.7). Now, define the gains k_i, $i = 2, 3, \cdots, n+1$, as

$$p^n + \frac{k_2}{k_1}p^{n-1} + \cdots + \frac{k_n}{k_1}p + \frac{k_{n+1}}{k_1} = (p+\lambda)^n \tag{3.4.8}$$

for a positive constant λ. Thus we have

$$\frac{k_{i+1}}{k_1} = C_n^i \lambda^i, \qquad i = 1, 2, \cdots, n, \tag{3.4.9}$$

where $C_n^i = \frac{n!}{i!(n-i)!}$. This means that all eigenvalues of the matrix A_1 are chosen as $-\lambda$.

Define the state transformation as

$$\tilde{x}_i = \lambda^{i-2} z_i, \qquad i = 2, \cdots, n+1. \tag{3.4.10}$$

Then, equation (3.4.7) can be written in terms of z as

$$\dot{z} = \lambda M z + B_1 \frac{\dot{\Psi}}{\lambda^{n-1}}, \tag{3.4.11}$$

where $z = \begin{bmatrix} z_2 & \cdots & z_{n+1} \end{bmatrix}^T$, and $n \times n$ matrix M

$$M = \begin{bmatrix} -C_n^1 & 1 & \cdots & \cdots & 0 \\ -C_n^2 & 0 & 1 & \cdots & 0 \\ \vdots & & & & \vdots \\ -C_n^{n-1} & 0 & 0 & \cdots & 1 \\ -C_n^n & 0 & 0 & \cdots & 0 \end{bmatrix}.$$

Define the Lyapunov function

$$W_1 = \frac{1}{\lambda} z^T P_1 z, \tag{3.4.12}$$

where P_1 is the positive definite solution of the Lyapunov equation $P_1 M + M^T P_1 = -I$. Differentiating W_1 along system (3.4.11) one obtains

$$\dot{W}_1 = -\|z\|^2 + 2z^T \frac{P_1}{\lambda} B_1 \frac{\dot{\Psi}(\cdot)}{\lambda^{n-1}}, \tag{3.4.13}$$

that, using the assumption A3.2, can be rewritten as

$$\dot{W}_1 \leq -\|z\|^2 + 2\lambda_{\max}(P_1)\|z\|\gamma_2/\lambda^n. \tag{3.4.14}$$

Take a value α, $0 < \alpha < 1$, it is easy to show that

$$\dot{W}_1 \leq -\alpha\|z\|^2 \tag{3.4.15}$$

if

$$\|z\| \geq \delta_z, \tag{3.4.16}$$

where $\delta_z = \frac{2\lambda_{\max}(P_1)\gamma_2}{(1-\alpha)\lambda^n}$ is a positive constant. As $\lambda_{\min}(P_1)\|z\|^2 \leq W_1(z) \leq \lambda_{\max}(P_1)\|z\|^2$, applying Corollary 5.3 of Theorem 5.1 of Khalil[4], one can conclude that if $\|z(0)\| \geq \delta_z$, there $\exists\, t_1$, $t_1 > 0$, such that

$$\|z(t)\| \leq \sqrt{\frac{\lambda_{\max}(P_1)}{\lambda_{\min}(P_1)}}\|z(0)\|e^{-\alpha/(2\lambda_{\max}(P_1))t}, \qquad \forall t < t_1 \tag{3.4.17}$$

and

$$\|z(t)\| \leq \sqrt{\frac{\lambda_{\max}(P_1)}{\lambda_{\min}(P_1)}}\delta_z, \qquad \forall t \geq t_1 \tag{3.4.18}$$

where

$$t_1 \leq \frac{2\lambda_{\max}(P_1)}{\alpha} \log\left(\frac{\|z\|}{\delta_z}\right). \tag{3.4.19}$$

As λ is always assumed to be larger than 1, we can observe from equation (3.4.10) that

$$\|z\| \leq \|\tilde{x}_{e1}\| \leq \lambda^{n-1}\|z\|.$$

Thus the previous expressions can be written in terms of $\tilde{x}_{e2}$ as

$$\|\tilde{x}_{e1}(t)\| \leq \lambda^{n-1}\sqrt{\frac{\lambda_{\max}(P_1)}{\lambda_{\min}(P_1)}}\|\tilde{x}_{e1}(0)\|e^{-\frac{\alpha}{2\lambda_{\max}(P_1)}t}, \qquad \forall t < t_1; \tag{3.4.20}$$

$$\|\tilde{x}_{e1}(t)\| \leq \lambda^{n-1}\sqrt{\frac{\lambda_{\max}(P_1)}{\lambda_{\min}(P_1)}}\delta_z, \qquad \forall t \geq t_1; \tag{3.4.21}$$

$$t_1 \leq \frac{2\lambda_{\max}(P_1)}{\alpha} \log\left(\frac{\|\tilde{x}_{e1}(0)\|}{\delta_z}\right). \tag{3.4.22}$$

Therefore, for a given positive constant δ, we can take λ such that

$$\begin{aligned} \delta &\geq \lambda^{n-1}\sqrt{\frac{\lambda_{\max}(P_1)}{\lambda_{\min}(P_1)}}\delta_z \\ &= \sqrt{\frac{\lambda_{\max}(P_1)}{\lambda_{\min}(P_1)}}\frac{2\lambda_{\max}(P_1)\gamma_2}{(1-\alpha)\lambda}. \end{aligned} \tag{3.4.23}$$

is satisfied. This will guarantee the exponential convergence of the observation error into

$$\|\tilde{x}_{e1}\| \leq \delta, \quad \forall t > t_1.$$

To complete the proof, it is necessary to show that gain k_1 can be chosen such that sliding condition (3.4.3) holds for all $t > 0$. It is obvious that

$$\begin{aligned} |\tilde{x}_2| &= |z_2| \leq \|z\| \\ &\leq \sqrt{\frac{\lambda_{\max}(P_1)}{\lambda_{\min}(P_1)}}\|z(0)\| \\ &\leq \sqrt{\frac{\lambda_{\max}(P_1)}{\lambda_{\min}(P_1)}}\|\tilde{x}_{e1}(0)\|, \qquad \forall t > 0. \end{aligned} \tag{3.4.24}$$

Therefore, for a given value of initial estimation error $\|\tilde{x}(0)\|$, the sliding condition will be fulfilled for all t if gain k_1 is chosen as

$$k_1 \geq \|\tilde{x}_{e1}(0)\|\sqrt{\frac{\lambda_{\max}(P_1)}{\lambda_{\min}(P_1)}}. \tag{3.4.25}$$

□

Remark 3.4.1 From the previous theorem we can also obtain bounds for the observer state errors $\tilde{x}_i$, $i = 2, \cdots, n, n+1$. From equations (3.4.3) and (3.4.18), it is obvious that

$$\begin{aligned} |\tilde{x}_i| &\leq \lambda^{i-2}\|z\| \\ &\leq \lambda^{i-2}\sqrt{\frac{\lambda_{\max}(P_1)}{\lambda_{\min}(P_1)}}\delta_z \leq \frac{\delta}{\lambda^{n+1-i}}, \quad i = 2, \cdots, n+1, \ \forall t > t_1. \end{aligned} \tag{3.4.26}$$

Remark 3.4.2 The choice of the observer gains cab be summarized as follows. α_i, $i = 1, 2, \cdots, n+1$ are chosen to make all poles of the Luenberger observer be real and equal to $-\xi$. Thus we have

$$\alpha_i = C_{n+1}^i \xi^i, \qquad i = 1, 2, \cdots, n+1, \tag{3.4.27}$$

where $C_{n+1}^i = \frac{(n+1)!}{i!*(n+1-i)!}$.

k_i, $i = 1, 2, \cdots, n+1$ are chosen as follows: k_1 is chosen according to equation (3.4.25); for a given small positive constant δ, from equation (3.4.23), we can obtain that λ must satisfy

$$\lambda \geq \sqrt{\frac{\lambda_{\max}(P_1)}{\lambda_{\min}(P_1)}}\frac{2\lambda_{\max}(P_1)\gamma_2}{(1-\alpha)\delta}. \tag{3.4.28}$$

Thus, from equations (3.4.9) and (3.4.25), we have

$$k_i \geq k_1 C_n^{i-1}\lambda^{i-1}, \qquad i = 2, \cdots, n+1. \tag{3.4.29}$$

Remark 3.4.3 In the above analysis, only the upper bound of the derivative of the perturbation is used. This may be reasonable when the control input is

bounded in a real system. However, when a complete observer and controller system is investigated, the more reasonable and strict assumption is to include the controller definition in the assumption. If the Lipschitiz condition in assumption A3.2 is considered, a error convergence to the origin will be resulted in.

Remark 3.4.4 A saturation function $\text{sat}(\chi, \epsilon_o)$ is used to replace the discontinuous function $\text{sgn}(\chi)$ so as to avoid the chatter of observer output. When the sliding condition (3.4.4) is satisfied, the observer will be guaranteed to enter the boundary layer $|\tilde{x}_1| \leq \epsilon_o$ for any initial condition $x_1(0)$. After replacing $\text{sgn}(\tilde{x}_1)$ with $\text{sat}(\tilde{x}_1, \epsilon_o)$, the error dynamics (3.4.2) becomes

$$\begin{cases} \dot{\tilde{x}}_1 &= \tilde{x}_2 - (\alpha_1 + \frac{k_1}{\epsilon_o})\tilde{x}_1 \\ &\vdots \\ \dot{\tilde{x}}_n &= \tilde{x}_{n+1} - (\alpha_n + \frac{k_n}{\epsilon_o})\tilde{x}_1 \\ \dot{\tilde{x}}_{n+1} &= -(\alpha_{n+1} - \frac{k_{n+1}}{\epsilon_o})\tilde{x}_1 + \dot{\Psi}. \end{cases} \tag{3.4.30}$$

The above error dynamics on boundary layer can be analyzed by using the same method for a high gain observer presented in Theorem 2.2. It is easy to show that after the system states enter the boundary layer $|\tilde{x}_1| \leq \epsilon_o$, $\tilde{x}_1$ will converge exponentially to a neighborhood of origin after a limited time period and remain in the boundary layer with the chosen gains k_i and α_i, $i = 1, \ldots, n+1$.

3.4.2 Design of a sliding mode state observer

For comparison with SMSPO, a sliding mode state observer (SMSO) for the nonlinear system (3.2.1) is designed with the output $y = x_1$. SMSO can be designed and analyzed by using the same method as SMSPO. The same subscripts is used for the convenience of presentation. In fact, SMSPO can be regarded as an extended-order conventional SMSO. It can estimate not only the system states, but also the perturbation term which is represented by the

fictitious state. However, the estimation error of the perturbation is critical to the accuracy of state estimation in SMSPO, as opposed to the upper bounds of the perturbation itself in SMSO. Consequently, the driving term of the error dynamics are reduced from the perturbation $\Psi(\cdot)$ in a SMSO to its estimation error $\tilde{\Psi}(\cdot)$ in a SMSPO. Hence, SMSPO will provide a better accuracy of state estimation. The signum function can also replaced by the saturation function to smooth the observer output. The results are briefly given as follows:

Sliding mode state observer

$$\begin{cases} \dot{\hat{x}}_1 &= \hat{x}_2 + \alpha_1 \tilde{x}_1 + k_1 \operatorname{sgn}(\tilde{x}_1) \\ &\cdots \\ \dot{\hat{x}}_n &= \alpha_n \tilde{x}_1 + k_n \operatorname{sgn}(\tilde{x}_1) + b_0 u. \end{cases} \tag{3.4.31}$$

Equations of error dynamics

$$\begin{cases} \dot{\tilde{x}}_1 &= \tilde{x}_2 - \alpha_1 \tilde{x}_1 - k_1 \operatorname{sgn}(\tilde{x}_1) \\ &\vdots \\ \dot{\tilde{x}}_n &= -\alpha_n \tilde{x}_1 - k_n \operatorname{sgn}(\tilde{x}_1) + \Psi. \end{cases} \tag{3.4.32}$$

Equations of reduced-order dynamics on sliding mode

$$\begin{cases} \dot{\tilde{x}}_2 &= -\frac{k_2}{k_1}\tilde{x}_2 + \tilde{x}_3 \\ \dot{\tilde{x}}_3 &= -\frac{k_3}{k_1}\tilde{x}_2 + \tilde{x}_4 \\ &\vdots \\ \dot{\tilde{x}}_n &= -\frac{k_n}{k_1}\tilde{x}_2 + \Psi(\cdot) \end{cases} \tag{3.4.33}$$

or

$$\dot{\tilde{x}}_{e2} = A_2 \tilde{x}_{e2} + B_2 \dot{\Psi}, \tag{3.4.34}$$

where $\tilde{x}_{e2} = \begin{bmatrix} \tilde{x}_2 & \cdots & \tilde{x}_n \end{bmatrix}^T$, and $(n-1) \times (n-1)$ matrix A_2 and $(n-1) \times 1$

matrix B_2 are

$$A_2 = \begin{bmatrix} -\frac{k_2}{k_1} & 1 & \cdots & \cdots & 0 \\ -\frac{k_3}{k_1} & 0 & 1 & \cdots & 0 \\ \vdots & & & & \vdots \\ -\frac{k_{n-1}}{k_1} & 0 & 0 & \cdots & 1 \\ -\frac{k_n}{k_1} & 0 & 0 & \cdots & 0 \end{bmatrix}, \qquad B_2 = \begin{bmatrix} 0 \\ \vdots \\ 0 \\ 1 \end{bmatrix}.$$

3.4.3 Design of combined sliding mode controller-observer

By using the estimated system states, a sliding function is defined:

$$\hat{S}_{\text{smcspo}} = \sum_{i=1}^{n} \rho_i (\hat{x}_i - y_d^{(i-1)}), \tag{3.4.35}$$

where $\rho_n = 1$, and ρ_i, $i = 1, \cdots, n$ are gains for a stable polynomial. As the true states are not available, the sliding surface depends on the estimated states. The actual sliding function is

$$S_{\text{smcspo}} = \sum_{i=1}^{n} \rho_i (x_i - y_d^{(i-1)}), \tag{3.4.36}$$

and the estimation error of the sliding function is

$$\tilde{S}_{\text{smcspo}} = S_{\text{smcspo}} - \hat{S}_{\text{smcspo}} = \sum_{i=1}^{n} \rho_i \tilde{x}_i. \tag{3.4.37}$$

The control u is chosen to enforce $\dot{\hat{S}}_{\text{smcspo}} \hat{S}_{\text{smcspo}} < 0$ outside a prescribed manifold $|\hat{S}_{\text{smcspo}}| < \epsilon_c$. A desired dynamic of $\hat{S}_{\text{smcspo}}$ is selected as

$$\dot{\hat{S}}_{\text{smcspo}} = -\zeta \hat{S}_{\text{smcspo}} - \varphi \ \text{sat}(\hat{S}_{\text{smcspo}}, \epsilon_c), \tag{3.4.38}$$

where ζ and φ are control gains, $\text{sat}(\hat{S}_{\text{smcspo}}, \epsilon_c)$ is a saturation function defined as equation (3.3.8) and used to eliminate the control chatter. In this equation, ϵ_c represents for the boundary layer thickness of sliding mode controller, as contrasted with the ϵ_o in sliding mode observer. To illustrate the advantages of SMSPO over SMSO, two sliding mode controllers are designed with SMSO and SMSPO, respectively.

Controller design via sliding mode state and perturbation observer

By using the estimated perturbation term $\hat{x}_{n+1}$ to cancel the system nonlinearities and uncertainties, the sliding mode controller is constructed as:

$$u = \frac{1}{b_0}\left[y_d^{(n)} - \hat{x}_{n+1} - \sum_{i=1}^{n-1}\rho_i(\hat{x}_{i+1} - y_d^{(i)}) - \zeta\hat{S}_{\text{smcspo}} - \varphi\ \text{sat}(\hat{S}_{\text{smcspo}}, \epsilon_c)\right]. \tag{3.4.39}$$

Differentiating equation (3.4.35) along system (3.4.1), and using the reduced error dynamics (3.4.6), one obtains

$$\dot{\hat{S}}_{\text{smcspo}} = \hat{x}_{n+1} + b_0 u + \frac{k_n}{k_1}\tilde{x}_2 - y_d^{(n)} + \sum_{i=1}^{n-1}\rho_i(\hat{x}_{i+1} - y_d^{(i)} + \frac{k_i}{k_1}\tilde{x}_2), \tag{3.4.40}$$

that, substituting u with control (3.4.39), leads to

$$\dot{\hat{S}}_{\text{smcspo}} = \sum_{i=1}^{n}\rho_i\frac{k_i}{k_1}\tilde{x}_2 - \zeta\hat{S}_{\text{smcspo}} - \varphi\ \text{sat}(\hat{S}_{\text{smcspo}}, \epsilon_c). \tag{3.4.41}$$

Therefore, the attractiveness condition of sliding function is

$$\zeta\left|\hat{S}_{\text{smcspo}}\right| + \varphi > \sum_{i=1}^{n}\rho_i\frac{k_i}{k_1}|\tilde{x}_2|, \tag{3.4.42}$$

which, using $k_1 > |\tilde{x}_2|_{\max}$ in equation (3.4.4), will be fulfilled if

$$\zeta\left|\hat{S}_{\text{smcspo}}\right| + \varphi > k_1\sum_{i=1}^{n}\rho_i\frac{k_i}{k_1}. \tag{3.4.43}$$

The above condition is obviously satisfied if gain φ is chosen as

$$\varphi > k_1\sum_{i=1}^{n}\rho_i\frac{k_i}{k_1}, \tag{3.4.44}$$

which, using equation (3.4.9), leads to

$$\varphi \geq k_1\sum_{i=1}^{n}\rho_i C_n^{(i-1)}\lambda^{(i-1)}. \tag{3.4.45}$$

This condition guarantees the existence of a sliding mode on the boundary layer $|\hat{S}_{\text{smcspo}}| \leq \epsilon_c$. From equation (3.4.37), we can obtain

$$\dot{\tilde{S}}_{\text{smcspo}} = \sum_{i=1}^{n-1}\rho_i\tilde{x}_{i+1} - \sum_{i=1}^{n}\rho_i\frac{k_i}{k_1}\tilde{x}_2 + \tilde{x}_{n+1}. \tag{3.4.46}$$

Using $\hat{S}_{\text{smcspo}} = S_{\text{smcspo}} - \tilde{S}_{\text{smcspo}}$ and equation (3.4.41), the actual S_{smcspo}-dynamics becomes

$$\dot{S}_{\text{smcpo}} + (\zeta + \frac{\varphi}{\epsilon_c})S_{\text{smcpo}} = (\zeta + \frac{\varphi}{\epsilon_c})\sum_{i=1}^{n}\rho_i\tilde{x}_i + \sum_{i=1}^{n-1}\rho_i\tilde{x}_{i+1} + \tilde{x}_{n+1}. \qquad (3.4.47)$$

As it can be seen, the driving term of S_{smcspo}-dynamics are the sum of the estimation errors of states and the estimation error of perturbation. From the bound of sliding surface $|S_{\text{smcspo}}| \leq \epsilon_c$, the bounds of the states tracking error can be obtained as follows:

$$\begin{aligned} |\hat{S}_{\text{smcspo}}| \leq \epsilon_c \;&\Rightarrow\; |S_{\text{smcspo}} - \tilde{S}_{\text{smcspo}}| \leq \epsilon_c \\ &\Rightarrow\; |S_{\text{smcspo}}| \leq |\tilde{S}_{\text{smcspo}}| + \epsilon_c \\ &\Rightarrow\; |S_{\text{smcspo}}| \leq |\textstyle\sum_{i=1}^{n}\rho_i\tilde{x}_i| + \epsilon_c \\ &\leq \tfrac{\delta}{\lambda^{n+1}}\textstyle\sum_{i=2}^{n}\rho_i\lambda^i + \epsilon_c, \qquad \forall t > t_1, \end{aligned} \qquad (3.4.48)$$

where t_1 is the time constant defined in equation (3.4.22). If the polynomial gains ρ_i are chosen as in equation (3.3.11), which make all poles of polynomial equal to $-\lambda_c$, thus, from equation (3.3.13), we have

$$\left|x^{(i)}(t) - x_d^{(i)}(t)\right| \leq (2\lambda_c)^i\frac{\epsilon_c}{\lambda_c^n} + \frac{\delta}{\lambda^{n+1}}\sum_{j=2}^{n}(\frac{\lambda}{\lambda_c})^j C_{n-1}^j, \quad i = 0, 1, \cdots, n-1. \qquad (3.4.49)$$

The previous analysis can be summarized as following theorem.

Theorem 3.2. *Consider system (3.2.1), and let assumptions A3.1 $\sim$ A3.3 hold. Design observer (3.4.1), with gains chosen from equations (3.4.27) to (3.4.29). Let δ be any arbitrary positive constant. Define the controller as equation (3.4.39) and the gains φ and ζ are chosen according to equation (3.4.45). Then the state tracking error will satisfy equation (3.4.49) after a short period of time t_1.*

Controller design via sliding mode state observer

For comparison, a sliding mode controller is designed based on a SMSO with system output $y = x_1$. To obtain desired dynamics described in equation

(3.4.38), a sliding mode controller is designed as

$$u = \frac{1}{b_0}\left[y_d^{(n)} - \sum_{i=1}^{n-1}\rho_i(\hat{x}_{i+1} - y_d^{(i)}) - \zeta\hat{S}_{\text{smcspo}} - \varphi\ \text{sat}(\hat{S}_{\text{smcspo}})\right]. \tag{3.4.50}$$

Differentiating equation (3.4.35) along system (3.4.31) , and using system (3.4.33), one obtains

$$\begin{aligned}\dot{\hat{S}}_{\text{smcspo}} &= \textstyle\sum_{i=1}^{n}\rho_i(\dot{\hat{x}}_i - y_d^{(i-1)}) \\ &= -y_d^{(n)} + \textstyle\sum_{i=1}^{n-1}\rho_i(\hat{x}_{i+1} - y_d^{(i)}) + \sum_{i=1}^{n}\frac{\rho_i k_i}{k_1}\tilde{x}_2 + b_0 u.\end{aligned} \tag{3.4.51}$$

Then the corresponding sliding surface dynamic under control (3.4.50) is

$$\dot{\hat{S}}_{\text{smcspo}} = \sum_{i=1}^{n}\rho_i\frac{k_i}{k_1}\tilde{x}_2 - \zeta\hat{S}_{\text{smcspo}} - \varphi\ \text{sat}(\hat{S}_{\text{smcspo}}). \tag{3.4.52}$$

Therefore, the attractiveness condition

$$\zeta\left|\hat{S}_{\text{smcspo}}\right| + \varphi > \left|\sum_{i=1}^{n}\rho_i\frac{k_i}{k_1}\right||\tilde{x}_2|, \tag{3.4.53}$$

can be fulfilled by choosing gain φ as

$$\varphi \geq k_1\sum_{i=1}^{n}\rho_i\frac{k_i}{k_1} \geq k_1\sum_{i=1}^{n}\rho_i C_{n-1}^{i-1}\lambda^{i-1}, \tag{3.4.54}$$

where $-\lambda$ is the poles of SMSO. And $k_1 \geq |\tilde{x}_2|_{\max}$ guarantees the existence of sliding mode in SMSO. Condition (3.4.54) will ensure the existence of sliding mode within the boundary layer $|\hat{S}_{\text{smcspo}}| \leq \epsilon_c$. From equations (3.4.37) and (3.4.33), we can obtain

$$\dot{\hat{S}}_{\text{smcspo}} = \sum_{i=1}^{n-1}\rho_i\tilde{x}_{i+1} - \sum_{i=1}^{n}\rho_i\frac{k_i}{k_1}\tilde{x}_2 + \Psi(\cdot). \tag{3.4.55}$$

Using $\hat{S}_{\text{smcspo}} = S_{\text{smcspo}} - \tilde{S}_{\text{smcspo}}$ and equation (3.4.41), the actual S_{smcspo}-dynamics becomes

$$\dot{S}_{\text{smcspo}} + (\zeta + \frac{\varphi}{\epsilon_c})S_{\text{smcspo}} = (\zeta + \frac{\varphi}{\epsilon_c})\sum_{i=1}^{n}\rho_i\tilde{x}_i + \sum_{i=1}^{n-1}\rho_i\tilde{x}_{i+1} + \Psi(\cdot). \tag{3.4.56}$$

From equations (3.4.56) and (3.4.47), it can be seen that the driving term of S_{smcspo}-dynamics in SMCSO are the estimation errors of states plus the perturbation itself, as contrasted with the estimation errors of states and the estimation error of perturbation in SMCSPO. This will result in the SMCSPO having better tracking performance than SMCSO.

3.4.4 Nonlinear adaptive control using continuous output feedback and SMSPO

In this section, a nonlinear adaptive control is designed by using continuous output feedback control and a SMSPO. The estimate of perturbation $\hat{x}_{n+1}$ is used to cancel the system nonlinearities and uncertainties so as to achieve the linearization of the original nonlinear system without requiring the detail system model. Utilizing the estimated states instead of the real ones, a linear feedback controller is designed for the equivalent linearized system. The controller is defined as:

$$u = v/b_0 - \hat{x}_{n+1}/b_0 \tag{3.4.57}$$

$$v = -K\hat{x}, \tag{3.4.58}$$

where $K = [k_1, k_2, \cdots, k_n]^T$ is the linear feedback controller gains, which make the matrix $A_0 = A - BK$ is Hurwitzian.

If attractive condition (3.4.4) is satisfied, the SMSPO will reach the sliding surface, that is $\tilde{x}_1 = 0$ and $\dot{\tilde{x}}_1 = 0$. Noting that $\hat{x}_{e1} = [\hat{x}_2, \cdots, \hat{x}_{n+1}]^T$, control (3.4.57) and (3.4.58) can be represented as:

$$u = \frac{1}{b_0}(-x_{n+1} - Kx + K_1\tilde{x}_{e1}), \tag{3.4.59}$$

where $K_1 = [k_2 \ \cdots \ k_n, \ 1]^T$.

Substituting control (3.4.59) into system (3.2.1), and using the state vari-

ables transformation (3.4.10), the closed-loop system can be represented by

$$\dot{x} = A_0 x + BK_1 z, \tag{3.4.60}$$

$$\dot{z} = \lambda M z + B_1 \frac{\dot{\Psi}(\cdot)}{\lambda^{n-1}}. \tag{3.4.61}$$

The stability result of closed-loop system (3.4.60) and (3.4.61) is represented by following theorem. To make the whole control system be exponentially stable, the function $\Psi(x,u,t)$ and $\dot{\Psi}(x,u,t)$ satisfy following assumption.

A3.4 The function $\Psi(x,u,t) : \mathcal{R}^n \times \mathcal{R} \times \mathcal{R}^+ \to \mathcal{R}$ and $\dot{\Psi}(x,u,t) : \mathcal{R}^n \times \mathcal{R} \times \mathcal{R}^+ \to \mathcal{R}$ are locally Lipschitz in their arguments over the domain of interest. In addition, $\Psi(0,0,0) = 0$ and $\dot{\Psi}(0,0,0) = 0$.

Theorem 3.3. *Consider system (3.2.1) and sliding mode state and perturbation observer (3.4.1), choose the observer gain given in equations (3.4.27) to (3.4.29), and let assumptions A3.1 ~ A3.4 hold. Define the control as that given by equations (3.4.57) and (3.4.58), then the origin of system (3.4.60) and (3.4.61) is exponentially stable.*

Proof: For system (3.4.60), we define the same Lyapunov function as

$$V_0(x) = x^T P_0 x \tag{3.4.62}$$

over a ball $B(0,r) \subset \mathcal{R}$, for some $r > 0$, and P_0 is the positive definite solution of the Lyapunov equation $P_0 A_0 + A_0^T P_0 = -I$. $\forall\ x \in B(0,r)$, we have

$$\lambda_{\min}(P_0)\|x\|^2 \le V_0(x) \le \lambda_{\max}(P_0)\|x\|^2, \tag{3.4.63}$$

$$\frac{\partial V_0}{\partial x} A_0 x \le -\|x\|^2, \tag{3.4.64}$$

$$\|\frac{\partial V_0}{\partial x}\| \le 2\lambda_{\max}(P_0)\|x\|. \tag{3.4.65}$$

For system (3.4.61), we define the same Lyapunov function $W_1(z)$ as equation (3.4.12).

Let us consider $V_2(x,z) = V_0(x) + \beta W_1(z)$, where β, $\beta > 0$ is to be determined, as a Lyapunov function candidate for system (3.4.60) and (3.4.61). Choose $\xi < r$;

Choose $\xi < r$; then, given Assumptions $A3.4$, $\forall\ (x,z) \in B(0,\xi) \times \|\eta\| \leq \xi = \Lambda$:

$$\|\dot{\Psi}(x,z)\| \leq L_1\|x\| + L_2\|z\|. \tag{3.4.66}$$

Using equations (3.4.63) to (3.4.65), equation (3.4.12), and the Young's inequality, it can be shown that, $\forall\ (x,z) \in \Lambda$, we have

$$\begin{aligned}
\dot{V}_2 &= -\|x\|^2 + 2x^T P_0 B K_1 z - \beta\|z\|^2 + 2\beta z^T P_1 B_1 \frac{\dot{\Psi}(\cdot)}{\lambda^n} \\
&\leq -\|x\|^2 - \beta\|z\|^2 + 2\|P_0\|\|K_1\|\|x\|\|z\| \\
&\quad + \frac{2\beta}{\lambda^n}\|P_1\|\|z\|(L_1\|x\| + L_2\|z\|) \\
&\leq -\|x\|^2 - \beta\|z\|^2 + (2\|P_0\|\|K_1\| + \frac{2L_1\beta}{\lambda^n}\|P_1\|)(\frac{\|x\|^2}{\epsilon_0} \\
&\quad + \epsilon_0\|z\|^2) + \frac{2L_2\beta}{\lambda^n}\|P_1\|\|z\|^2 \\
&\leq -\tfrac{1}{2}\|x\|^2 - \tfrac{\beta}{2}\|z\|^2 - b_1\|x\|^2 - b_2\|z\|^2,
\end{aligned} \tag{3.4.67}$$

where $b_1 = \frac{1}{2} - \frac{2}{\epsilon_0}(\|K_1\|\|P_0\| + \frac{\beta L_1\|P_1\|}{\lambda^n})$, $b_2 = \frac{\beta}{2} - \frac{2\beta L_2\|P_1\|}{\lambda^n} - 2\epsilon_0(\|P_0\|\|K_1\| + \frac{\beta L_1\|P_1\|}{\lambda^n})$, and $\epsilon_0 > 0$.

Now choose β small enough and $\epsilon_0 \geq \epsilon_0^* = 4\|K_1\|\|P_0\| + \frac{4\beta L_1\|P_1\|}{\lambda^n}$ such that $b_1 > 0$, and then choose $\epsilon_2^* = \beta/(\epsilon_0^{*2} + 4\beta L_4\|P_4\|)$, $\forall\ \epsilon \leq \epsilon_2^*$, $b_2 > 0$. Then, it can be shown that

$$\dot{V} \leq -\min(1/2, \beta/(2\epsilon))[\|x\|^2 + \|z\|^2]. \tag{3.4.68}$$

Thus we can conclude that the origin of system (3.4.60) and (3.4.61) is exponentially stable. □

The designed controller is adaptive to the time varying unknown parameters, system nonlinear dynamics and external disturbances. When there does not exist uncertainties and external disturbances and the exact system nonlinearities is obtainable, such a controller provides the same performance as the

state exact feedback non-linear controller. But when there exists uncertainties, this controller performs much better. Moreover, this controller use state and perturbation estimate to realize the whole controller; it needs only one measurable output and can be easily implemented.

3.5 Example

In this section, simulation of the control of nonlinear system without known system model are performed using proposed adaptive sliding mode control scheme. Consider a second nonlinear system used in [31] in the form of equation (3.2.1) as

$$\begin{cases} \dot{x}_1 &= x_2 \\ \dot{x}_2 &= f(x) + (b(x) - b_0)u + d(t) + b_0 u \\ y &= x_1, \end{cases} \tag{3.5.1}$$

where $x = (x_1, x_2)^T$, $f(x,t) = -(2+\sin(\pi t))x_1^3 - 5(3+\cos(\pi t))\sin(x_2)$, $b(x) = 1 + 0.5\sin(t)$, $b_0 = 2$, and $d(t) = 5\sin(10\pi t)$. The system, initially at the state of $x_1(0) = 5$ and $x_2(0) = 0$, is required to track the desired trajectory $y_d(t) = 5\sin(t)$. For system (3.5.1), we have perturbation

$$\begin{aligned} \Psi(x,u,t) &= f(x,t) + (b(x,t) - b_0)u + d(t) - y_r^{(2)}(t) \\ &= -(2+\sin(\pi t))x_1^3 - 5(3+\cos(\pi t))\sin(x_2) \\ &\quad +5\sin(10\pi t) + (-1 + 0.5\sin(t))u + 5\sin(t) \\ &\leq 3|x_1|^3 + 1.5|u| + 40. \end{aligned}$$

Case 1: Classical SMC

From the initial state condition and control $u = 0$, the bound of the perturbation $|\Psi(x,u,t)|_{\max} = |f(x) + d(t)| \leq 400$. Parameters of a classical SMC (3.3.14) are chosen as follows. $\rho_1 = 20$ and $\rho_2 = 1$ such that make $\lambda_c = -20$; $\varphi = 500$, $\zeta = 20$, and $\epsilon_c = 0.1$. The tracking error response is shown in Figure 3.1 and the control output is shown in Figure 3.2. The unknown perturbation $f(x) + d(t)$ is shown in Figure 3.3.

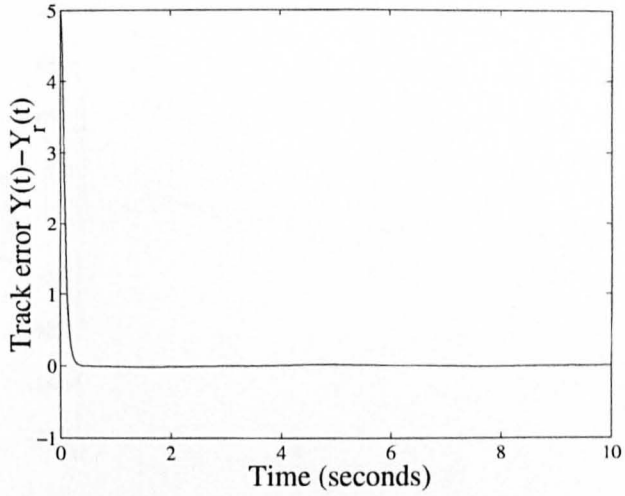

Figure 3.1: Tracking error response $y - y_r$ with SMC

Case 2: Sliding mode controller with perturbation observer

Parameters of a SMPO (3.3.1) are selected to be $\alpha_1 = 2 \times 10^3$, $\alpha_2 = 1 \times 10^6$, $k_1 = 1000$,$k_2 = 3500$, and $\epsilon_o = 0.05$, where ϵ_o is the thickness of boundary layer. Parameters of SMCPO (3.3.22) are chosen as $\rho_1 = 20$ and $\rho_2 = 1$ such that make $\lambda_c = -20$; $\varphi = 100$, $\zeta = 20$, and $\epsilon_c = 0.05$. Note that due to the usage of perturbation estimate $\hat{\Psi}(\cdot)$, the value of φ is decreased from 400 in SMC to 100. The tracking error, perturbation estimate and control are shown in Figures 3.4, 3.5 and 3.6. It can be seen from Figures 3.2 and 3.5 that the control output becomes smaller.

Case 3: Sliding mode controller with state and perturbation observer

Parameters of a SMSPO (3.4.1) are selected to be $\alpha_1 = 300$, $\alpha_2 = 3 \times 10^4$, $\alpha_3 = 1 \times 10^6$, $k_1 = 100$, $k_2 = 4 \times 10^5$, $\alpha_3 = 4 \times 10^8$ and $\epsilon_o = 0.5$. Parameters of SMCSPO (3.4.39) are chosen as $\rho_1 = 20$ and $\rho_2 = 1$ such that make $\lambda_c = -20$; $\varphi = 100$, $\zeta = 20$, and $\epsilon_c = 0.5$. The tracking error, perturbation estimate and control are shown in Figures 3.7, 3.8 and 3.9. The estimate error of x_1 and x_2 are shown in Figures 3.10.

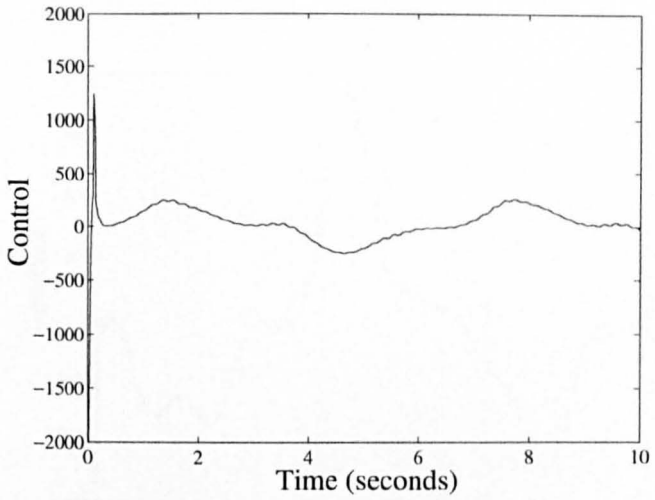

Figure 3.2: Control output with SMC

3.6 Conclusion

In this chapter, the output feedback control of nonlinear system based on sliding mode state and perturbation observer has been investigated. By use of the estimate of perturbation to replace the upper bound of perturbation, a conservative control input is avoided and so that the tracking accuracy is improved by the reasonable control. The feedback linearization of nonlinear system using the estimation of the perturbation from SMSPO have also been investigated. In each case, the complete stability analysis for the controller and observer has been given. The simulation results on an example have also been presented.

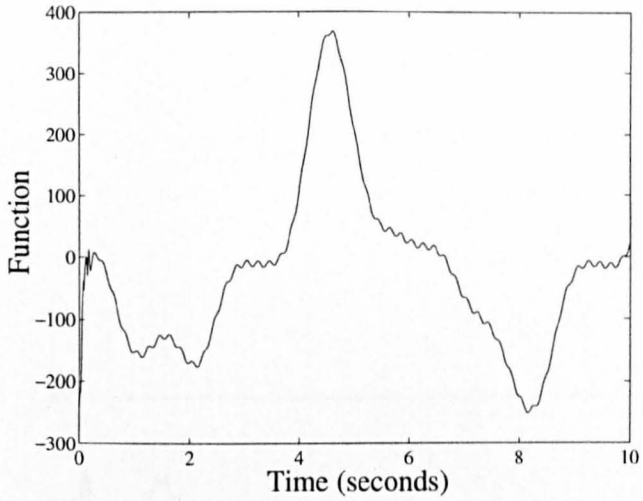

. Figure 3.3: Perturbation $f(x) + d(t)$ with SMC

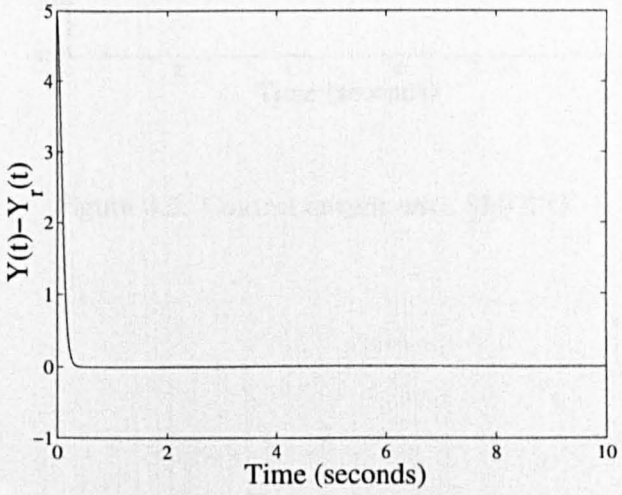

Figure 3.4: Tracking error response $y - y_r$ with SMCPO

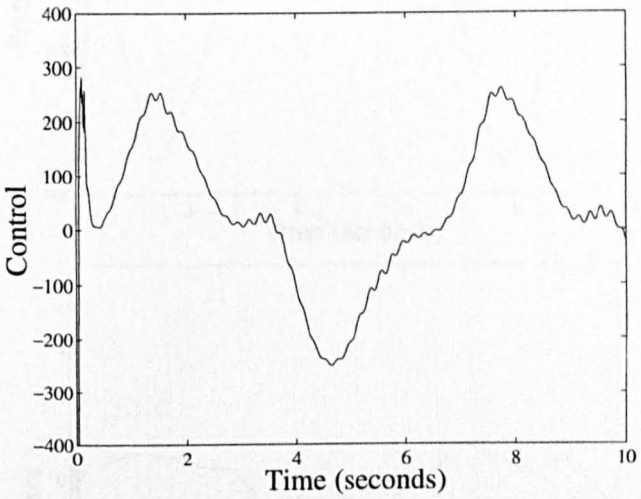

Figure 3.5: Control output with SMCPO

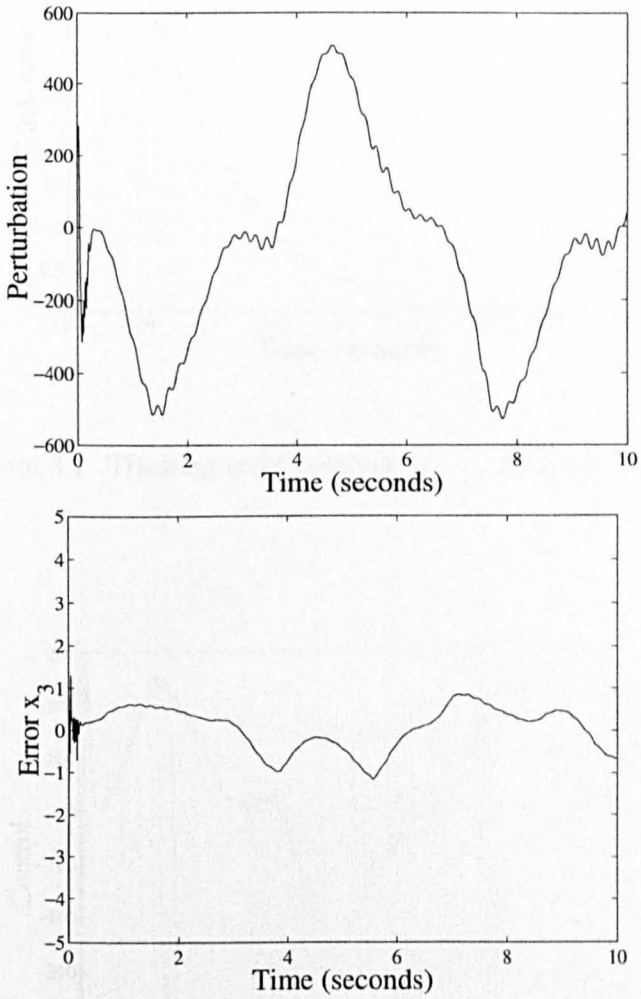

Figure 3.6: Perturbation $f(x) + d(t)$ with SMCPO

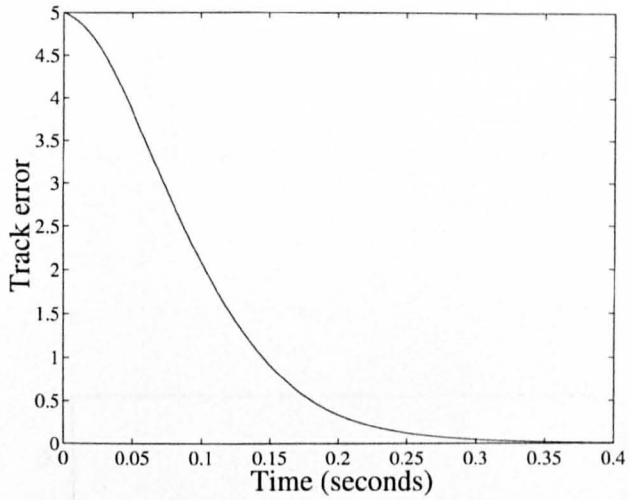

Figure 3.7: Tracking error response $y - y_r$ with SMCSPO

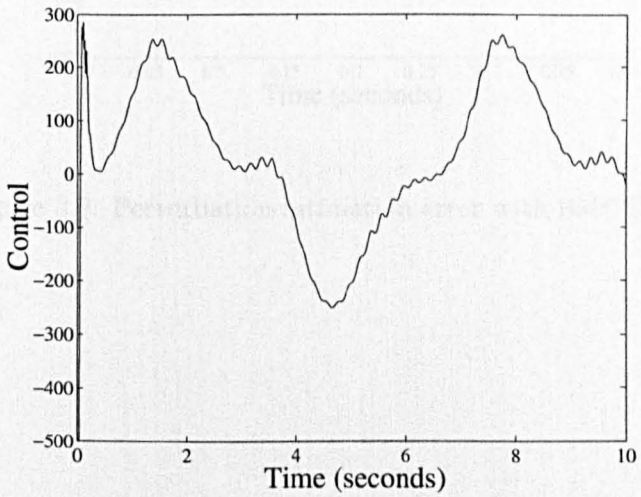

Figure 3.8: Control output with SMCSPO

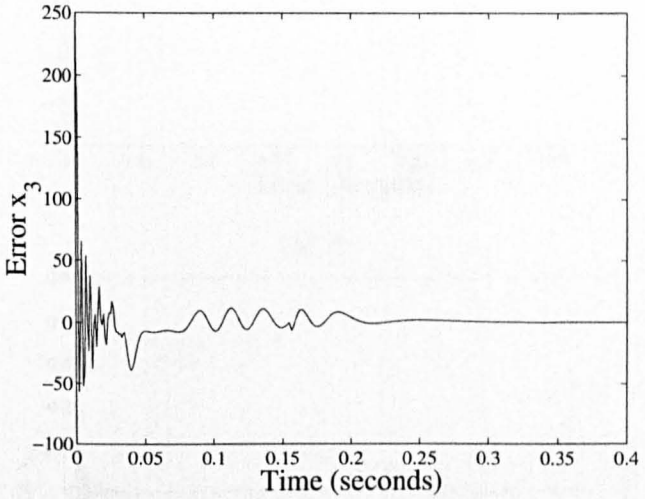

Figure 3.9: Perturbation estimation error with SMCSPO

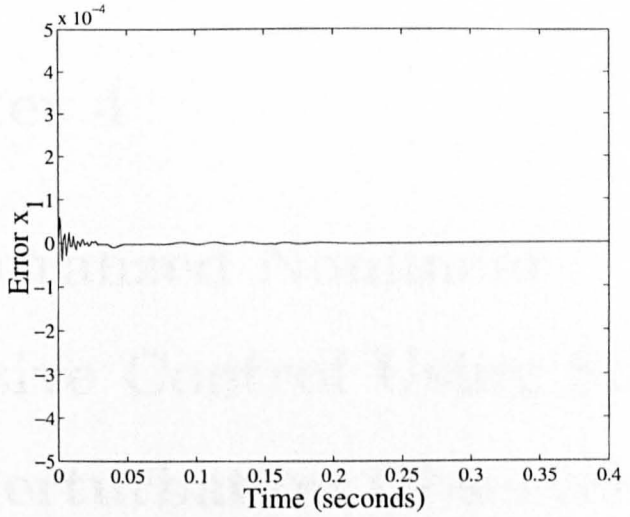

(a) $\tilde{x}_1$

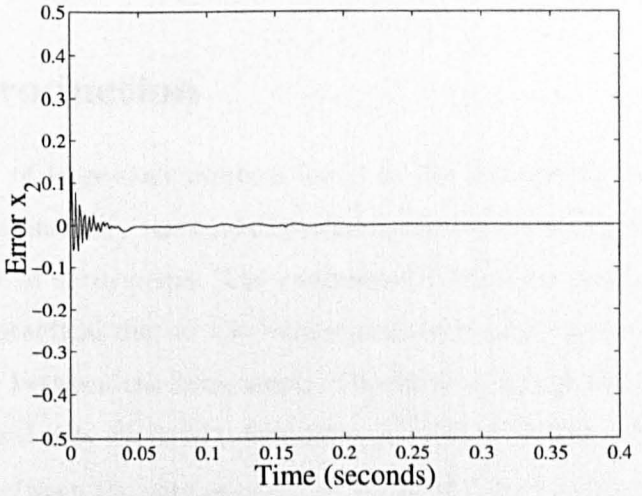

(b) $\tilde{x}_2$

Figure 3.10: Estimate error of SMSPO

Chapter 4

Decentralized Nonlinear Adaptive Control Using State and Perturbation Observer

4.1 Introduction

A number of large-scale systems found in the real world, such as electric power systems, industry manipulators and computer networks, are often composed of a set of subsystems. The centralized control for large-scale systems is usually impractical due to the requirement of a large amount of information exchange between the subsystems. Therefore, a decentralized control law developed based only on local information is often preferable. Because of the interactions between the subsystems, the design of a decentralized controller is in general more difficult than that of the centralized control [134].

Modelling a large-scale system is always difficult or impossible due to its complexity. The uncertainties of the large-scale system appear not only in local subsystems but also from interactions. And the fundamental uncertainties encountered in the decentralized controller design arise from the strength of

the interaction between the subsystems. Therefore, the decentralized robust control or adaptive control of both linear and nonlinear large-scale system with uncertainties are practically significant and have been well developed in recent years [135]. The standard M-matrix conditions have been proposed in [136] and used for the design of a decentralized adaptive controller. The stability of the controlled large-scale system is ensured if there exists a positive definite M-matrix which is related to the bound of the interactions. It is noted that these schemes suffer from some severe drawbacks. For example, the positive definiteness of the M-matrix is hard to verify because it involves unknown constants. In addition, the relative degree of each local subsystem of the decentralized system can not be larger than two. High gain stabilization techniques were proposed in [137] to design decentralized adaptive control which need not resort to any M-matrix condition, but at a price of assuming the standard strict matching condition about the uncertainties. Using the deterministic approach to uncertain systems, nonadaptive decentralized controllers have been designed using the possible bounds on the interactions to drive the nominal subsystem to the equilibrium state [138].

Though several decentralized nonadaptive or adaptive control schemes have been proposed to handle bounded or unbounded interactions, most of these works are based on the assumptions that the interactions are either bounded by constants or first-order polynomials in states, or they are in slow time variation. In [139], a class of large-scale system, with the assumption that the interactions between subsystems are bounded by a known or unknown pth-order polynomial in states were considered.

Most works in decentralized control focus on state-feedback and less attention has been paid to the decentralized output feedback problem of large-scale nonlinear systems. Based on adaptive output feedback control in the centralized control, a decentralized adaptive regulator was designed for systems which have the observer canonical form[140]. Recently, the decentralized adap-

tive asymptotic tracking for a new class of large-scale systems using nonlinear output feedback is proposed [135]. This approach does not require any matching conditions on the parametric uncertainties nor growth conditions of any kind on the subsystem and interacting output nonlinearities. Decentralized reduced-order filters are presented to recover the unmeasured states. In most of the adaptive control schemes, the linear or nonlinear parametric condition are assumed and only unknown constant parameters or slow time-varying parameters can be treated.

In this chapter, decentralized nonlinear adaptive control (DNAC) of large-scale systems is investigated based on the state and perturbation observer. During the design of DNAC, high gain observer and sliding mode observer have been used to estimate system states and perturbation, respectively. Three control schemes, decentralized nonlinear adaptive controller with high gain observer, decentralized nonlinear adaptive sliding mode controller with sliding mode observer and decentralized nonlinear adaptive control using continuous feedback control and sliding mode observer, have been developed. The nonlinearities and uncertainties existing in each subsystems and the interactions between the subsystems are included in the system perturbation and estimated by the function estimation method. Most importantly, the usage of the estimate of the perturbation, instead of its bound, will result in a reasonable control output.

This chapter is organized as follows. In Section 4.2, the problem statement is presented. Then Section 4.3 develops a decentralized nonlinear adaptive control via a high gain state and perturbation observer and presents the stability results. In Section 4.4, the decentralized sliding mode control scheme is designed based on a sliding mode state and perturbation observer. In this section a decentralized states feedback sliding mode controller is presented for comparison at first. Decentralized nonlinear adaptive control using continuous feedback control and sliding mode observer is also presented. In Section

4.5, the benchmark example of double inverted pendulums on carts is used to illustrate these control strategies. Finally conclusion will be given in section 6.

4.2 Problem statement

Consider a large-scale nonlinear system Q which is composed of N interconnected subsystems q_i, $i = 1, \cdots, N$. Each subsystem q_i may be presented as:

$$q_i : \begin{cases} \dot{x}_{i1} &= x_{i2} \\ \dot{x}_{i2} &= x_{i3} \\ &\vdots \\ \dot{x}_{in_i} &= f_i(x_i) + g_i(x_i)u_i(t) + z_i(x) + d_i(x_i, t) \\ y_i &= x_{i1}, \end{cases} \tag{4.2.1}$$

where $x_i = [x_{i1}, x_{i2}, \cdots, x_{in_i}]^T \in \mathcal{R}^{n_i}$ is the state vector of q_i, $x = [x_1^T, \cdots, x_N^T]^T \in \mathcal{R}^n$ the state vector of whole system, $n = \sum_{i=1}^{N} n_i$; $u_i(t) \in \mathcal{R}$ the control input of q_i; $y_i \in \mathcal{R}$ the output of system q_i; $f_i(x_i) : \mathcal{R}^{n_i} \to \mathcal{R}$ the unknown continuous function; $g_i(x_i) : \mathcal{R}^{n_i} \to \mathcal{R}$ unknown control gain; $z_i(x) : \mathcal{R}^n \to \mathcal{R}$ the strength of interactions from other subsystems; $d_i(x_i, t) \in \mathcal{R}^{n_i} \times \mathcal{R}^+ \to \mathcal{R}$ the external disturbance of subsystem q_i.

The perturbation of subsystems q_i, which represents the combined effect of nonlinearities, uncertainties, external disturbance and interactions between subsystems, is defined as

$$\Psi_i(x, u, t) = f_i(x_i) + z_i(x) + d_i(x_i, t) + (g_i(x_i) - g_{i0})u_i, \tag{4.2.2}$$

where g_{i0} is a known constant control gain. And we assume the known part of the system nonlinearities $f_{i0}(x_i) = 0$ for simplification.

Then system (4.2.1) may be represented in a matrix form as

$$q_i : \dot{x}_i = A_i x_i + B_i[\Psi_i + g_{i0}u_i], \tag{4.2.3}$$

where

$$A_i = \begin{bmatrix} 0 & 1 & 0 & \cdots & 0 \\ 0 & 0 & 1 & \cdots & 0 \\ \vdots & & & & \vdots \\ 0 & 0 & 0 & \cdots & 1 \\ 0 & 0 & 0 & \cdots & 0 \end{bmatrix}_{n_i \times n_i}, \quad B_i = \begin{bmatrix} 0 \\ 0 \\ \vdots \\ 0 \\ 1 \end{bmatrix}_{n_i \times 1}. \tag{4.2.4}$$

After introducing a *fictitious state* to represent the perturbation: $x_{i(n_i+1)} = \Psi_i(x, u, t)$, subsystem q_i can be rewritten in a $(n_i + 1)$-order state equation as

$$\begin{cases} \dot{x}_{ie} &= A_{i1}x_{ie} + B_{i2}g_{i0}u_i + B_{i1}\dot{\Psi}(\cdot) \\ y_i &= C_{i1}x_{ie}, \end{cases} \tag{4.2.5}$$

where $\dot{\Psi}(\cdot)$ is the derivative of perturbation $\Psi(\cdot)$ and

$$x_{ie} = \begin{bmatrix} x_{i1} \\ x_{i2} \\ \vdots \\ x_{in_i} \\ x_{i(n_i+1)} \end{bmatrix}, \quad A_{i1} = \begin{bmatrix} 0 & 1 & \cdots & \cdots & 0 \\ 0 & 0 & 1 & \cdots & 0 \\ \vdots & & & & \vdots \\ 0 & 0 & 0 & \cdots & 1 \\ 0 & 0 & 0 & \cdots & 0 \end{bmatrix}_{(n_i+1)\times(n_i+1)},$$

$$B_{i2} = \begin{bmatrix} 0 \\ 0 \\ \vdots \\ 1 \\ 0 \end{bmatrix}_{(n_i+1)\times 1}, \quad B_{i1} = \begin{bmatrix} 0 \\ 0 \\ \vdots \\ 0 \\ 1 \end{bmatrix}_{(n_i+1)\times 1}, \quad C_{i1} = \begin{bmatrix} 1 \\ 0 \\ \vdots \\ 0 \\ 0 \end{bmatrix}^T_{(n_i+1)\times 1}.$$

Defining the desired track state vector $x_{ri} = [y_{ri}, y_{ri}^{(1)}, \cdots, y_{ri}^{(n_i)}]^T$, and the tracking error vector $e_i = x_i - x_{ri} = [e_{i1}, e_{i2}, \cdots, e_{in_i}]^T$, system (4.2.3) may be rewritten for the tracking problem as

$$q_i : \dot{e}_i = A_i e_i + B_i[\Psi_i - y_{ri}^{(n_i)} + g_{i0}u_i]. \tag{4.2.6}$$

The following assumptions are made on system (4.2.1):

A4.1 g_{i0} is chosen to satisfy:

$$|g_i(x_i)/g_{i0} - 1| \leq \theta_i < 1, \tag{4.2.7}$$

where θ_i is a positive constant.

A4.2 The function $\Psi_i(x,u,t) : \mathcal{R}^n \times \mathcal{R} \times \mathcal{R}^+ \to \mathcal{R}$ and $\dot{\Psi}_i(x,u,t) : \mathcal{R}^n \times \mathcal{R} \times \mathcal{R}^+ \to \mathcal{R}$ are locally Lipschitz in their arguments over the domain of interest and globally bounded in x:

$$|\Psi_i(x,u,t)| \leq \gamma_{i1}, \quad |\dot{\Psi}_i(x,u,t)| \leq \gamma_2,$$

where γ_{i1} and γ_{i2} are positive constants. In addition, $\Psi_i(0,0,0) = 0$ and $\dot{\Psi}_i(0,0,0) = 0$.

A4.3 The desired output y_{ri} and its up to n_ith-order derivatives $(y_{ri}^{(1)}, \cdots, y_{ri}^{(n_i)})$ are bounded, i.e., $|y_{rj}^{(l)}| \leq h_j$, $l = 1, \cdots, n_i$, $j = 1, \cdots N$, where h_j is a positive constant.

Our control problem is formulated as follows. Under assumptions $A4.1 \sim A4.3$, find out the decentralized, output-feedback control of the form

$$\dot{\hat{x}}_i = \nu_i(t, \hat{x}_i, y_i), \qquad u_i = \mu_i(t, \hat{x}_i, y_i), \tag{4.2.8}$$

such that, the state x_i can track stably the desired state x_{ri} and for any positive constant ϵ, the tracking error e_i will converge into a neighbourhood around origin

$$\|e_i\| \leq \epsilon \qquad \text{and} \qquad |y_i(t) - y_{ri}(t)| \leq \epsilon, \tag{4.2.9}$$

where $\hat{x}_i$ is the estimate of system state x_i, ν_i and μ_i are nonlinear functions.

4.3 Decentralized nonlinear adaptive control using high gain state and perturbation observer

In this section, the design of a (n_i+1)th-order high gain state observer is designed to estimate the system states and perturbation when the subsystem output $y_i = x_{i1}$ is available. Then the estimates of the states and perturbation of subsystem are employed to design a decentralized adaptive output feedback linearization control law. The singular perturbation method is used to analyze the stability of the closed-loop system which include the controller and observer.

4.3.1 Design of a HGSPO for subsystem q_i

The high gain state and perturbation observer for subsystem q_i (4.2.5) is designed as

$$\dot{\hat{x}}_{ie} = A_{i1}\hat{x}_{ie} + B_{i2}g_{i0}u_i + H_i(y - C_{i1}\hat{x}_{ie}). \tag{4.3.1}$$

The observer gain H_i is chosen as

$$H_i = \begin{bmatrix} \alpha_{i1}/\epsilon_i \\ \alpha_{i2}/\epsilon_i^2 \\ \vdots \\ \alpha_{in_i}/\epsilon_i^{n_i} \\ \alpha_{n_i+1}/\epsilon_i^{n_i+1} \end{bmatrix}, \tag{4.3.2}$$

where ϵ_i, $0 < \epsilon_i < 1$ is a positive constant to be specified and the positive constants α_{ij}, $j = 1, 2, \cdots, n_i+1$, are chosen such that the roots of

$$s^{n+1} + \alpha_{i1}s^n + \cdots + \alpha_{in_i}s + \alpha_{i(n_i+1)} = 0$$

are in the open left-half complex plan.

Throughout this chapter, $\tilde{x}_{ij} = x_{ij} - \hat{x}_{ij}$ refers to the estimation error of x_{ij} whereas $\hat{x}_{ij}$ symbolizes the estimated quantity of x_{ij}. Defining the estimation error vector as $\tilde{x}_{ie} = x_{ie} - \hat{x}_{ie}$, the error dynamics of observer (4.3.1) becomes

$$\dot{\tilde{x}}_{ie} = (A_{i1} - H_i C_{i1})\tilde{x}_{ie} + B_{i1}\dot{\Psi}_i(\cdot). \tag{4.3.3}$$

For the purpose of analysis, the observer error dynamics are replaced by the equivalent dynamics of the scaled estimation error

$$\eta_{ij} = \frac{\tilde{x}_{ij}}{\epsilon_i^{n+1-j}}, \qquad 1 \le j \le n_i + 1.$$

Hence, we have $\hat{x}_{ie} = x_{ie} - D_i(\epsilon_i)\eta_i$ where

$$\begin{aligned} \eta_i &= [\eta_{i1}, \eta_{i2}, \cdots, \eta_{i(n_i+1)}]^T, \\ D_i(\epsilon_i) &= \mathrm{diag}[\epsilon_i^{n_i+1}, \cdots, \epsilon_i, 1]_{(n_i+1)\times(n_i+1)}. \end{aligned}$$

Then the error dynamics of observer (4.3.3) can be represented as

$$\begin{aligned} \dot{\eta}_i &= D_i^{-1}(\epsilon_i)(A_{i1} - H_i C_{i1}) D_i(\epsilon_i)\eta_i + D_i^{-1}(\epsilon_i) B_{i1}\dot{\Psi}_i(\cdot) \\ &= \tfrac{1}{\epsilon_i} A_{i2}\eta_i + B_{i1}\dot{\Psi}_i(\cdot), \end{aligned} \tag{4.3.4}$$

where

$$A_{i2} = \begin{bmatrix} -\alpha_{i1} & 1 & \cdots & \cdots & 0 \\ -\alpha_{i2} & 0 & 1 & \cdots & 0 \\ \vdots & \vdots & \vdots & \ddots & \vdots \\ -\alpha_{in_i} & 0 & 0 & \cdots & 1 \\ -\alpha_{i(n_i+1)} & 0 & 0 & \cdots & 0 \end{bmatrix}$$

is a Hurwitzian.

The analysis of the convergence of HGSPO is similar to the HGSPO designed in Chapter 2. The observer gains can be chosen such that the estimation error $\tilde{x}_{i1}$ will converge exponentially to a small neighbourhood that is arbitrarily close to origin. Here, we only give the results in following theorem.

Theorem 4.1. *Consider system (4.2.1), design a high gain state and perturbation observer (4.3.1) for each subsystem q_i and choose gains H_i described in*

equation (4.3.2). If assumptions A4.1 ~ A4.2 hold for some values g_{i0}, γ_{i1} *and* γ_{i2}, *then given any positive constant* $\delta_{\text{spo}_i} > 0$, *there exits a positive constant* $\epsilon^*_{\text{spo}_i}$, *such that* $\forall \epsilon_i$, $0 < \epsilon_i < \epsilon^*_{\text{spo}_i}$, *from the initial observer error* $\tilde{x}_{ie}(0)$, *the observer error* $\tilde{x}_{ie}$ *converges exponentially into the neighborhood*

$$\|\tilde{x}_{ie}\| \leq \delta_{\text{spo}_i}.$$

Proof: Refer to Theorem 2.2 in Chapter 2.

4.3.2 Decentralized nonlinear adaptive control using HGSPO

Using the estimate of perturbation $\hat{x}_{i(n_i+1)}$ to compensate the system nonlinearities, uncertainties and the interactions between subsystems, and the estimate of system states $\hat{x}_i$ to replace the true states, a decentralized adaptive output feedback linearization controller of subsystem q_i is designed as

$$u_i = v_i/g_{i0} - (\hat{x}_{i(n_i+1)} - y_{ri}^{(n_i)})/g_{i0}, \tag{4.3.5}$$

$$v_i = -K_i(\hat{x}_i - x_{ir}), \tag{4.3.6}$$

where $K_i = [k_{i1}, k_{i2}, \cdots, k_{in_i}]^T$ is the linear feedback controller gains, which are chosen to make $A_{i0} = A_i - B_i K_i$ Hurwitzian.

Note that $\hat{x}_i = x_i - D_i'(\epsilon_i)\eta_i'$, $\hat{x}_{i(n_i+1)} = x_{i(n_i+1)} - \eta_{i(n_i+1)}$, where $D_i'(\epsilon_i) = \text{diag}[\epsilon_i^{n_i+1}, \cdots, \epsilon_i]_{(n_i)\times(n_i)}$ and $\eta_i' = [\eta_{i1}, \eta_{i2}, \cdots, \eta_{in_i}]^T$. Control (4.3.5) can be represented as:

$$u_i = \frac{1}{g_{i0}}(-x_{i(n_i+1)} + y_{ri}^{(n_i)} - K_i e_i + K_{i1} D_i(\epsilon_i)\eta_i), \tag{4.3.7}$$

where $K_{i1} = [K_i, 1]$.

Substituting control (4.3.7) into system (4.2.6), the closed-loop system can be represented by

$$\dot{e}_i = A_{i0} e_i + B_i K_{i1} D_i(\epsilon_i)\eta_i, \tag{4.3.8}$$

$$\epsilon_i \dot{\eta}_i = A_{i2}\eta_i + \epsilon_i B_{i1} \dot{\Psi}_i(e_i, D_i(\epsilon_i)\eta_i). \tag{4.3.9}$$

Note that the bound of control u_i should big enough so that the estimate of perturbation $\hat{x}_{i(n_i+1)}$ can be used to realize the cancellation of the real perturbation $x_{i(n_i+1)}$.

System (4.3.8) and (4.3.9) represents a standard singular perturbed system, and $\eta_i = 0$ is the unique solution of system (4.3.9) when $\epsilon_i = 0$. The reduced system, obtained by substituting $\eta_i = 0$ in system (4.3.8), is as:

$$\dot{e}_i = A_{i0} e_i. \tag{4.3.10}$$

The boundary-layer system, obtained by applying the state variable transformation $\tau_i = t/\epsilon_i$ to system (4.3.9) and then setting $\epsilon_i = 0$, is given by

$$\frac{d\eta_i}{d\tau_i} = A_{i2}\eta_i. \tag{4.3.11}$$

Theorem 4.2. *Consider subsystem q_i (4.2.1), design a high gain state and perturbation observer(4.3.1), and choose the observer gain described in equation (4.3.2), and let assumptions A4.1 $\sim$ A4.3 hold; then, $\exists \epsilon_{i2}^*$, $\epsilon_{i2}^* > 0$, so that, $\forall\ \epsilon_i$, $0 < \epsilon_i < \epsilon_{i2}^*$, system (4.3.8) and (4.3.9) is exponentially stable. Moreover, property (4.2.9) holds.*

Proof: As A_{i0} is a Hurwitz matrix, we know that the reduced system (4.3.10) is exponentially stable in a region of $\mathcal{R}_i$ which includes the origin. Thus, we can define a Lyapunov function

$$V_{i0}(e_i) = e_i^T P_{i0} e_i \tag{4.3.12}$$

over a ball $B(0, r_i) \subset \mathcal{R}_i$, for some $r_i > 0$; and P_{i0} is the positive definite solution of the Lyapunov equation $P_{i0}A_{i0} + A_{i0}^T P_{i0} = -I$. $\forall\ e_i \in B(0, r)$, we have

$$\lambda_{\min}(P_{i0})\|e_i\|^2 \leq V_{i0}(e_i) \leq \lambda_{\max}(P_{i0})\|e_i\|^2, \tag{4.3.13}$$

$$\frac{\partial V_{i0}}{\partial e_i} A_{i0} e_i \leq -\|e_i\|^2, \tag{4.3.14}$$

$$\|\frac{\partial V_{i0}}{\partial e_i}\| \leq 2\lambda_{\max}(P_{i0})\|e_i\|. \tag{4.3.15}$$

The boundary-layer system (4.3.11) is also exponentially stable in a region of $\mathcal{Q}_i$ which includes the origin. Thus we define the Lyapunov function $V_{i2}(\eta_i) = \eta_i^T P_{i2}\eta_i$, where P_{i2} is the positive definite solution of the Lyapunov equation $P_{i2}A_{i2} + A_{i2}^T P_{i2} = -I$. This function satisfies

$$\lambda_{\min}(P_{i2})\|\eta_i\|^2 \leq V_{i2}(\eta_i) \leq \lambda_{\max}(P_{i2})\|\eta_i\|^2, \tag{4.3.16}$$

$$\frac{\partial V_{i2}}{\partial \eta_i}A_{i2}\eta_i \leq -\|\eta_i\|^2, \tag{4.3.17}$$

$$\|\frac{\partial V_{i2}}{\partial \eta_i}\| \leq 2\lambda_{\max}(P_{i2})\|\eta_i\|. \tag{4.3.18}$$

Let us consider $V_i = V_{i0}(e_i) + \beta_i V_{i2}(\eta_i)$, where β_i, $\beta_i > 0$ is a constant to be determined, as a Lyapunov function candidate for system (4.3.8) and (4.3.9). Choosing $\xi < r_i$; then, given Assumptions $A4.1 \sim A4.2$, $\forall\ (e_i, \eta_i) \in B(0,\xi) \times \|\eta_i\| \leq \xi = \Lambda_i$, we have

$$\|\dot{\Psi}(x, \eta_i, t)\| \leq L_{i1}\|e_i\| + L_{i2}\|\eta_i\|. \tag{4.3.19}$$

Using equations (4.3.13) $\sim$ (4.3.18), and the Young's inequality, it can be shown that, $\forall (e_i, \eta_i) \in \Lambda_i$, we have

$$\begin{aligned}
\dot{V}_i &= \tfrac{\partial V_{i0}}{\partial e_i}(A_{i0}e_i + B_i\eta_i) + \beta_i \tfrac{\partial V_{i2}}{\partial \eta_i}(\tfrac{A_{i2}\eta_i}{\epsilon_i} + B_{i1}\dot{\Psi}_i(\cdot)) \\
&\leq -\|e_i\|^2 - \tfrac{\beta_i}{\epsilon_i}\|\eta_i\|^2 + 2\beta_i L_{i2}\|P_{i2}\|\|\eta_i\|^2 + (2\|P_{i0}\| \\
&\quad +2\beta_i L_{i1}\|P_{i2}\|)\|e_i\|\|\eta_i\| \\
&\leq -\|e_i\|^2 - \tfrac{\beta_i}{\epsilon_i}\|\eta_i\|^2 + 2\beta_i L_{i2}\|P_{i2}\|\|\eta_i\|^2 \\
&\quad +(2\|P_{i0}\| + 2\beta_i L_{i1}\|P_{i2}\|)(\tfrac{1}{\epsilon_{i0}}\|e_i\|^2 + \epsilon_i\|\eta_i\|^2) \\
&\leq -\tfrac{1}{2}\|e_i\|^2 - \tfrac{\beta_i}{2\epsilon_i}\|\eta_i\|^2 - b_{i1}\|e_i\|^2 - b_{i2}\|\eta_i\|^2,
\end{aligned} \tag{4.3.20}$$

where $b_{i1} = \frac{1}{2} - \frac{2}{\epsilon_{i0}}(\|P_{i0}\| + \beta_i L_{i1}\|P_{i2}\|)$, $b_{i2} = \frac{\beta_i}{2\epsilon_i} - 2\beta_i(\epsilon_{i0} * L_{i1} + L_{i2})\|P_{i2}\| - 2\epsilon_i\|P_{i0}\|$, and $\epsilon_i > 0$. Now choose β_i small enough and $\epsilon_i \geq \epsilon_i^* = 4\|P_{i0}\| + 4\beta_i L_{i1}\|P_{i2}\|$ such that $b_{i1} > 0$, and then choose $\epsilon_{i1}^* = \beta_i/({\epsilon_{i0}^*}^2 + 4\beta_i L_{i2}\|P_{i2}\|)$, $\forall \epsilon_i$, $\epsilon_i \leq \epsilon_{i1}^*$, it can be shown that

$$\dot{V} \leq -\min(1/2, \beta_i/(2\epsilon_i))[\|e_i\|^2 + \|\eta_i\|^2]. \tag{4.3.21}$$

Thus we can conclude that the origin of system (4.3.8) and (4.3.9) is exponentially stable. As the tracking error $e_i = x_i - x_{ir}$ will converge exponentially to zero, the state x_i can track the desired state x_{ri} asymptotically and finally the following asymptotic tracking property is achieved

$$\lim_{t\to\infty} |y_i(t) - y_{ri}(t)| = 0.$$

□

4.4 Decentralized nonlinear adaptive control with sliding mode state and perturbation observer

In this section, the sliding mode state and perturbation observer is designed for the decentralized output feedback control of the interconnected large-scale nonlinear system. First the design of a decentralized state feedback sliding mode controller for a subsystem is briefly reviewed. Then after designing a sliding mode state and perturbation observer, the decentralized sliding mode controller and linear feedback linearization controller are investigated respectively.

4.4.1 Decentralized state feedback sliding mode controller

In this section, let assume the full states are measurable for design of a decentralized sliding mode controller. For subsystem q_i, define the sliding surface $S_{\text{smc}_i}(e_i)$ as

$$S_{\text{smc}_i}(e_i) = \sum_{j=1}^{n_i} \rho_{ij}(x_{ij} - y_{ri}^{(j-1)}) = \sum_{j=1}^{n} \rho_{ij} e_{ij}, \tag{4.4.1}$$

where coefficients ρ_{ij}, $j = 1, \cdots, n_i - 1$ and $\rho_{in_i} = 1$, are constants and the polynomial $s^{n_i-1} + \rho_{i(n_i-1)}s^{n_i-2} + \cdots + \rho_{i2}s + \rho_{i1}$ is Hurwitzian.

Differentiating equation (4.4.1) along system (4.2.6), one obtains

$$\dot{S}_{\mathrm{smc_i}} = -y_{ri}^{(n_i)} + \sum_{j=1}^{n_i-1} \rho_{ij} e_{i(j+1)} + \Psi_i(\cdot) + g_{i0} u_i. \tag{4.4.2}$$

A sliding mode controller is designed as

$$u_i = \frac{1}{g_{i0}} \left[y_r^{(n_i)} - \sum_{j=1}^{n_i-1} \rho_{ij} e_{i(j+1)} - \zeta_i S_{\mathrm{smc_i}} - \varphi_i \, \mathrm{sgn}(S_{\mathrm{smc_i}}) \right], \tag{4.4.3}$$

where ζ_i and φ_i are control gains and they are determined to fulfill the attractive condition of sliding surface $S_{\mathrm{smc_i}}$ as follows:

$$\zeta_i \, |S_{\mathrm{smc_i}}| + \varphi_i > |\Psi_i(\cdot)|_{\max}. \tag{4.4.4}$$

From assumption $A3$, $\Psi_i(\cdot) \leq \gamma_{i1}$; thus, the above condition is obviously satisfied if gain φ_i is chosen such that

$$\varphi_i \geq \gamma_{i1}. \tag{4.4.5}$$

To avoid the control chattering, the signum function $\mathrm{sgn}(\chi)$ can be replaced with a unit saturation function $\mathrm{sat}(\chi, \epsilon_{c_i})$, where ϵ_{ci} is the boundary layer thickness of the sliding mode controller. Moreover, the corresponding $S_{\mathrm{smc_i}}$ dynamics within the boundary layer is not desired to exhibit high frequency oscillation either. Consider the dynamics behaviour of $S_{\mathrm{smc_i}}$, once it penetrates into the boundary layer given $|S_{\mathrm{smc_i}}| \leq \epsilon_{ci}$:

$$\dot{S}_{\mathrm{smc_i}} + (\zeta_i + \frac{\varphi_i}{\epsilon_{c_i}}) S_{\mathrm{smc_i}} = \Psi_i(\cdot). \tag{4.4.6}$$

This equation acts as a low-pass filter against the perturbation and

$$\omega_i = \zeta_i + \frac{\varphi_i}{\epsilon_{c_i}} \tag{4.4.7}$$

is the tuneable break frequency. In order to eliminate the influence of the perturbation, this frequency has an upper bound ω_{maxi}. This can be achieved by choosing a boundary layer ϵ_{ci} as:

$$\epsilon_{c_i} = \frac{\varphi_i}{\omega_{\mathrm{maxi}} - \zeta_i}. \tag{4.4.8}$$

It is desired to keep ϵ_{c_i} as small as possible for track precision. However, for a given bandwidth bound ω_{maxi}, it can be easily shown from equation (4.4.8) that when φ_i increases due to the increase of perturbations, so does ϵ_{c_i}. Therefore, this choice of ϵ_{ci} introduces a trade-off between robustness and tracking accuracy.

4.4.2 Design a sliding mode state and perturbation observer for q_i

As it is difficult to obtain the bound of the perturbation, the upper bound of perturbation in the worst case is employed for determination of the control gain (4.4.5). This results in a conservative and high gain for practical applications. In fact, most often the worst conditions in which the perturbation takes its upper bound does not occur. Therefore, these conservative gains are not necessary. In this section, the perturbation estimation will be applied to remedy this problem in which a high control gain is utilized due to the use of upper bound. When the upper bound is replaced by the estimate of perturbation, a low and reasonable control gain will result in. Moreover, although the upper bound of the derivative of perturbation is required to guarantee the estimation accuracy and may result in the conservative high gains for observer, those conservative gains are only included in the observer-loop, rather than in the controller law. Such properties will be illustrated as follows. In fact, as the interaction strengths between subsystems are included in the perturbation of each subsystem, the procedure of the decentralized controller design for the subsystem can be treated similarly to the analysis of SISO system in Chapter 3. Here we briefly review the results as follows.

For subsystem q_i in system (4.2.5), with the measurement $y_i = x_{i1}$, a $(n_i +$

1)th-order sliding mode observer is designed as:

$$\begin{cases} \dot{\hat{x}}_{i1} &= \hat{x}_{i2} + \alpha_{i1}\tilde{x}_{i1} + k_{i1}\,\mathrm{sgn}(\tilde{x}_{i1}) \\ &\vdots \\ \dot{\hat{x}}_{n_i} &= \hat{x}_{i(n_i+1)} + \alpha_{in_i}\tilde{x}_{i1} + k_{in_i}\,\mathrm{sgn}(\tilde{x}_{i1}) + g_{i0}u_i \\ \dot{\hat{x}}_{n_i+1} &= \alpha_{i(n_i+1)}\tilde{x}_{i1} + k_{i(n_i+1)}\,\mathrm{sgn}(\tilde{x}_{i1}), \end{cases} \tag{4.4.9}$$

where $\tilde{x}_{i1} = x_{i1} - \hat{x}_{i1}$, k_{ij} and α_{ij}, $j = 1, \cdots, n_i + 1$, are positive coefficients. The constants α_{ij} are chosen as same as in that for designing a Luenberger observer(which corresponds to $k_{ij} = 0$, $j = 1, \cdots, n_i + 1$) so as to place the poles of the Luenberger observer at the desired locations in the left half side of complex plane.

From equations (4.2.5) and (4.4.9), the error dynamics of observer can be obtained as:

$$\begin{cases} \dot{\tilde{x}}_{i1} &= \tilde{x}_{i2} - \alpha_{i1}\tilde{x}_{i1} - k_{i1}\,\mathrm{sgn}(\tilde{x}_{i1}) \\ &\vdots \\ \dot{\tilde{x}}_{in_i} &= \tilde{x}_{i(n_i+1)} - \alpha_{in_i}\tilde{x}_{i1} - k_{in_i}\,\mathrm{sgn}(\tilde{x}_{i1}) \\ \dot{\tilde{x}}_{i(n_i+1)} &= -\alpha_{i(n_i+1)}\tilde{x}_{i1} - k_{i(n_i+1)}\,\mathrm{sgn}(\tilde{x}_{i1}) + \dot{\Psi}_i. \end{cases} \tag{4.4.10}$$

The sliding surface is defined as $S_{\mathrm{spo}_i}(\tilde{x}_i) = \tilde{x}_{i1} = 0$. Introducing the Lyapunov function $V_{\mathrm{spo}_i} = \frac{1}{2}S^2_{\mathrm{spo}_i}$, the sliding surface is attractive if $\dot{V}_{\mathrm{spo}_i} \leq 0$ $\forall\ \tilde{x}_i \notin S_{\mathrm{spo}_i}$. The condition for the existence of sliding mode is:

$$\begin{cases} \tilde{x}_{i2} \leq k_{i1} + \alpha_{i1}\tilde{x}_{i1}, & \text{if } \tilde{x}_{i1} > 0; \\ \tilde{x}_{i2} \geq -k_{i1} + \alpha_{i1}\tilde{x}_{i1}, & \text{if } \tilde{x}_{i1} < 0. \end{cases} \tag{4.4.11}$$

Such a condition can be guaranteed by choosing k_{i1} as follows:

$$k_{i1} \geq |\ \tilde{x}_{i2}\ |_{\max}\,. \tag{4.4.12}$$

Under the above condition, it is guaranteed that the system will reach the sliding surface at $t = t_s$ and remain on the sliding surface $S_{\mathrm{spo}_i} = 0$, $\forall t \geq t_s$. Actually, the observer dynamics can start in the sliding mode, if $\hat{x}_{i1}(0)$ can be taken as $x_{i1}(0)$.

By applying $\tilde{x}_{i1} = 0$ and $\dot{\tilde{x}}_{i1} = 0$ when the sliding mode takes place, the equivalent control can be obtained as the same as which is described in Chapter 3, that is

$$[\,\mathrm{sgn}(\tilde{x}_{i1})]_{\mathrm{eq}} = \frac{1}{k_{i1}}\tilde{x}_{i2}, \tag{4.4.13}$$

The equivalent control is not the control signal which is actually applied to the system but it may be thought of as the control signal which is applied 'on average' to maintain the sliding motion. In fact, it is the low frequency components of the real control signal[15].

Substituting equation (4.4.13) to system (4.4.10), the resulting error dynamics on the sliding mode take the form :

$$\dot{\tilde{x}}_{ie1} = A_{i3}\tilde{x}_{ie1} + B_{i3}\dot{\Psi}_i, \tag{4.4.14}$$

where $\tilde{x}_{ie1} = \begin{bmatrix} \tilde{x}_{i2} & \cdots & \tilde{x}_{i(n_i+1)} \end{bmatrix}^T$, and $n_i \times n_i$ matrix A_{i3} and $n_i \times 1$ matrix B_{i3} are as follows respectively:

$$A_{i3} = \begin{bmatrix} -\frac{k_{i2}}{k_{i1}} & 1 & \cdots & \cdots & 0 \\ -\frac{k_{i3}}{k_{i1}} & 0 & 1 & \cdots & 0 \\ \vdots & & & & \vdots \\ -\frac{k_{in_i}}{k_{i1}} & 0 & 0 & \cdots & 1 \\ -\frac{k_{i(n_i+1)}}{k_{i1}} & 0 & 0 & \cdots & 0 \end{bmatrix}, \qquad B_{i3} = \begin{bmatrix} 0 \\ \vdots \\ 0 \\ 1 \end{bmatrix}.$$

The following theorem states the convergence of sliding mode observer.

Theorem 4.3. *Consider system (4.2.5), and design a sliding mode state and perturbation observer (4.4.9). If assumptions A4.1 ~ A4.3 hold for some value γ_{i1} and γ_{i2}, then given any constant δ_i, gains k_{ij}, and α_{ij}, $j = 1, \cdots, n_i + 1$, can be chosen such that the observer error $\tilde{x}_{ie1}$ converges exponentially into the neighbourhood*

$$\|\tilde{x}_{ie1}\| \leq \delta_i.$$

Proof: Refer to Theorem 3.3.

Remark 4.4.1: Like Theorem 3.3, all poles of A_{i3} are placed to $-\lambda_i$. Thus, gains k_{ij}, $j = 2, 3, \cdots, n_i + 1$ are chosen as

$$\frac{k_{i(j+1)}}{k_{i1}} = C_{n_i}^j \lambda_i^j, \qquad j = 1, 2, \cdots, n_i, \tag{4.4.15}$$

where $C_{n_i}^j = \frac{n_i!}{j!(n_i-j)!}$. Define the change of variables as

$$\tilde{x}_{ij} = \lambda_i^{j-2} z_{ij}, \qquad j = 2, \cdots, n_i + 1. \tag{4.4.16}$$

Equation (4.4.14) can be written in terms of z_i as

$$\dot{z}_i = \lambda_i M_i z_i + B_{i3} \frac{\dot{\Psi}_i}{\lambda_i^{n_i-1}}, \tag{4.4.17}$$

where $z_i = \begin{bmatrix} z_{i2} & \cdots & z_{i(n_i+1)} \end{bmatrix}^T$, and

$$M_i = \begin{bmatrix} -C_{n_i}^1 & 1 & \cdots & \cdots & 0 \\ -C_{n_i}^2 & 0 & 1 & \cdots & 0 \\ \vdots & & & & \vdots \\ -C_{n_i}^{n_i-1} & 0 & 0 & \cdots & 1 \\ -C_{n_i}^{n_i} & 0 & 0 & \cdots & 0 \end{bmatrix}_{n_i \times n_i}.$$

Let matrix P_{i3} be the positive definite solution of the Lyapunov equation $P_{i3}M_i + M_i^T P_{i3} = -I$.

Remark 4.4.2 Bounds for the observer errors $\tilde{x}_{ij}$, $j = 2, \cdots, n_i, n_i + 1$, can be obtained as follows:

$$|\tilde{x}_{ij}| \leq \frac{\delta_i}{\lambda_i^{n_i+1-j}}, \quad j = 2, \cdots, n_i + 1, \ \forall t > t_1. \tag{4.4.18}$$

Remark 4.4.3 The choice of the observer gains can be summarized as follows. α_{ij}, $j = 1, 2, \cdots, n_i + 1$ are chosen to make all poles of the Luenberger observer be real and negative $-\xi$. Thus we have

$$\alpha_{ij} = C_{n_i+1}^j \xi^j, \qquad j = 1, 2, \cdots, n_i + 1, \tag{4.4.19}$$

where $C_{n_i+1}^{j} = \frac{(n_i+1)!}{j!(n_i+1-j)!}$.

For a given value of initial estimation error $\|\tilde{x}_{ie1}(0)\|$, the sliding mode condition will be fulfilled for all t if gain k_{i1} is chosen as

$$k_{i1} \geq \|\tilde{x}_{ie1}(0)\| \sqrt{\frac{\lambda_{\max}(P_{i3})}{\lambda_{\min}(P_{i3})}}. \tag{4.4.20}$$

For a given small positive constant δ_i, λ_i must satisfy

$$\lambda_i \geq \sqrt{\frac{\lambda_{\max}(P_{i3})}{\lambda_{\min}(P_{i3})}} \frac{2\lambda_{\max}(P_{i3})\gamma_{i2}}{(1-\alpha_i)\delta_i}, \tag{4.4.21}$$

where α_i is a constant, $0 < \alpha_i < 1$. Thus, from equations (4.4.15) and (4.4.20), we have

$$k_{i(j+1)} = k_{i1} C_{n_i}^{j} \lambda^j, \qquad j = 1, 2, \cdots, n_i. \tag{4.4.22}$$

4.4.3 Design of combined sliding mode controller-observer

Using the estimate of states to replace the true states, the sliding surface $\hat{S}_{\text{smc}_i}$ for subsystem q_i is defined as:

$$\hat{S}_{\text{smc}_i} = \sum_{j=1}^{n_i} \rho_{ij}(\hat{x}_{ij} - y_{ri}^{(j-1)}) = \sum_{j=1}^{n_i} \rho_{ij}(e_{ij} - \tilde{x}_{ij}), \tag{4.4.23}$$

where coefficients ρ_{ij}, $j = 1, \cdots, n_i - 1$, and $\rho_{in_i} = 1$ are constants and the polynomial $s^{n_i-1} + \rho_{i(n_i-1)}s^{n_i-2} + \cdots + \rho_{i2}s + \rho_{i1}$ is Hurwitzian. As the true states are not available, the sliding surface depends on the estimated states. The actual sliding function is defined in equation (4.4.1) and the error of the sliding surface is

$$\tilde{S}_{\text{smc}_i} = \sum_{j=1}^{n_i} \rho_{ij}\tilde{x}_{ij}. \tag{4.4.24}$$

Control u_i is chosen to enforce $\dot{\hat{S}}_{\text{smc}_i}\hat{S}_{\text{smc}_i} < 0$ outside a prescribed manifold. A desired $\hat{S}_{\text{smc}_i}$ is selected as

$$\dot{\hat{S}}_{\text{smc}_i} = -\zeta_i \hat{S}_{\text{smc}_i} - \varphi_i \,\text{sat}(\hat{S}_{\text{smc}_i}, \epsilon_{c_i}), \tag{4.4.25}$$

where ζ_i and φ_i are control gains, $\text{sat}(\hat{S}_{\text{smc}_i}, \epsilon_{c_i})$ is defined as equation (3.3.8) and used to eliminate the control chattering. In this equation, ϵ_{c_i} represents for the boundary layer thickness of sliding mode controller, as contrasted with the ϵ_{o_i} in the sliding mode observer.

Using the estimated perturbation $\hat{x}_{i(n_i+1)}$ to cancel the nonlinearities, uncertainties and the interactions between subsystems, the sliding mode controller is constructed as

$$u_i = \frac{1}{g_{i0}} \left[y_{ri}^{(n_i)} - \hat{x}_{i(n_i+1)} - \sum_{j=1}^{n_i-1} \rho_{ij} (\hat{x}_{i(j+1)} - y_{ri}^{(j)}) - \zeta_i \hat{S}_{\text{smc}_i} - \varphi_i \, \text{sat}(\hat{S}_{\text{smc}_i}, \epsilon_{c_i}) \right]. \tag{4.4.26}$$

Differentiating equation (4.4.23) along system (4.4.9), and using the reduced error dynamics (4.4.14), one obtains

$$\dot{\hat{S}}_{\text{smc}_i} = \hat{x}_{i(n_i+1)} + g_{i0} u_i - y_{ri}^{(n_i)} + \sum_{j=1}^{n_i-1} \rho_{ij} (\hat{x}_{i(j+1)} - y_{ri}^{(j)}) + \sum_{j=1}^{n_i} \rho_{ij} \frac{k_{ij}}{k_{i1}} \tilde{x}_{i2}, \tag{4.4.27}$$

that, substituted with control (4.4.26), leads to

$$\dot{\hat{S}}_{\text{smc}_i} = \sum_{j=1}^{n_i} \rho_j \frac{k_{ij}}{k_{i1}} \tilde{x}_{i2} - \zeta_i \hat{S}_{\text{smc}_i} - \varphi_i \, \text{sat}(\hat{S}_{\text{smc}_i}, \epsilon_{c_i}). \tag{4.4.28}$$

Therefore, the attractiveness condition of sliding mode controller is

$$\zeta_i \left| \hat{S}_{\text{smc}_i} \right| + \varphi_i > \sum_{j=1}^{n_i} \rho_{ij} \frac{k_{ij}}{k_{i1}} |\tilde{x}_{i2}|, \tag{4.4.29}$$

which, using equation (4.4.12), $k_{i1} > |\tilde{x}_{i2}|_{\max}$, will be fulfilled if

$$\zeta_i \left| \hat{S}_{\text{smc}_i} \right| + \varphi_i \geq k_{i1} \sum_{j=1}^{n_i} \rho_{ij} \frac{k_{ij}}{k_{i1}}. \tag{4.4.30}$$

The above condition is obviously satisfied if gain φ_i is chosen such that

$$\varphi_i \geq k_{i1} \sum_{j=1}^{n_i} \rho_{ij} \frac{k_{ij}}{k_{i1}}, \tag{4.4.31}$$

which, using equation (4.4.15), leads to

$$\varphi_i \geq k_{i1} \sum_{j=1}^{n_i} \rho_{ij} C_{n_i}^{(j-1)} \lambda_i^{(j-1)}. \tag{4.4.32}$$

This condition guarantees the existence of a sliding mode within the boundary layer $|\hat{S}_{\text{smc}_i}| \leq \epsilon_{c_i}$. From equation (4.4.24), we can obtain the error dynamics of the sliding mode as

$$\dot{\hat{S}}_{\text{smc}_i} = \sum_{j=1}^{n_i} \rho_{ij}\tilde{x}_{i(j+1)} - \sum_{j=1}^{n_i} \rho_{ij}\frac{k_{ij}}{k_{i1}}\tilde{x}_{i2}. \tag{4.4.33}$$

Using $S_{\text{smc}_i} = \hat{S}_{\text{smc}_i} + \tilde{S}_{\text{smc}_i}$ and equation (4.4.28), the actual sliding mode dynamics becomes

$$\dot{S}_{\text{smc}_i} + (\zeta_i + \frac{\varphi_i}{\epsilon_{c_i}})S_{\text{smc}_i} = (\zeta_i + \frac{\varphi_i}{\epsilon_{c_i}})\sum_{j=1}^{n_i} \rho_{ij}\tilde{x}_{ij} + \sum_{j=1}^{n_i} \rho_{ij}\tilde{x}_{i(j+1)}. \tag{4.4.34}$$

It can be seen that the driving term of $\hat{S}_{\text{smc}_i}$-dynamics are reduced to the sum of the estimation errors of states and the perturbation. The bound of the output track error can also be obtained as follows:

$$\begin{aligned} |\hat{S}_{\text{smc}_i}| \leq \epsilon_{c_i} \quad &\Rightarrow \quad |\hat{S}_{\text{smc}_i} - \tilde{S}_{\text{smc}_i}| \leq \epsilon_{c_i} \\ &\Rightarrow \quad |S_{\text{smc}_i}| \leq |\tilde{S}_{\text{smc}_i}| + \epsilon_{c_i} \\ &\Rightarrow \quad |S_{\text{smc}_i}| \leq |\textstyle\sum_{j=1}^{n_i} \rho_{ij}\tilde{x}_{ij}| + \epsilon_{c_i} \\ &\leq \tfrac{\delta_i}{\lambda_i^{n_i+1}} \textstyle\sum_{j=2}^{n_i} \rho_{ij}\lambda_i^j + \epsilon_{c_i}, \ \forall t > t_1, \end{aligned} \tag{4.4.35}$$

where t_1 is the time constant defined in equation (3.4.22). If the polynomial gains ρ_{ij} in equation (4.4.1) are chosen to make all poles of polynomial equal to $-\lambda_{c_i}$, thus, from equation (3.3.13), we have

$$|x_i^{(j)}(t) - x_{di}^{(j)}(t)| \leq (2\lambda_{c_i})^j \frac{\epsilon_{c_i}}{\lambda_{c_i}^{n_i}} + \frac{\delta_i}{\lambda_i^{n_i+1}} \sum_{l=2}^{n} (\frac{\lambda_i}{\lambda_{c_i}})^l C_{n-1}^l, \ \ j = 0, 1, n-1. \tag{4.4.36}$$

From the previous analysis, the Lyapunov function candidate can be defined as $V = \sum_{i=1}^{N} V_i$, where $V_i = \frac{1}{2}\hat{S}_{\text{smc}_i}^2$, for the large-scale system (4.2.1), thus the stability analysis of the whole system can be summarized as follows.

Theorem 4.4. *For large-scale nonlinear system (4.2.1), let assumptions A4.1 ~ A4.3 hold. For each subsystem q_i, design observer (4.4.9), with gains properly chosen properly according to equations (4.4.19) and (4.4.22), and controller*

as described by equation (4.4.26) with gains φ_i are chosen properly according to (4.4.32). Then for any bounded initial condition, the system state x_i is bounded and will track the desired x_{ri} when S_{smc_i} converge to boundary layer $|S_{\text{smc}_i}| < \epsilon_{c_i}$, and the state track error $y_i(t) - y_{ri}(t)$ satisfies equation (4.4.36).

4.4.4 Decentralized nonlinear adaptive control with continuous output feedback and SMSPO

In this section, design of a decentralized nonlinear adaptive control using continuous output feedback and the state and perturbation estimates from SMSPO for subsystem q_i is discussed. The estimate of perturbation $\hat{x}_{i(n_i+1)}$ is used to compensate the nonlinearities, uncertainties and interactions of subsystem q_i so as to achieve the decentralized control of global system. Utilizing the estimated states instead of the real ones, a linear continuous feedback controller, rather than a sliding mode controller, is designed for the equivalent linearized subsystem. The controller has the form of:

$$u_i = v_i/g_{i0} - \hat{x}_{i(n_i+1)}/g_{i0} \tag{4.4.37}$$

$$v_i = -K_i\hat{x}_i, \tag{4.4.38}$$

where $K_i = [k_{i1}, k_{i2}, \cdots, k_{in_i}]^T$ is the linear feedback controller gains, which are chosen to make the matrix $A_{i0} = A_i - B_iK_i$ Hurwitzian.

If the attractive condition (4.4.12) is satisfied, the sliding mode observer (4.4.9) will reach the sliding surface and then stay on it, that is $\tilde{x}_{i1} = 0$ and $\dot{\tilde{x}}_{i1} = 0$ and the dynamics on the sliding surface satisfies equations (4.4.14). Noting that $\hat{x}_{ie1} = [\hat{x}_{i2}, \hat{x}_{i3}, \cdots, \hat{x}_{i(n_i+1)}]^T$, control (4.4.37) and (4.4.38) can be represented as:

$$u_i = \frac{1}{g_{i0}}(-x_{i(n_i+1)} - K_ix_i + K_{i1}\tilde{x}_{ie1}), \tag{4.4.39}$$

where $K_{i1} = [k_{i2},\ k_{i3}\ \cdots\ k_{in_i},\ 1]^T$.

Substituting control (4.4.37) into system (4.2.1) and using the variables transform given by equation (4.4.16), the closed-loop system with controller and observer can be represented by

$$\dot{x}_i = A_{i0}x_i + B_iK_{i1}z_i, \tag{4.4.40}$$

$$\dot{z}_i = \lambda_i M_i z_i + B_{i1}\frac{\dot{\Psi}_i(\cdot)}{\lambda_i^{n_i-1}}. \tag{4.4.41}$$

The stability analysis of system (4.4.40) and (4.4.41) is similar to that discussed in Chapter 3. Here, the results are summarized briefly as following theorem.

Theorem 4.5. *Consider large-scale system (4.2.1), for each subsystem q_i design a sliding mode state and perturbation observer (4.4.9), choose the observer gains described in equations (4.4.19) ~ (4.4.22), and let assumptions A4.1 ~ A4.3 hold. Define control as given by equations (4.4.37) and (4.4.38), then the origin of system (4.4.40) and (4.4.41) is stable.*

4.5 Application of decentralized nonlinear control in input/output linearization of MIMO nonlinear system

In this section, the proposed decentralized nonlinear control schemes are applied to the input/output linearization of MIMO nonlinear system. After the nonlinear system is transferred to a nonlinear normal form, a state and perturbation observer is designed for the subsystem. By using the estimate of system states and perturbation, the input/output linearization will be achieved without the detail system model and with output feedback for MIMO nonlinear system.

The method of input/output linearization has been well described in [1]. A

multi-input multi-output (MIMO) affine nonlinear system is represented by

$$\dot{x} = f(x) + \sum_{j=1}^{m} g_j(x)u_j \tag{4.5.1}$$

$$y = h(x), \tag{4.5.2}$$

where, $x \in \mathcal{R}^n$, $u \in \mathcal{R}^m$, $y \in \mathcal{R}^m$, $f : \mathcal{R}^n \to \mathcal{R}^n$, $g_j \in g$ and $g : \mathcal{R}^n \to \mathcal{R}^{n\times m}$, $h : \mathcal{R}^n \to \mathcal{R}^m$, f, g and h are assumed as C^∞ functions of their arguments, defined on $\mathcal{R}^n$.

In the input/output linearization procedure, the output y_i is differentiated, with respect to time, several times until at least one of the control input u_j appears.

The ith subsystem has a r_ith-order relative degree, if r_i is the smallest integer such that, for at least one of $g_j(x), j = 1, \cdots, m$,

- $\mathcal{L}_{g_j}(\mathcal{L}_f^k(h_i(x))) = 0$, $\forall\, x$ in a neighbourhood of x_0, $k = 0, 1, \cdots, r_i - 2$;
- $\mathcal{L}_{g_j}(\mathcal{L}_f^{r_i-1}(h_i(x))) \neq 0$, $\forall\, x$ in a neighbourhood of x_0;

then the r_ith derivative of y_i with respect to time could be written as

$$\frac{d^{r_i}y_i}{dt^{r_i}} = \mathcal{L}_f^{r_i}(h_i(x)) + \sum_{j=1}^{m} \mathcal{L}_{g_j}(\mathcal{L}_f^{r_i-1}(h_i(x)))u_j, \tag{4.5.3}$$

where $x_0 \in \mathcal{R}^n$, $\mathcal{L}_f(\phi(x)) : \mathcal{R}^n \to R$ and $\mathcal{L}_{g_j}(\phi(x)) : \mathcal{R}^n \to R$, representing the Lie derivative of $\phi(x)$ with respect to $f(x)$ and $g_j(x)$ respectively, and

$$\begin{aligned} \mathcal{L}_f^0(h_i(x)) &= h_i(x) \\ \mathcal{L}_f^k(h_i(x)) &= \left[\frac{\partial}{\partial x}\mathcal{L}_f^{k-1}(h_i(x))\right] f(x) \\ \mathcal{L}_{g_j}\left(\mathcal{L}_f^k(h_i(x))\right) &= \left[\frac{\partial}{\partial x}\mathcal{L}_f^k(h_i(x))\right] g_j(x). \end{aligned}$$

Equation (4.5.3) can be written in a matrix form as follows:

$$D(d/dt)y = A(x) + B(x)u, \tag{4.5.4}$$

where

$$A(x) = [\mathcal{L}_f^{r_1}(h_1(x)) \cdots \mathcal{L}_f^{r_m}(h_m(x))]^T,$$

$$B(x) = \begin{bmatrix} \mathcal{L}_{g_1}(\mathcal{L}_f^{r_1-1}(h_1(x))) & \cdots & \mathcal{L}_{g_m}(\mathcal{L}_f^{r_1-1}(h_1(x))) \\ \mathcal{L}_{g_1}(\mathcal{L}_f^{r_m-1}(h_m(x))) & \cdots & \mathcal{L}_{g_m}(\mathcal{L}_f^{r_m-1}(h_m(x))) \end{bmatrix},$$

and $D(d/dt) \equiv \text{diag}[d^{r_i}/dt^{r_i}]$.

If $B(x)$ is nonsingular, a control law is obtained in the following form

$$u = B(x)^{-1}[-A(x) + v], \tag{4.5.5}$$

where $v \in \mathcal{R}^m$ is a new input vector. The control law of equation (4.5.5) yields m de-coupled linear SISO systems:

$$D(d/dt)y = v. \tag{4.5.6}$$

It should be mentioned that the controller (4.5.5) works based on accurate mathematical cancellation of the nonlinear terms $A(x)$ and $B(x)$. Exact cancellation is almost impossible due to model simplification, parameter uncertainty, and computational errors. If system uncertainties are present, the system can no longer be linearized as that shown in equation (4.5.6).

In this section, a perturbation is introduced to represent the combined effect of system nonlinearities, uncertainties and external disturbances of the ith subsystem. Then the perturbation term is represented by a fictitious state and an extended-order sliding mode observer is employed to estimate the system states and the fictitious state. The estimate of the fictitious state is used to achieve the cancellation of system nonlinearities and perturbations, which realize the system decoupling and the input/output linearization of the ith nonlinear subsystem. These are discussed as follows.

For the ith subsystem of system (4.5.4), let

$$\Psi_i(x,u,t) = \mathcal{L}_f^{r_i}(h_i(x)) + \sum_{j=1,\neq i}^{m} \mathcal{L}_{g_j}(\mathcal{L}_f^{r_i-1}(h_i(x)))u_j + (b_i(x) - b_{i0})u_i, \tag{4.5.7}$$

then equation (4.5.3) can be rewritten as

$$\frac{d^{r_i}y_i}{dt^{r_i}} = \Psi_i(x,u,t) + b_{i0}u_i, \tag{4.5.8}$$

where $\Psi(x,u,t)$ is defined as a fictitious state, e.g. system perturbation which represents the combined effect of the system nonlinearties, uncertainties and external disturbances of the ith subsystem; $b_i(x) = \mathcal{L}_{g_i}(\mathcal{L}_f^{r_i-1}(h_i(x)))$ and b_{i0} is a constant control gain which will be determined later.

Thus for the ith subsystem, the same controller as described in sections 4.3 and 4.4 can be designed. If the internal dynamic of MIMO system is asymptotically stable, the whole system is stable under the decentralized controller. Thus the input/output linearization will be achieved without the detail system model and with only partial state feedback for MIMO nonlinear system.

4.6 Simulation results

Consider a system which is composed of two inverted pendulums on two carts, interconnected by a moving spring, shown in Figure 4.1., This system was studied as an example in the literature of decentralized control [141, 139, 135]. Let assume that the pivot position of the moving spring is a function of time and it can change along the full length of the pendulums. For this example this motion of the carts is specified as sinusoidal trajectories. The input to each pendulum is the torque u_i, $i = 1,2$, applied at the pivot point. The objective of the decentralised adaptive controller is to control each pendulum with mass independently so that each pendulum tracks its own desired reference trajectory while the connected spring and carts are moving.

Defining the state vectors $x_1 = (x_{11}, x_{12})^T$ and $x_2 = (x_{21}, x_{22})^T$, where $x_{11} = \theta_1$, $x_{12} = \dot{\theta}_1$, $x_{21} = \theta_2$, $x_{22} = \dot{\theta}_2$. The dynamic equations of the system

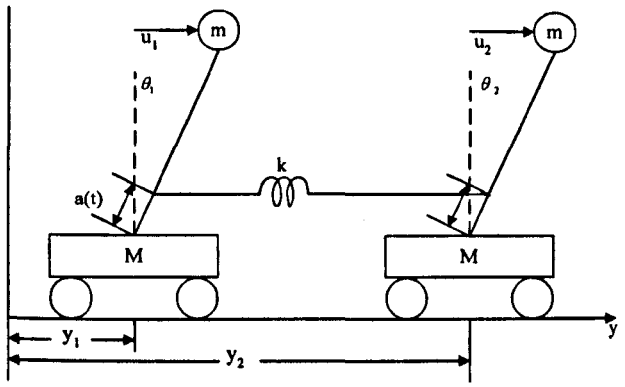

Figure 4.1: Two inverted pendulums on carts

can be described as

$$q_1: \begin{cases} \dot{x}_{11} = x_{12} \\ \dot{x}_{12} = \left(\frac{g}{cl} - \frac{ka(t)(a(t)-cl)}{cml^2}\right) x_{11} + \frac{1}{cml^2} u_1 \\ \qquad + \frac{ka(t)(a(t)-cl)}{cml^2} x_{21} - \beta_1 x_{12}^2 - \frac{k(a(t)-cl)}{cml^2}(s_1(t) - s_2(t)) \end{cases},$$

$$q_2: \begin{cases} \dot{x}_{21} = x_{22} \\ \dot{x}_{22} = \left(\frac{g}{cl} - \frac{ka(t)(a(t)-cl)}{cml^2}\right) x_{21} + \frac{1}{cml^2} u_2 \\ \qquad + \frac{ka(t)(a(t)-cl)}{cml^2} x_{11} - \beta_1 x_{22}^2 - \frac{k(a(t)-cl)}{cml^2}(s_2(t) - s_1(t)) \end{cases}, \tag{4.6.1}$$

where u_1 and u_2 are the control torques applied to the pivot point of each pendulum, $\beta_1 = m/M \cdot \sin(x_{11})$, $\beta_2 = m/M \cdot \sin(x_{21})$, l the length of of the pendulum, $c = m/(m+M)$, k and g spring and gravity constants, respectively. In the simulation study, let choose $g = l = 1$, $k = 1$, $m = M = 10$, then $c = 0.5$ and $\beta_i \leq 1$. The available system outputs are $y_1 = x_{11}$ and $y_2 = x_{21}$. The desired system outputs are chosen as $y_{r1} = \sin(3t)$ and $y_{r2} = \sin(t)$. Let $s_1(t) = \sin(\omega_1 t)$, and $s_2(t) = L + \sin(\omega_2 t)$, where $\omega_1 \neq \omega_2$ and L is the natural length of the spring. We also select $L = 2$ and set $a(t) = \sin(5t)$, $\omega_1 = 2$, $\omega_2 = 3$. We assume that the control gain is known so that we choose $g_{10} =$

$g_{20} = g_1 = g_2 = \frac{1}{cml^2} = 0.2$. For subsystem q_1 and q_2, we have perturbation

$$\begin{aligned}
\Psi_1 &= \left(2 - \tfrac{1}{5}\sin(5t)(\sin(5t) - 0.5)\right) x_{11} + \tfrac{1}{5}\sin(5t)(\sin(5t) - 0.5)x_{21} \\
&\quad - \sin(x_{11})x_{12}^2 - \tfrac{1}{5}(\sin(5t) - 0.5)(\sin(2t) - \sin(3t) - 2) \\
&\leq 2.1x_{11} + x_{12}^2 + 0.3x_{21} + 1.2, \\
\Psi_2 &= \left(2 - \tfrac{1}{5}\sin(5t)(\sin(5t) - 0.5)\right) x_{21} + \tfrac{1}{5}\sin(5t)(\sin(5t) - 0.5)x_{11} \\
&\quad - \sin(x_{21})x_{22}^2 - \tfrac{1}{5}(\sin(5t) - 0.5)(2 + \sin(3t) - \sin(2t)) \\
&\leq 2.1x_{21} + x_{22}^2 + 0.3x_{11} + 1.2.
\end{aligned}$$

Case 1: Decentralized nonlinear adaptive controller via HGSPO

The parameters of the third-order high gain observer (4.3.1) are chosen as: $\alpha_{i1} = 300$, $\alpha_{i2} = 2.7 \times 10^5$, $\alpha_{i3} = 1 \times 10^6$, $\epsilon_i = 0.1$, $i = 1, 2$. The parameters of controller (4.3.5) and (4.3.6) are chosen as: $k_{i1} = 100$, $k_{i2} = 20$,$i = 1, 2$. Figures 4.2 and 4.3 show simulations results where both subsystems are controlled with DNAC-HGSPO . Figures 4.4 and 4.5 show the estimates of the states and perturbation of subsystem q_1.

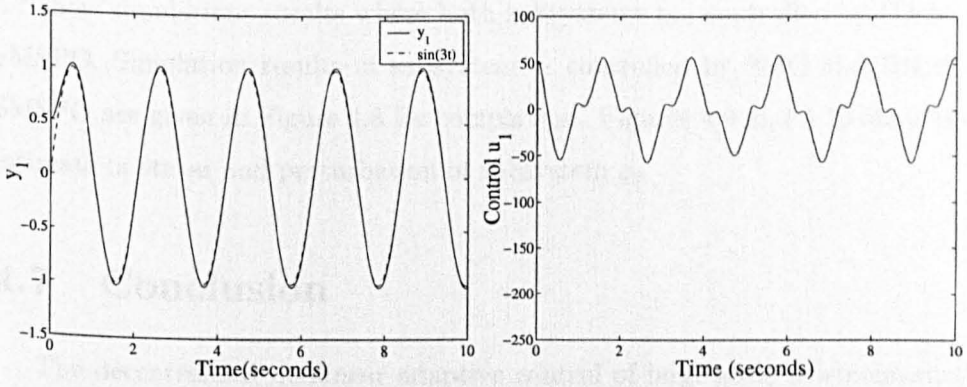

(a) y_1 (b) u_1

Figure 4.2: System responses of q_1 with the DNAC-HGSPO

Case 2: Decentralized nonlinear adaptive controller controller via SMSPO

The parameters of third-order sliding mode observer (4.4) are chosen as: $\alpha_{i1} = 150$, $\alpha_{i2} = 7.5 \times 10^3$, $\alpha_{i3} = 1.25 \times 10^4$, $\epsilon_{o_i} = 0.01$, $k_{i1} = 10$, $k_{i2} =$

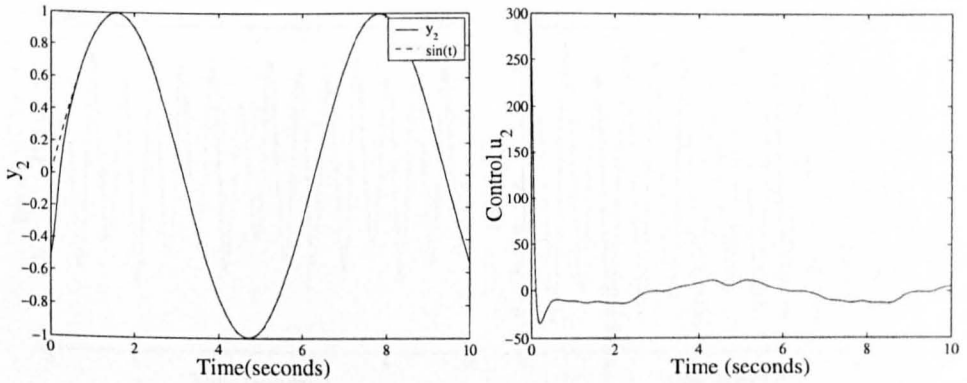

(a) y_2 (b) u_2

Figure 4.3: System responses of q_2 with the DNAC-HGSPO

$k_{i2} = 9\times10^5$, $i = 1, 2$. The parameters of DNAC-SMSPO (4.4.26) are chosen as: $\rho_{i1} = 20$, $\rho_{i2} = 1$, $\zeta_i = 2$, $\varphi_i = 5$, $\epsilon_{c_i} = 0.1$, $i = 1, 2$. Parameters of decentralized SMC (4.4.3) are chosen as same as DNAC-SMSPO (4.4.26). Figures 4.6 and 4.7 show simulations results where both subsystems are controlled by DNAC-SMSPO. Simulation results of subsystem q_1 controlled by SMC and DNAC-SMSPO are given in Figure 4.8 for comparison. Figures 4.9 and 4.10 show the estimate of states and perturbation of subsystem q_2.

4.7 Conclusion

The decentralized nonlinear adaptive control of large-scale interconnected systems via state and perturbation observer has been investigated in this chapter. Two kinds of state and perturbation observers, high gain observer and sliding mode observer, have been studied respectively for estimating the nonlinearities, uncertainties and interactions of subsystems. Three control schemes, decentralized nonlinear adaptive control with high gain observer, decentralized nonlinear adaptive sliding mode control with sliding mode observer and decen-

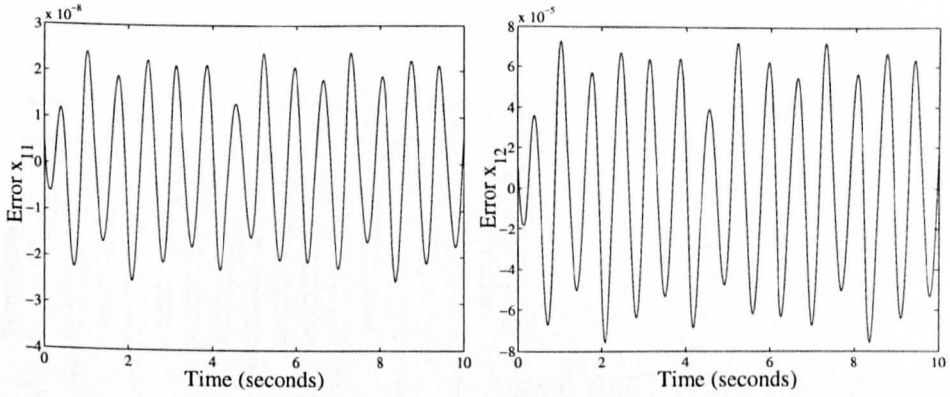

(a) $\tilde{x}_{11}$ (b) $\tilde{x}_{12}$

Figure 4.4: High gain observer responses of q_1

tralized nonlinear adaptive control with continuous feedback control and sliding mode observer, have been developed together with the study of their stability analysis. These control schemes have also been applied to the input/output linearization of MIMO nonlinear systems which leads to decoupling of the large-scale system. Finally, the design of decentralized nonlinear adaptive controller for the inverted double pendulums on carts, without using the velocity measurements and system model, has been undertaken.

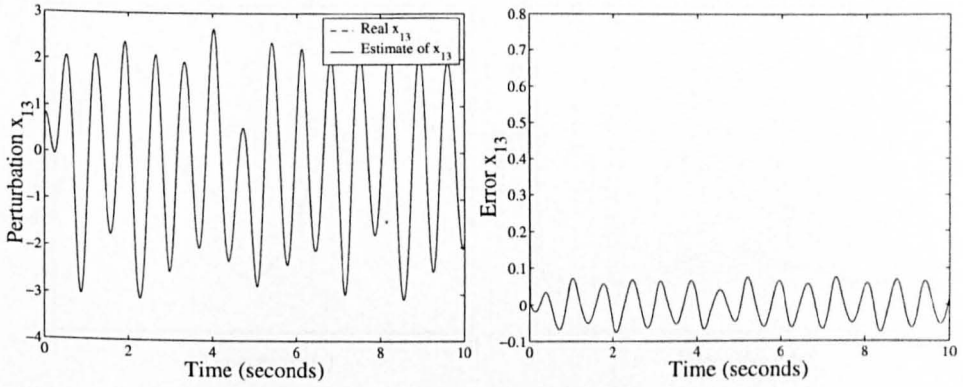

(a) Ψ_1 (b) $\tilde{\Psi}_1$

Figure 4.5: High gain observer responses of q_1

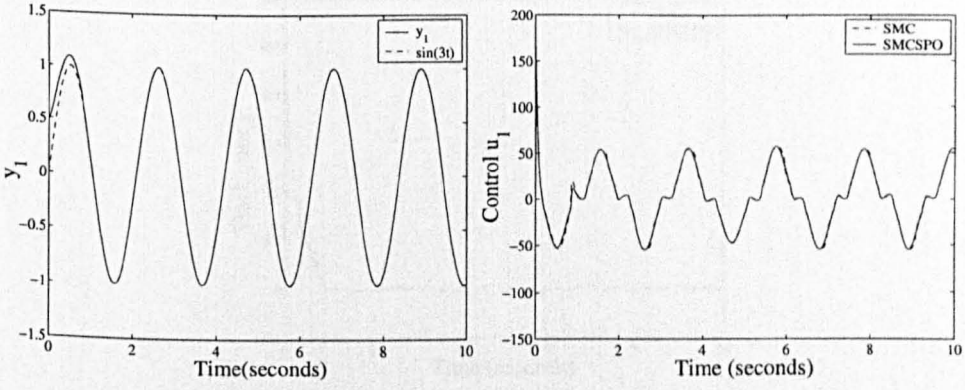

(a) y_1 (b) u_1

Figure 4.6: System responses of q_1 with the DNAC-SMSPO

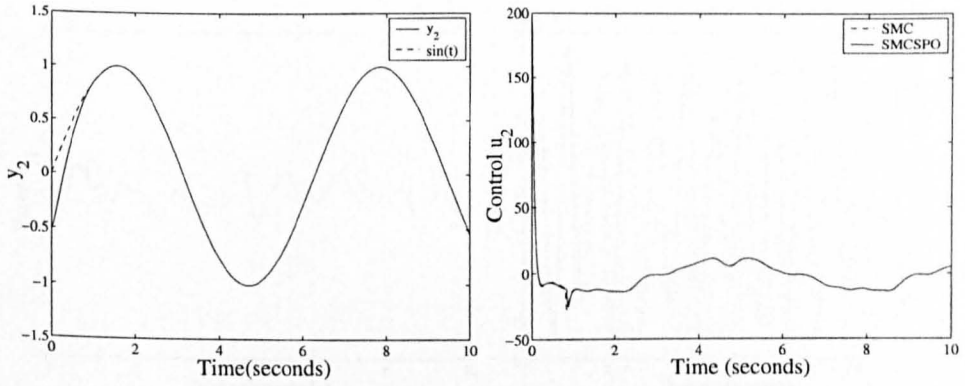

(a) y_2 (b) u_2

Figure 4.7: System responses of q_2 with the DNAC-SMSPO

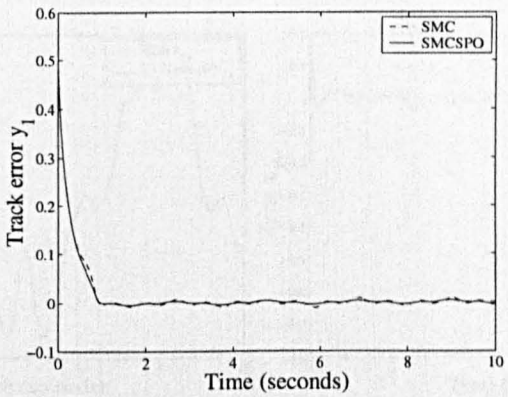

$y_1 - y_{r1}$

Figure 4.8: Tracking error comparing between SMC and DNAC-SMSPO

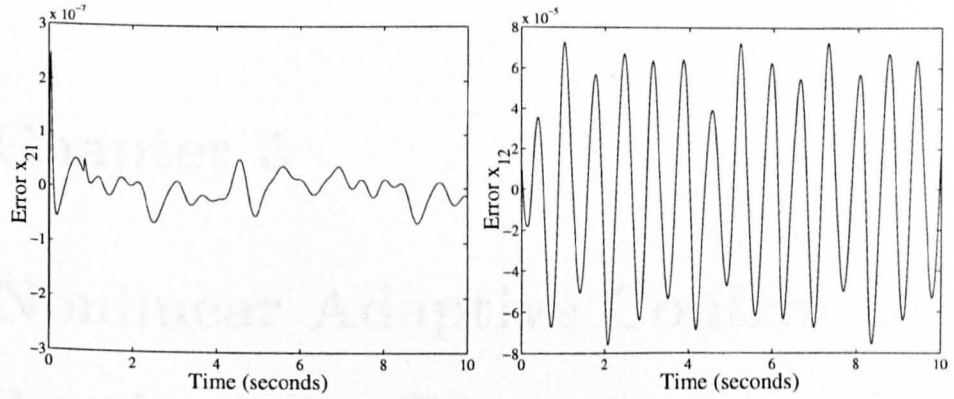

(a) $\tilde{x}_{21}$ (b) $\tilde{x}_{22}$

Figure 4.9: Sliding mode observer responses of q_2 with the SMSPO

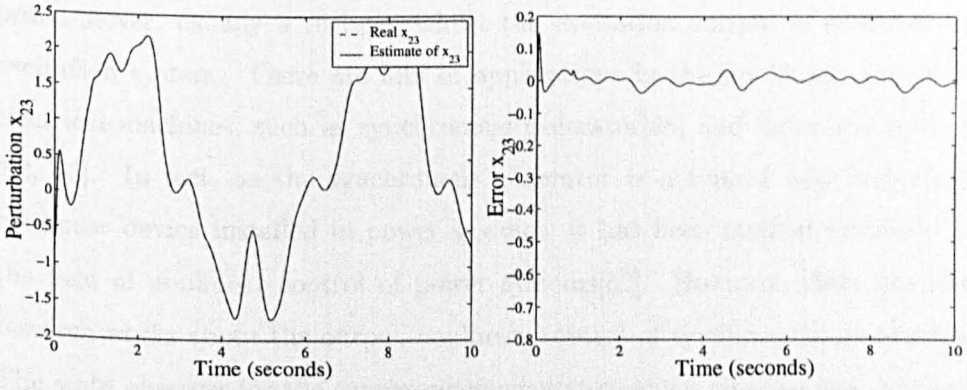

(a) Ψ_1 (b) $\tilde{\Psi}_1$

Figure 4.10: Sliding mode observer responses of q_2 with the SMSPO

Chapter 5

Nonlinear Adaptive Control Of Synchronous Generators

5.1 Introduction

Synchronous generator is used almost exclusively in power systems as a source of electrical energy. The generator is supplied with real power for a prime mover, usually a turbine, whilst the excitation current is provided by excitation system. There are lots of applications in the nonlinear control of electrical machines, such as synchronous generator[85] and induction motors [92, 93]. In fact, as the synchronous generator is a typical and important nonlinear device installed in power systems, it has been studied intensely in the field of nonlinear control of power systems[82]. However, there are less research works about the output nonlinear control of synchronous generators. The state observer for the synchronous generator which requires the accurate nonlinear model was studied and applied to the nonlinear field voltage control for generators in [83, 84].

This chapter investigates the application of the adaptive nonlinear control (NAC) for the excitation control of synchronous generators. The nonlinear

adaptive control is basically an input/output feedback linearizing control of nonlinear systems but it employs output feedback and perturbation estimation. An extended-order sliding mode observer is used to estimate system states and perturbation. The estimate of states and perturbation allows the input/output linearization of the nonlinear system without the requirement of accurate model. This constitutes a real-time compensation mechanism against the uncertainties and perturbations. The designed controller is able to deal with the uncertainties of parameters, unknown system dynamics and external disturbances. The new NAC has advantages in simple structure and robust performance.

The synchronous generator with an Automatic Voltage Regulator (AVR) installed for regulation of generator terminal voltage is considered. Only one measurement, generator relative rotor angle, is needed to form feedback control. The design of NAC does not need an accurate power system model and other measurements, but it can provide better control performance, compared with the state feedback linearization control (FLC) which relies on the full system states and detailed nonlinear system model.

Simulation studies based on a single-machine quasi-infinite bus power system are undertaken to evaluate the proposed approach. The simulation results show that the NAC can provide superior performance in comparison with that obtained from the conventional model based state feedback linearizing controller. The chapter is organized as follows. Section 5.2 describes the generator model in a single machine infinite bus power system. The design of the nonlinear adaptive excitation controller is discussed in Section 5.3. The state feedback linearizing controller is also included in Section 5.3 for comparison. The simulation results are presented in Sections 5.4 and 5.5 concludes the chapter.

5.2 Synchronous generator model

The controller design is undertaken in a single-machine infinite-bus system which is illustrated in Figure 5.1. The generator is connected to an infinite bus through a transformer and two parallel transmission lines. A third-order simplified model, called one axis or E'_q-model, is adopted for the nonlinear state feedback linearization control of synchronous generators. As the regulation of generator terminal voltage is also an important object of the generator excitation control, most of the modern generators are equipped with an Automatic Voltage Regulator (AVR). The AVR is also included in the system equations. The whole system dynamics are described as follows:

$$\begin{cases} \dot{\delta} &= \omega - \omega_0 \\ \dot{\omega} &= \frac{\omega_0}{2H}[P_m - \frac{D}{\omega_0}(\omega - \omega_0) - P_e] \\ \dot{E}'_q &= \frac{1}{T'_{do}}(u + E_{f0} - E_q + V_r) \\ \dot{V}_r &= \frac{K_a}{T_a}(V_{ref} - V_t) - \frac{V_r}{T_a}, \end{cases} \tag{5.2.1}$$

where

$$\begin{aligned} P_e &= E'_q I_q + (X_q - X'_d) I_d I_q \\ I_d &= \frac{1}{X'_{ds}}\left(E'_q - V_s \cos(\delta)\right) \\ I_q &= \frac{V_s \sin(\delta)}{X_{qs}} \\ E_q &= E'_q + (X_d - X'_d) I_d \\ V_t &= \sqrt{V_d^2 + V_q^2} \\ V_d &= X_q I_q \\ V_q &= E'_q - X'_d I_d, \end{aligned}$$

where δ denotes the relative rotor angle, in rad; ω the generator speed, in rad/s; ω_0 the system speed, in rad/s; E_q and E'_q the transient voltage and voltage behind the quadrature-axis, respectively; P_m the mechanical power input from the prime mover and assumed to be constant, in $p.u.$; P_e the electrical

power output of the generator, in *p.u.*; H the inertia coefficient of rotor, in seconds; T'_{do} the direct axis transient short circuit time constant, in seconds; D the damping constant of the generator, in *p.u.*; X_d, X'_d the synchronous and transient impedances in the d-axis, respectively ; X_q the synchronous impedance in the q-axis; $X'_{ds} = X'_d + X_T + X_s$, $X_{qs} = X_q + X_T + X_s$, X_T and X_s the impedances of the transformer and transmission line, respectively; u the excitation control, in *p.u.*; I_d and I_q the generator currents in the d-axes and q-axes, respectively; V_d and V_q the generator terminal voltage in the d-axes and q-axes, respectively; V_t and V_{ref} the generator terminal voltage and its reference value, respectively; V_r, K_a and T_a the control output, control gain and time constant of AVR, respectively; E_{f0} the initial excitation voltage and V_s the voltage of the infinite bus.

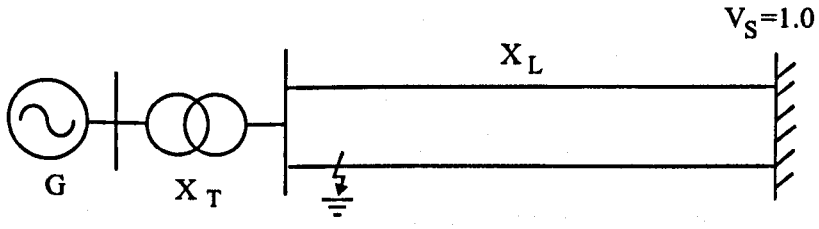

Figure 5.1: The single-machine infinite-bus power system

5.3 Nonlinear adaptive controller design

By defining state variables as :

$$x = [x_1 \ x_2 \ x_3 \ x_4]^\top = [\delta - \delta_0 \ \ \omega - \omega_0 \ \ E'_q \ \ V_r]^\top,$$

the state equations of system (5.2.1) can be rewritten in a matrix form as

$$\begin{aligned}\dot{x} &= \begin{bmatrix} x_2 \\ \frac{\omega_0}{2H}\left[P_m - \frac{D}{\omega_0}x_2 - P_e(x)\right] \\ \frac{1}{T'_{do}}\left[E_{f0} - E_q(x) + x_4\right] \\ \frac{K_a}{T_a}\left[V_{\text{ref}} - V_t(x)\right] - \frac{x_4}{T_a} \end{bmatrix} + \begin{bmatrix} 0 \\ 0 \\ \frac{1}{T'_{do}} \\ 0 \end{bmatrix} u \\ y &= h(x) = x_1. \end{aligned} \tag{5.3.1}$$

For this system, we have

$$\begin{aligned} \mathcal{L}_g h(x) &= 0 \\ \mathcal{L}_f h(x) &= x_2 \\ \mathcal{L}_g\mathcal{L}_f h(x) &= 0 \\ \mathcal{L}_f^2 h(x) &= \frac{\omega_0}{2H}\left[P_m - \frac{D}{\omega_0}x_2 - P_e(x)\right] \\ \mathcal{L}_g\mathcal{L}_f^2 h(x) &= \frac{-\omega_0 V_s \sin x_1 + \delta_0}{2HT'_{do}X'_{ds}}. \end{aligned}$$

As $\mathcal{L}_g\mathcal{L}_f^2 h(x) \neq 0, \quad \forall \delta \neq k\pi, \quad k = 0, 1, 2, \cdots$, system (5.3.1) has relative degree $r = 3$. The 3rd-order derivative of y with respect to time could be obtained as

$$\frac{d^3 y}{dt^3} = a(x) + b(x)u, \tag{5.3.2}$$

where

$$\begin{aligned} a(x) &= \mathcal{L}_f^3 h(x) = -\frac{\omega_0 V_s}{2HX'_{ds}} x_2 x_3 \cos(x_1 + \delta_0) \\ &+ \frac{D\dot{x}_2}{2H} - \frac{\omega_0 V_s^2 (X'_{ds} - X_{qs})}{2HX_{qs}X'_{ds}} x_2 \cos(2x_1 + 2\delta_0) \\ &+ \frac{\omega_0 V_s \sin(x_1 + \delta_0)(-E_{f0} + E_q(x) - x_4)}{2HT'_{do}X'_{ds}}, \end{aligned} \tag{5.3.3}$$

$$b(x) = \mathcal{L}_g\mathcal{L}_f^2 h(x) = \frac{-\omega_0 V_s \sin x_1 + \delta_0}{2HT'_{do}X'_{ds}}. \tag{5.3.4}$$

Define the system perturbation as

$$\Psi(x, u, t) = a(x) + (b(x) - b_0)u, \tag{5.3.5}$$

then equation (5.3.2) can be rewritten as

$$\frac{d^3y}{dt^3} = \Psi(x,u,t) + b_0 u \tag{5.3.6}$$

where b_0 is a constant and chosen as $b_0 < b(x)/2$, as $b(x)$ is negative and bounded when the synchronous generator operates under a normal operation condition.

By defining new state variables: $z_1 = y$, $z_2 = dy/dt = x_2$, $z_3 = d^2y/dt^2 = \dot{x}_3$ and $z_4 = \Psi(\cdot)$, a new system equation is obtained as

$$\begin{cases} \dot{z}_1 &= z_2 \\ \dot{z}_2 &= z_3 \\ \dot{z}_3 &= z_4 + b_0 u \\ \dot{z}_4 &= \dot{\Psi}(\cdot) \\ y &= z_1. \end{cases} \tag{5.3.7}$$

A fourth-order sliding mode observer is designed as discussed in section (3.4.1). As the generator speed will not shift far away from the synchronous speed even when a fault occurs, the maxima of $|\tilde{z}_2|_{\max}$ is relative small. Thus it is easy to choose the gain k_1 so as to guarantee the existence of sliding mode referring to equations (3.4.3) and (3.4.4). With the estimates of states and perturbation, a control law described by equations (3.4.57) and (3.4.58) can be obtained:

$$u = v/b_0 - \hat{z}_4/b_0, \tag{5.3.8}$$

$$v = -a_1\hat{z}_1 - a_2\hat{z}_2 - a_3\hat{z}_3. \tag{5.3.9}$$

As the relative degree of system (5.3.1) is $r = 3$, the remaining internal system dynamics is

$$\dot{V}_r = \frac{K_a}{T_a}(V_{\text{ref}} - V_t(x)) - \frac{V_r}{T_a}.$$

Note that when $z_i = 0$, $i = 1,2,3$, $V_t(x) = V_{\text{ref}}$, thus the zero dynamics of system (5.3.1) is :

$$\dot{V}_r = -\frac{1}{T_a}V_r.$$

It is exponentially stable. The structure of the NAC connected to the generator excitation system together with an AVR is shown in Figure 5.2.

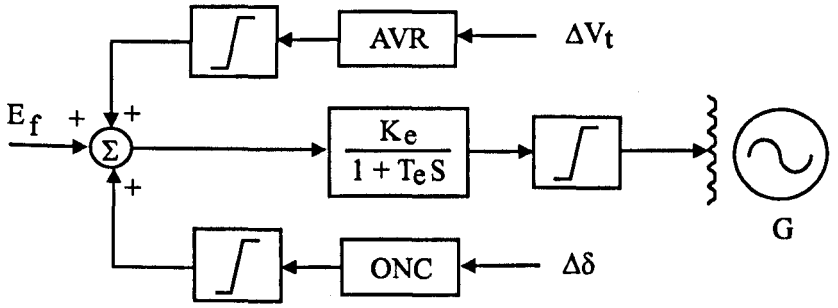

Figure 5.2: The excitation control system with NAC and AVR equipped

5.3.1 Design of state feedback linearizing controller

The design of the state feedback linearizing control (FLC) of the synchronous generator has been well studied [104, 87, 114]. An AVR is always combined directly with FLC to achieve the regulation of the terminal voltage. By subtracting the AVR in equation (5.3.1), the control of FLC, u_{flc}, can be obtained from equations (5.3.2) as:

$$u_{\text{flc}} = \frac{v - a(x)}{b(x)} - V_r. \tag{5.3.10}$$

Control (5.3.10) can be realized by the measurable local variables of the generator as follows [87, 114]:

$$\begin{aligned} u_{\text{flc}} = &-E_{f0} + V_t + \frac{Q_e X_d}{V_t} + T'_{do}\frac{d}{dt}\left(V_t + \frac{Q_e X'_d}{V_t}\right) \\ &-\frac{T_{do}}{P_e}\left(V_t + \frac{Q_e X'_d}{V_t}\right)\left(\frac{dP_e}{dt} + \frac{D}{\omega_0}\dot{\omega} + \frac{2H}{\omega_0}v\right) \end{aligned} \tag{5.3.11}$$

where Q_e is the output reactive power of generator, $v = -a_1 z_1 - a_2 z_2 - a_3 z_3$ is the control of the equivalent linear system.

5.3.2 Remarks

Remark 5.1: It is assumed that the synchronous machine is stable under a proper control. Thus the system states and perturbation term are bounded so as to guarantee the existence of appropriate gains of the sliding mode observer.

Remark 5.2: The NAC has great merit in that only one variable measurement, relative rotor angle, is required for implementation of the nonlinear control. There are some methods available now for measuring the relative rotor angle [142]. Using another measurable variable, such as the rotor speed, is also under investigation.

Remark 5.3: It is well known that the AVR can inject negative damping into the system while the power system operates at high power loading with a leading power factor, in particular in a long distance tie-line transmission system. The nonlinearity injected into the system by adding the AVR was not considered in the design of the previous state feedback linearizing controllers. In fact, when the rotor angle is chosen as the system output and the AVR is installed, the synchronous generator cannot be exactly input-to-state linearized. It only can be input/output linearized as in the NAC design procedure.

Remark 5.4: Regarding a real power system, the following three aspects should be considered in design: (1) the fifth-order, or even seventh-order, differential equation may be required as a accurate model to represent the dynamics of a synchronous generator; (2) The mechanical power P_m is an input of the system, and, in principle, it can be used for control although its dynamics is extremely slow compared with the fast-acting dynamics of the excitation input u. The mechanical power input should be considered as an external disturbance; and (3) V_s and X_s are two parameters which characterize the external network and they are uncertain in power system operation. If these three factors were considered in FLC design, the system nonlinearity could not be cancelled completely by the FLC. This will result in degradation of the control performance

inevitably. However, the NAC has a simple structure and its design does not rely on the accurate system model. It can deal with the system nonlinearities and uncertainties through real-time compensation.

5.4 Simulation results

Simulation studies have been undertaken on a single-machine infinite-bus power system, shown in Figure 5.1. The system parameters are given as following: $X_d = 1.0\,p.u.$, $X'_d = 0.4\,p.u.$, $X_q = 0.6\,p.u.$, $X_T = 0.12\,p.u.$, $X_L = 1.0\,p.u.$, $D = 0.008$, $T'_{do} = 5.0\,s$ and $H = 4.34\,s$. The excitation system parameters are: $K_e = 1$ and $T_e = 0$. The limit of the excitation voltage is: $\pm 9.0\,p.u.$ The AVR parameters are: $K_A = 200$, $T_A = 0.01\,s$. The system normal operation conditions are $\delta_0 = 0.6981\,rad$, $P_e = 0.4732\,p.u.$, $V_t = 1.1145\,p.u.$ and $\omega_0 = 314.15$. As the advantages of the nonlinear controller over other controllers, such as PID controller, power system stabilizer and linear optimal controller etc., have been discussed in [104, 87], only the proposed NAC and its comparison with the FLC will be simulated in this chapter.

The parameters of the fourth-order sliding observer are chosen as: $\alpha_1 = 200$, $\alpha_2 = 1.5 \times 10^4$, $\alpha_3 = 5 \times 10^5$ and $\alpha_4 = 6.25 \times 10^6$ so as to place all the poles of the Luenberger observer at -50; $\beta_1 = 50$, $\beta_2 = 1.5 \times 10^4$, $\beta_3 = 1.5 \times 10^6$, $\beta_4 = 5 \times 10^7$ so as to set the error dynamic on the sliding mode with all poles at $\lambda = -100$. It should be mentioned that the sliding observer is set with high gains to guarantee the quick and accurate tracking performance when the fault happens.

The controller parameters in equation (5.3.9) are chosen as $a_1 = 1000$, $a_2 = 300$, $a_3 = 30$ so as to place the poles of the linear system at -10. Both NAC and FLC use the same parameters for the control of the linear system. The constant control gain in (5.3.9) is chosen as $b_0 = -10$. The performances of the controller are investigated with a three-phase-to-ground short-circuit fault

occurring at the sending end of the transmission lines, as shown in Figure 5.1. The fault duration is 0.1 s. The robustness of the controller is evaluated in the cases of system parameters uncertainties, variation of system operation conditions and inter-area oscillation disturbance, respectively.

5.4.1 Control performance evaluation

Figures 5.3, 5.4 and 5.5 show the system responses of the rotor angle and terminal voltage to the fault. From the figure, it can be seen that the NAC has a better performance than the FLC, with a more smooth damping provided. Although a better performance of FLC can be obtained after optimizing its parameters, the NAC performs at least the same as FLC in this case. Note that the FLC uses the full states and the known parameters of the simulation system, but the NAC only employs one measurement without requiring the details of the system information.

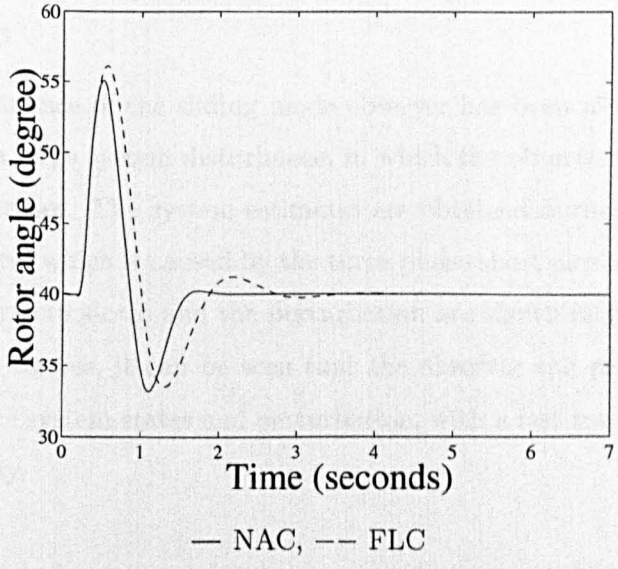

Figure 5.3: The rotor angle responses to three-phase short-circuit fault

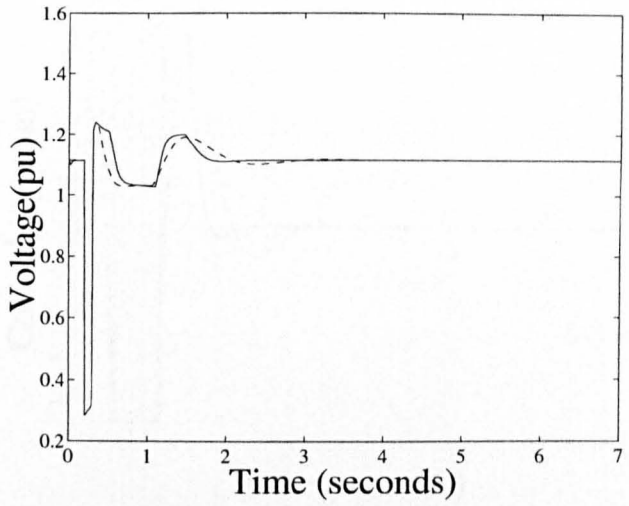

— NAC, -- FLC

Figure 5.4: Terminal voltage V_t responses to three-phase short-circuit fault

5.4.2 Observer performance and perturbation estimation

The performance of the sliding mode observer has been monitored during the period of a large system disturbance, in which the observer functions fully in its nonlinearities. The system estimates are obtained during the generator transient process which is caused by the three-phase short circuit. The estimation error of system states and the perturbation are shown in Figures 5.6 and 5.7. From the figures, it can be seen that the observer can provide accurate estimates of the system states and perturbation, with a fast track rate without any phase delay.

5.4.3 Robustness against parameters uncertainties

The variation of system parameters is considered for robustness evaluation of the NAC. In this case, the FLC is designed with inaccurate system param-

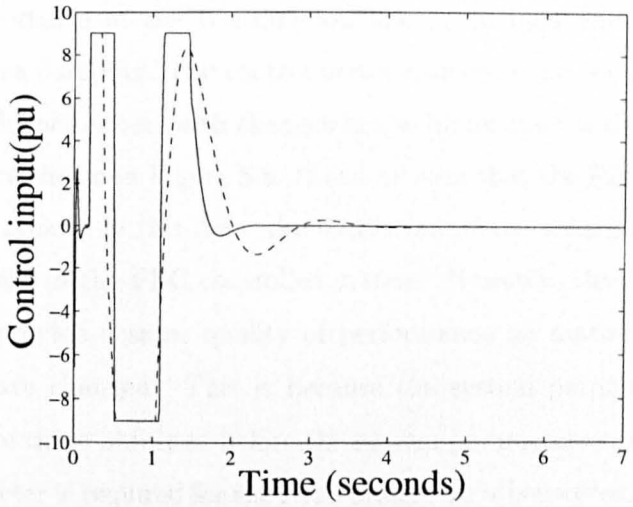

Excitation voltage u,— NAC, -- FLC

Figure 5.5: Excitation voltage u (three-phase short-circuit fault)

eters. In the system simulation, $T'_{do} = 5.0$ and $H = 4.34$ are given. The values of T'_{do} and H decreased by 20% from their original values are used in the FLC. The system responses to the fault are shown at Figure 5.9. A big difference between the FLC and NAC performances has been identified, with and without accurate parameters. However, as only the bound values of system states are required in the NAC design, inaccurate parameters will not influence the NAC performance with choice of some conservative bound values. It is worth pointing out that the NAC owns such a merit as it focuses on the nonlinearity estimation, rather than the parameters estimation involved in conventional adaptive control schemes.

5.4.4 Variation of operation conditions

The two controllers are evaluated with variation of system parameter, X_s, which is caused by switching off one transmission line after the fault. In this

case, the impedance of the transmission line is doubled and the generator suffers from less damping. The control performances of the two controllers are compared with each other, with changes in the impedance of the transmission lines, which are shown in Figure 5.8. It can be seen that the FLC performance has degraded greatly in this case. An oscillation of the generator rotor angle has been caused in the FLC controlled system. However, the NAC can still, in this case, provide a same quality of performance no matter what system parameters have changed. This is because the system parameters installed in the FLC are those obtained before the system parameters change, while no system parameter is required for the NAC design. In other words, the nonlinear observer is able to track the variations of system operation conditions.

5.4.5 Effect of inter-area oscillation

The NAC design is based on a single-machine infinite bus power system (SMIB). The design is undertaken for the generator which has low inertia and is connected to a high inertia external system by a long tie-line. It is concerned that the SMIB-designed nonlinear controller may not perform well in the presence of inter-area modes oscillation. Thus it will be necessary to evaluate the SMIB-designed NAC on a more realistic multi-machine power system model with different oscillation frequencies. One approach named *single-machine quasi-infinite bus*, where the infinite bus is modulated in magnitude by inter-area-type frequencies, can be used in the simulation of the SMIB system [112]. We choose $V_s = 1.0 + 0.12 * \sin(5t)$, corresponding to an inter-area fundamental frequency of 5Hz. In order to show the difference between the NAC and FLC performances clearly, a relatively high inter-area fundamental frequency 5Hz is chosen here. The responses are shown in Figures 5.10 $\sim$ 5.12. The FLC provides weak damping of oscillation. Again, the NAC has the same satisfactory performance as that obtained without the inter-area oscillation

simulated. This shows that the NAC can completely reject the effect of the inter-area disturbance. The estimation of system perturbation is also shown in Figures 5.10 $\sim$ 5.12. Similar observations can be made with respect to the un-modelled prime-mover dynamics.

5.5 Conclusion

A nonlinear adaptive controller has been proposed for excitation control of synchronous generators based on a state and perturbation observer. The designed controller possesses a great robustness to deal with parameter uncertainties and varying system operation conditions. Moreover, the NAC can also take unmodelled system dynamics into account and reject external disturbances automatically, as the system dynamics is estimated from real-time measurements. Furthermore, the NAC has a simple structure and can be implemented easily in practice with a single measurement. The simulation results show that the NAC has a better control performance, especially greater robustness, compared with the FLC which requires full system states and accurate system system model to design.

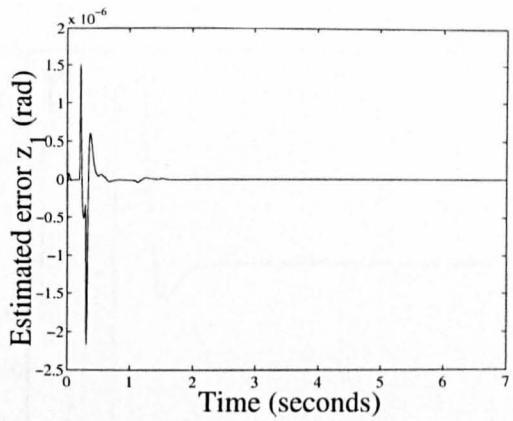

(a) $\tilde{z}_1$

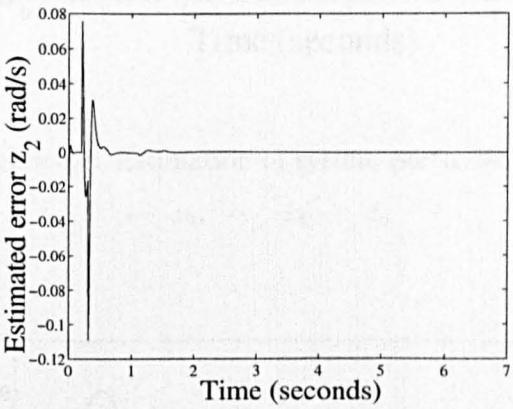

(b) $\tilde{z}_2$

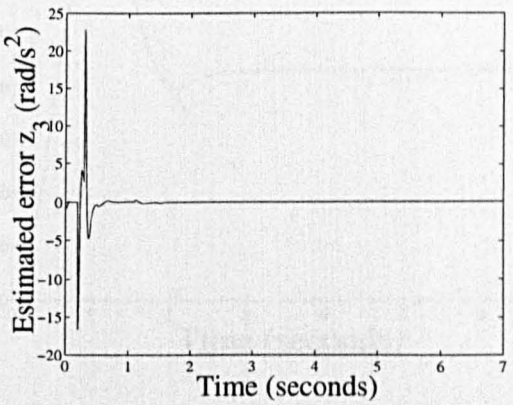

(c) $\tilde{z}_3$

Figure 5.6: Estimation error of states during the fault period

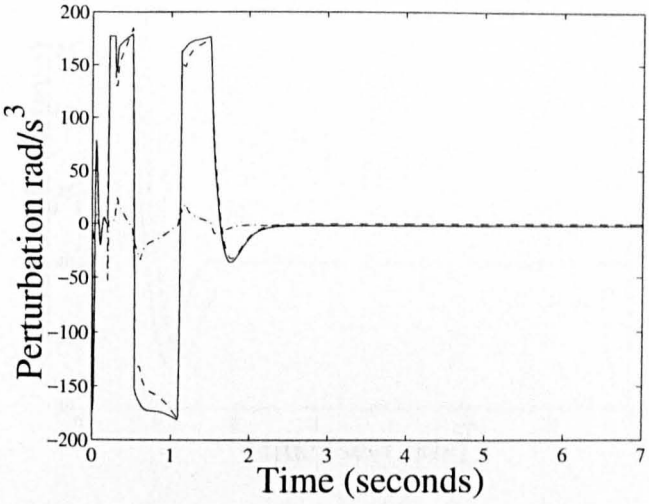

Figure 5.7: Estimation of system perturbation

— z_4, $\cdots$ $\hat{z}_4$ − . $\tilde{z}_4$

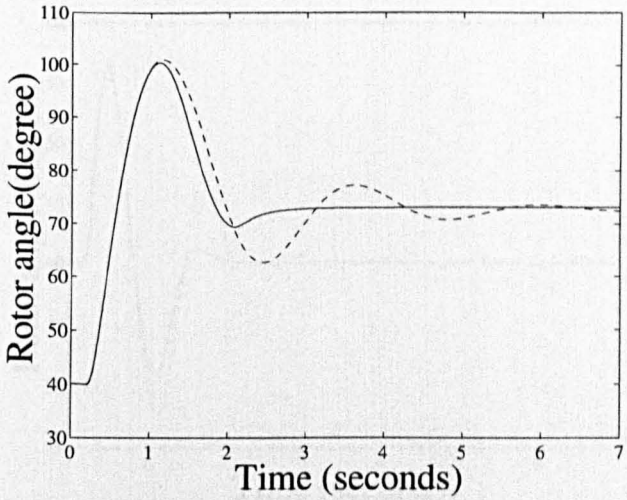

Figure 5.8: Response with operation condition variation

Rotor angle δ, — NAC, − − FLC

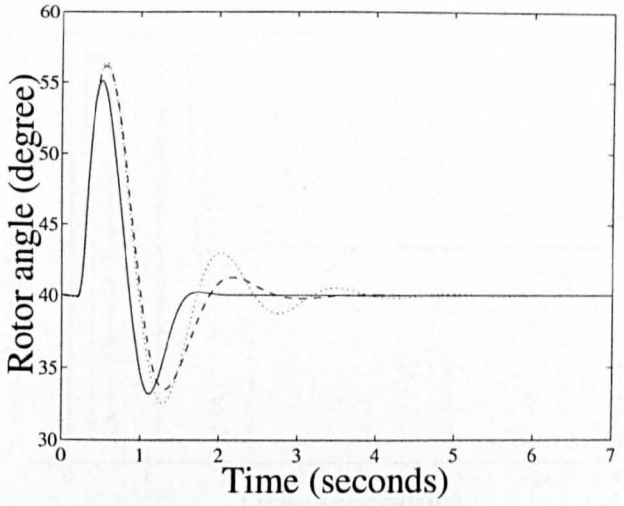

Figure 5.9: Robustness with parameters uncertainty

Rotor angle δ

— NAC, –. NAC robust test

– – FLC, ··· FLC robust test

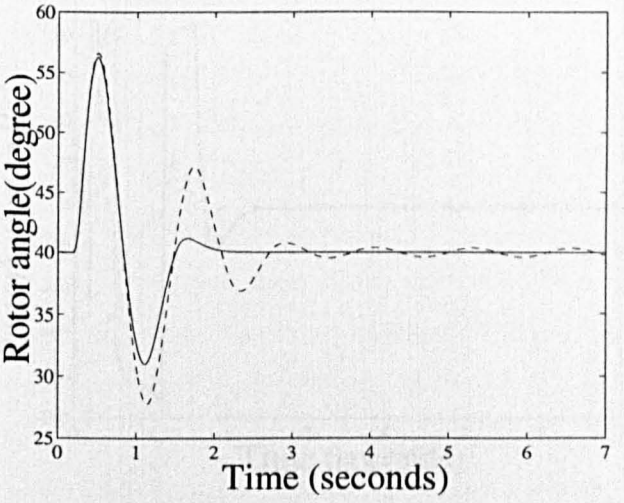

— NAC, – – FLC

Figure 5.10: Rotor angle response in the presence of persistent inter-area type disturbance

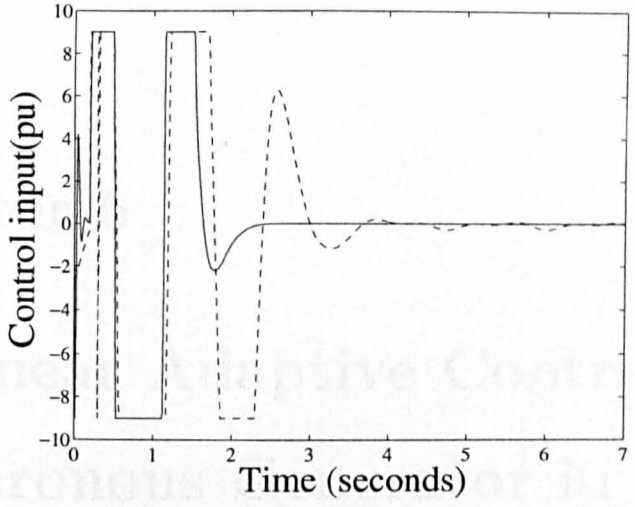

Figure 5.11: Excitation voltage u in the presence of persistent inter-area type disturbance

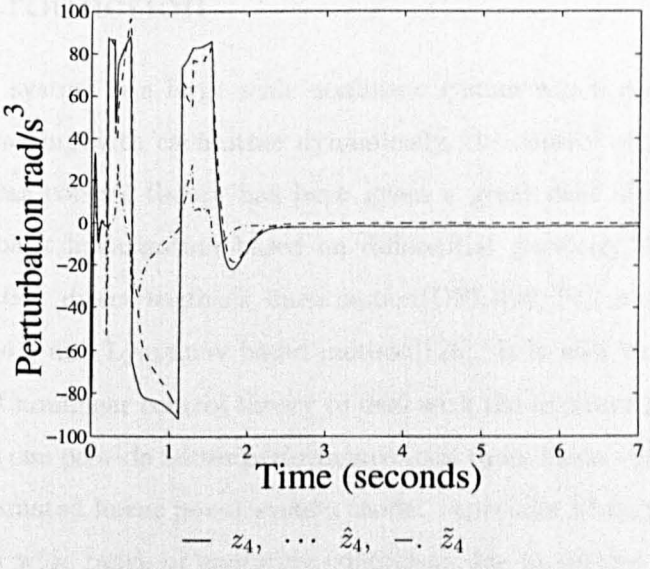

Figure 5.12: Perturbation estimation in the presence of persistent inter-area type disturbance

Chapter 6

Nonlinear Adaptive Control of Synchronous Generator in Multi-Machine Power Systems

6.1 Introduction

As power system is a large scale nonlinear system which consists of subsystems interacting with each other dynamically, the control of power system using nonlinear control theory has been given a great deal of attention[82], such as feedback linearization based on differential geometry method(FLC) [86, 87, 88, 104], direct feedback linearization(DFL)[90, 91], nonlinear adaptive control[143] and Lyapunov based method[126]. It is well known that the application of nonlinear control theory to deal with the inherent power system nonlinearities can provide better performance than those linear controller based on an approximated linear power system model, especially when power system operates on a wide range of operating conditions due to various disturbances and different load commands.

In a multi-machine power system, a decentralized controller with local mea-

surements is preferred for industry practice. When the synchronous generator is modelled as a simplified third order model, a nonlinear decentralized controller can be developed based on FLC method and the electrical machine theory [86, 87, 88]. It can deal with the variation of operation condition. In [90], a DFL nonlinear compensator is designed first to alleviate part of system nonlinearities and then a robust method is used to deal with the remaining nonlinearities. After the nonlinear power system is transferred to a linear system with matched nonlinearities, in [126] a Lyapunov based design, and in [144] a DFL method, is utilized to design a nonlinear decentralized controller. Most of these nonlinear controllers are based on state feedback, in which the complete accessibility to full system states is commonly assumed. In practice, it is not always feasible and economical to measure all system state variables. To resolve the problem, the state observer was studied and applied to the nonlinear field voltage control of generators [84]. In this method, the exact system nonlinear model is still required to design a nonlinear state observer.

In this chapter, a nonlinear and adaptive decentralized excitation control of synchronous generator in multi-machine power system is investigated by using the sliding mode states and perturbation observer. Two kinds of decentralized output feedback controller are investigated: a decentralized controller based on a fully linearizable model of multi-machine power system and a decentralized input/output linearizing controller. During the design of the first kind of controller, the synchronous generator is described in a simplified three-order model; Whilst the second decentralized controller is based on a detailed power system model in which the synchronous generator is modelled using a five-order differential equations and an AVR is included for the regulation for terminal voltage. Finally, these two different design procedures result in the same type of controller for each subsystem.

For each subsystem, a perturbation term (fictitious state) is introduced to represent the combined effect of system nonlinearities, uncertainties and inter-

connections of another subsystem. Based on the subsystem, a sliding mode observer is designed to estimate the system states and the fictitious state without requiring the knowledge of system nonlinear functions and parameters. The estimated states and perturbation is then used to realize the feedback linearizing control. This leads to de-coupling the multi-machine power system into subsystems automatically without ignoring any system interaction. Consequently, a nonlinear output decentralized controller based on local measurements is obtained.

Simulation studies are undertaken in a three-machine power system to evaluate the effectiveness of the controller. The simulation results are provided to demonstrate the merits of the novel nonlinear output control strategy. The designed controller requires only one output variable, generator rotor angle, to formulate its control law. Simulation studies undertaken in a three-machine power system show the effectiveness of the proposed control scheme.

This chapter is organized as follows. Section 2 describes the design based on fully linearizable multi-machine power system model, including the system model, the design of the nonlinear state feedback linearizing controller(FLC) design which will be used for comparison with the DNAC. The input/output linearizing control design is given in section 4. The simulation results are presented in section 5 and the conclusion is given in section 6.

6.2 Design of controller based on fully linearizable system model

6.2.1 Dynamic model of a multi-machine power system

A multi-machine power system with $n+1$ machines, in which the $(n+1)$-th machine is chosen as the reference machine and the fast-speed excitation system is utilized on each machine, can be described by a nonlinear dynamic

model as follows [76, 86, 87]:

$$\begin{aligned} \dot{\delta}_i &= \omega_i - \omega_0 \\ \dot{\omega}_i &= \frac{\omega_0}{2H_i}\left[P_{mi} - \frac{D_i}{\omega_0}(\omega_i - \omega_0) - P_{ei}\right] \\ \dot{E}'_{qi} &= \frac{1}{T'_{doi}}[u_i - E_{qi}], \qquad i = 1,\ 2, \cdots,\ n, \end{aligned} \tag{6.2.1}$$

where

$$\begin{aligned} E_{qi} &= E'_{qi} + (x_{di} - x'_{di})I_{di} \\ I_{di} &= B_{ii}E'_{qi} - \sum_{j=1, j\neq i}^{n} E'_{qj}y_{ij}\cos(\delta_i - \delta_j - \alpha_{ij}) \\ P_{ei} &= G_{ii}E'^2_{qi} + E'_{qi}\sum_{j=1, j\neq i}^{n} E'_{qj}y_{ij}\sin(\delta_i - \delta_j - \alpha_{ij}), \end{aligned}$$

where δ_i denotes the relative rotor angle, in rad; ω_i the generator speed, in rad/s; ω_0 the system speed, in rad/s; E_{qi}, E'_{qi} and E''_{qi} the voltage, transient voltage and sub-transient voltage in q-axis, respectively; E''_{di} sub-transient voltage in d-axis; P_{mi} the mechanical power input from the prime mover and assumed to be constant, in $p.u.$; P_{ei} the electrical power output of the generator, in $p.u.$; H_i the inertia coefficient of rotor, in seconds; T'_{d0i}, T''_{d0i} and T''_{q0i} the d-axis transient, d-axis sub-transient and q-axis sub-transient short circuit time constant, in seconds, respectively; x_{di}, x'_{di} and x''_{di} the synchronous, transient and sub-transient impedances in the d-axis, respectively ; x_{qi} and the synchronous impedance in the q-axis; u_i the excitation control, in $p.u.$; I_{di} and I_{qi} the generator currents in the d-axes and q-axes, respectively; V_{di} and V_{qi} the generator terminal voltage in the d-axes and q-axes, respectively; V_{ti} and V_{refi} the generator terminal voltage and its reference value, respectively; V_{ri}, K_{ai} and T_{ai} the control output, control gain and time constant of AVR, respectively; E_{fd0i} the initial excitation voltage; subscript i denotes the variables of the ith machine; and subscript 0 the initial value of variable.

Let $z_{i1} = \delta_i$, $z_{i2} = \omega_i$, $z_{i3} = E'_{qi}$, then the system state model can be obtained

as:

$$\begin{aligned} \dot{z}_i &= \mathcal{F}_i(z) + \mathcal{G}_i(z)u_i \\ y_i &= \mathcal{H}_i(z), \qquad\qquad i = 1, 2, \cdots, n, \end{aligned} \tag{6.2.2}$$

where

$$\mathcal{F}_i(z) = \begin{bmatrix} z_{i2} - \omega_0 \\ \frac{\omega_0}{2H_i}\Big(P_{mi} - \frac{D_i}{\omega_0}(z_{i2} - \omega_0) - G_{ii}z_{i3}^2 \\ \qquad -z_{i3}\sum_{j=1,j\neq i}^{n} z_{j3}y_{ij}\sin(z_{i1} - z_{j1} - \alpha_{ij})\Big) \\ -\frac{1}{T'_{doi}}\left((1 + (x_{di} - x'_{di})B_{ii})z_{i3}\right. \\ \qquad \left. -(x_{di} - x'_{di})\sum_{j=1,j\neq i}^{n} z_{j3}y_{ij}\cos(z_{i1} - z_{j1} - \alpha_{ij})\right) \end{bmatrix}$$

$$\mathcal{G}_i(z) = [0 \;\; 0 \;\; 1/T'_{doi}]^T$$

$$\mathcal{H}_i(z) = z_{i1} - \delta_{i0}.$$

Define $z_i \triangleq [z_{i1}\, z_{i2}\, z_{i3}]^T$, $z \triangleq [z_1^T \;\; z_2^T \;\; \cdots \;\; z_n^T]^T$, $y \triangleq [y_1 \;\; y_2 \;\; \cdots \;\; y_n]^T$, and $u \triangleq [u_1 \;\; u_2 \;\; \cdots \;\; u_n]^T$, the state equations of the whole multi-machine system is represented as

$$\begin{aligned} \dot{z} &= \mathcal{F}(z) + \mathcal{G}(z)u \\ y &= \mathcal{H}(z), \end{aligned} \tag{6.2.3}$$

where $z \in \mathbb{R}^{3n}$ represent the state variables, $u \in \mathbb{R}^n$ the control input, and $y \in \mathbb{R}^n$ the measured outputs. $\mathcal{F}$, $\mathcal{G}$ and $\mathcal{H}$ are sufficiently smooth in a domain $\mathcal{S} \subset \mathbb{R}^{3n}$ and are defined as follows:

$$\begin{aligned} \mathcal{F}(z) &= [\mathcal{F}_1^T(z) \;\; \mathcal{F}_2^T(z) \;\; \cdots \;\; \mathcal{F}_n^T(z)]^T \\ \mathcal{G}(z) &= \text{block diag}[\mathcal{G}_1(z) \;\; \mathcal{G}_2(z) \;\; \cdots \;\; \mathcal{G}_n(z)] \\ \mathcal{H}(z) &= [\mathcal{H}_1(z) \;\; \mathcal{H}_1(z) \;\; \cdots \;\; \mathcal{H}_n(z)]^T. \end{aligned}$$

It has been shown that system (6.2.3) can be linearized by choosing a state variable transformation and a nonlinear feedback control law [104, 86, 87]. There exists a diffeomorphism $T : \mathcal{S} \to \mathbb{R}^{3n}$, defined as

$$x = T(z) = \left[\mathcal{H}_1(z), L_{\mathcal{F}}\mathcal{H}_1(z), L_{\mathcal{F}}^2\mathcal{H}_1(z), \mathcal{H}_2(z), \cdots, \mathcal{H}_n(z), L_{\mathcal{F}}\mathcal{H}_n(z), L_{\mathcal{F}}^2\mathcal{H}_n(z)\right]^T, \tag{6.2.4}$$

where $x \triangleq [x_{11}, x_{12}, x_{13}, \cdots, x_{i1}, x_{i2}, x_{i3}, \cdots, x_{n1}, x_{n2}, x_{n3}]^T$ and $x_{i1} = z_{i1} - \delta_{i0}$, $x_{i2} = z_{i2} - \omega_0$, $x_{i3} = \dot{z}_{i2}$. The nonlinear transformation, $x = T(z)$, leads to a system model with respect to the new state variables x from system (6.2.3):

$$\begin{aligned} \dot{x}_{i1} &= x_{i2} \\ \dot{x}_{i2} &= x_{i3} \\ \dot{x}_{i3} &= \alpha_i(x) + \textstyle\sum_{j=1}^{n} \beta_{ij}(x) u_j \\ y_i &= x_{i1}, \qquad\qquad i = 1, \cdots, n, \end{aligned} \tag{6.2.5}$$

where

$$\alpha_i(x) = \left(L_{\mathcal{F}}^3 \mathcal{H}_i(z)\right)|_{z=T^{-1}(x)} \tag{6.2.6}$$

$$\begin{aligned} L_{\mathcal{F}}^3 \mathcal{H}_i(z) &= \sum_{j=1}^{n} \left(\frac{\partial \dot{\omega}_i}{\partial z_{j1}} \mathcal{F}_{j1}(z) + \frac{\partial \dot{\omega}_i}{\partial z_{j2}} \mathcal{F}_{j2}(z) + \frac{\partial \dot{\omega}_i}{\partial z_{j3}} \mathcal{F}_{j3}(z) \right) \\ &= \frac{-\omega_0}{2H_i} \sum_{j=1}^{n} \left(\frac{\partial P_{ei}}{\partial E'_{qj}} \mathcal{F}_{j3}(z) + \frac{\partial P_{ei}}{\partial \delta_j} \mathcal{F}_{j1}(z) \right) + \frac{D_i}{2H_i} \mathcal{F}_{i2}(z) \end{aligned} \tag{6.2.7}$$

$$\beta_{ij}(x) = \left(L_{\mathcal{G}_j} L_{\mathcal{F}}^2 \mathcal{H}_i(z)\right)|_{z=T^{-1}(x)} \tag{6.2.8}$$

$$\begin{aligned} L_{\mathcal{G}_j} L_{\mathcal{F}}^2 \mathcal{H}_i(z) &= \frac{\partial \dot{\omega}_i}{\partial E'_{qj}} \frac{1}{T'_{doj}} \\ &= \frac{-\omega_0}{2H_i T'_{doj}} \frac{\partial P_{ei}}{\partial E'_{qj}} \qquad j = 1, 2, \ldots, n, \end{aligned} \tag{6.2.9}$$

and

$$L_{\mathcal{F}} \mathcal{H}_i(z) = \frac{\partial \mathcal{H}_i(z)}{\partial z} \mathcal{F}(z),$$

$$L_{\mathcal{G}_j} L_{\mathcal{F}} \mathcal{H}_i(z) = \frac{\partial \left(L_{\mathcal{F}} \mathcal{H}_i(z)\right)}{\partial z} \mathcal{G}_j(z),$$

are the Lie derivatives of $\mathcal{H}_i(z)$ along $\mathcal{F}(z)$, and $L_{\mathcal{F}} \mathcal{H}_i(z)$ along $\mathcal{G}_j(z)$, respectively[1].

It should be mentioned that the DNAC is undertaken based on the system model (6.2.5) in which the nonlinearities satisfy the matching condition.

6.2.2 Design of the decoupled state feedback linearizing controller

The system in form (6.2.5) can be exactly linearized by a nonlinear state feedback control

$$u = [\beta(x)]^{-1}(v - \alpha(x)), \tag{6.2.10}$$

and the following linear system is derived

$$\begin{aligned} \dot{x}_{i1} &= x_{i2} \\ \dot{x}_{i2} &= x_{i3} \\ \dot{x}_{i3} &= v_i, \quad i = 1, \cdots, n, \end{aligned} \tag{6.2.11}$$

where $\alpha(x) = \{\alpha_i(x)\}_{n\times 1}$, $\beta(x) = \{\beta_{ij}(x)\}_{n\times n}$ and $v = [v_1, v_2, \cdots, v_n]^T$ is the control of linear system (6.2.11).

Equation (6.2.10) is a centralised control law and its implementation requires all the system states. Design of a decoupled control law is desired and it has been well studied [86, 114, 87]. From system (6.2.1), we can obtain:

$$\begin{aligned} \frac{d}{dt}P_{ei} &= \sum_{j=1}^{n}\left(\frac{\partial P_{ei}}{\partial E'_{qj}}\frac{dE'_{qj}}{dt} + \frac{\partial P_{ei}}{\partial \delta_j}\frac{d\delta_j}{dt}\right) \\ &= \sum_{j=1}^{n}\left(\frac{\partial P_{ei}}{\partial E'_{qj}}\mathcal{F}_{j3} + \frac{\partial P_{ei}}{\partial \delta_j}\mathcal{F}_{j1} + \frac{\partial P_{ei}}{\partial E'_{qj}}\frac{1}{T'_{doj}}u_j\right). \end{aligned} \tag{6.2.12}$$

From equations (6.2.7), (6.2.9) and (6.2.12), the following equation can be given:

$$\alpha_i(z) = -\frac{\omega_0}{2H_i}\frac{dP_{ei}}{dt} + \frac{D_i}{2H_i}\dot{\omega}_i - \sum_{j=1}^{n}\beta_{ij}u_j. \tag{6.2.13}$$

Substituting equation (6.2.13) into system (6.2.5), the decoupled model of system (6.2.5) can be obtained as:

$$\begin{aligned} \dot{x}_{i1} &= x_{i2} \\ \dot{x}_{i2} &= x_{i3} \\ \dot{x}_{i3} &= -\tfrac{\omega_0}{2H_i}(\dot{P}_{ei} - \tfrac{D_i}{\omega_0}(\dot{\omega}_i)), \qquad i = 1, 2, \cdots, n. \end{aligned} \tag{6.2.14}$$

Based on the synchronous generator theory, we can derive another form of the active power of ith machine and its derivative as follows:

$$P_{ei} = E'_{qi}I_{qi} + (X_{qi} - X'_{di})I_{qi}I_{di} \tag{6.2.15}$$

$$\frac{d}{dt}P_{ei} = I_{qi}\frac{d}{dt}E'_{qi} + E'_{qi}\frac{d}{dt}I_{qi} + (X_{qi} - X'_{di})\frac{d}{dt}(I_{di}I_{qi}). \tag{6.2.16}$$

Substituting equation (6.2.16) and the third equation of system (6.2.1) into system (6.2.14) again, we can obtain:

$$\dot{x}_{i3} = f_i(x) + b_i(x)u_i, \tag{6.2.17}$$

where $f_i(x)$ and $b_i(x)$ are given as follows:

$$f_i(x) = \frac{-\omega_0}{2H_i}\left(\frac{D_i}{\omega_0}\dot{\omega}_i + E'_{qi}\dot{I}_{qi} + (x_{qi} - x'_{di})\frac{d}{dt}(I_{di}I_{qi})\right) + \frac{\omega_0 I_{qi}}{2H_i T'_{doi}}E_{qi} \tag{6.2.18}$$

$$b_i(x) = \frac{-\omega_0 I_{qi}}{2H_i T'_{doi}}. \tag{6.2.19}$$

It can be seen that $b_i(x)$ is a nonzero variable within a normal range of the generator operation. Thus, system (6.2.14) is linearizable and it can be linearized exactly by introducing a state feedback control:

$$u_i = \frac{v_i - f_i(x)}{b_i(x)}, \tag{6.2.20}$$

$$v_i = -a_{i1}(\delta_i - \delta_{i0}) - a_{i2}(\omega_i - \omega_0) - a_{i3}\dot{\omega}_i, \tag{6.2.21}$$

where a_{ij}, $j = 1, 2, 3$, are feedback gains and they can be determined by a linear optimal control strategy.

Substituting equations (6.2.18) and (6.2.19) into equation (6.2.20), we can obtain the decoupled state feedback excitation control of the $i-$th machine as follows:

$$u_i = E_{qi} - \frac{T'_{doi}}{I_{qi}}\left[\frac{2H_i}{\omega_0}v_i + \frac{D_i}{\omega_0}\dot{\omega}_i + E'_{qi}\frac{d}{dt}I_{qi} + (x_{qi} - x'_{di})\frac{d}{dt}(I_{di}I_{qi})\right]. \tag{6.2.22}$$

PAGE MISSING IN ORIGINAL

then the third equation of (6.2.5) can be rewritten as

$$\dot{x}_{i3} = \Psi_i(x, u, t) + b_{i0}u_i, \tag{6.2.25}$$

where $\Psi(x, u, t)$ is defined as 'perturbation'. Introducing a fictitious state $x_{i4} = \Psi_i(x(t), u(t), t)$ to represent the perturbation, system (6.2.5) becomes:

$$\begin{aligned} \dot{x}_{i1} &= x_{i2} \\ \dot{x}_{i2} &= x_{i3} \\ \dot{x}_{i3} &= x_{i4} + b_{i0}u_i \\ \dot{x}_{i4} &= \dot{\Psi}_i(\cdot) \\ y_i &= x_{i1} \qquad\qquad i = 1, 2, \cdots, n, \end{aligned} \tag{6.2.26}$$

where $x_{ij}(0) = 0$, $j = 1,\ 2,\ 3$, $x_{i4}(0) = -b_{i0}E_{qi0}$, $\dot{\Psi}_i(0) = 0$,
$b_{i0} = (-\omega_0 I_{qi0})/(2H_i T'_{doi})$.

It is reasonable to assume that the power system under a proper control is stable. The boundary values of the system states can be estimated based on the maximum value of the states, when a three-phase-to-ground fault occurs at the terminal of the generator, which gives a most severe disturbance to the machine. During the fault, the electric power P_{ei} will change from P_{mi} to around zero within a short period of time, Δ. Therefore, the boundary values can be obtained as follows:

$$\begin{aligned} |\, x_{i3} \,| &\leq \frac{\omega_0 P_{mi}}{2H_i} \\ |\, x_{i4} \,| &\leq \frac{\omega_0 P_{mi}}{2H_i \Delta} \\ |\, \dot{\Psi}_i(\cdot) \,| &\leq \frac{\omega_0 P_{mi}}{2H_i \Delta^2}. \end{aligned}$$

6.2.5 Design of decentralized nonlinear adaptive controller

For system (6.2.26), design a fourth-order sliding mode observer as described in Chapter 3. With proper selection of the observer parameters, the

estimate of the system states and the perturbation will converge to their real values quickly, e.g. $\hat{x}_{ij} \to x_{ij}$, $j = 1, \cdots, 3$ and $\hat{x}_{i4} \to \Psi(\cdot)$. Then, the estimated states can be used to replace the real system states to design the linear state feedback control v_i. The complete control law for system (6.2.5) is given as follows:

$$u_i = v_i/b_{i0} - \hat{x}_{i4}/b_{i0}, \tag{6.2.27}$$

$$v_i = -a_{i1}\hat{x}_{i1} - a_{i2}\hat{x}_{i2} - a_{i3}\hat{x}_{i3}, \tag{6.2.28}$$

where a_{ij}, $j = 1, 2, 3$, are gains of the linear feedback controller and the estimated perturbation $\hat{x}_{i4}$ will function as a real-time compensation to cancel the system nonlinearities and uncertainties.

6.2.6 Summarization and remarks

The basic scheme of DNAC can be summarized as follows:

Step 1: Transform the fully linearized nonlinear system (6.2.3) to the nominal nonlinear system (6.2.5), as described in section 6.2.1;

Step 2: Define the perturbation term and fictitious state to represent all the uncertainties, external disturbances and known and unknown nonlinearities of the nonlinear system (6.2.5), as described in section 6.2.4;

Step 3: Design an extended-order sliding mode observer to estimate the perturbation and the system states, as addressed in section 6.2.5;

Step 4: Employ the estimated perturbation and states to implement the control law, equations (6.2.27) and (6.2.28), as in section 6.2.5.

6.3 Controller design based on input/output linearizing system model

6.3.1 The detailed model of a multi-machine power system

Considering the fast-acting excitation system utilized on each machine, a fifth-order model is employed to represent the machine together with a first-order dynamic model of an Automatic Voltage Regulator (AVR) which is used to describe the regulation of generator terminal voltage. The multi-machine power system including n machines can be described by n interconnected subsystems as follows:

$$\begin{aligned}
\dot{\delta}_i &= \omega_i - \omega_0 \\
\dot{\omega}_i &= \tfrac{\omega_0}{2H_i}[P_{mi} - P_{ei}] \\
\dot{E}'_{qi} &= \tfrac{1}{T'_{doi}}[u_i + E_{fd0i} + U_{ri} - E_{qi}] \\
\dot{E}''_{qi} &= \tfrac{1}{T''_{doi}}[-E''_{qi} + E'_{qi} - (x'_{di} - x''_{di})I_{di}] + \dot{E}'_{qi} \\
\dot{E}''_{di} &= \tfrac{1}{T''_{qoi}}[-E''_{di} - (x'_{qi} - x''_{qi})I_{qi}] \\
\dot{U}_{ri} &= \tfrac{K_{ai}}{T_{ai}}(U_{refi} - U_{ti}) - \tfrac{U_{ri}}{T_{ai}},
\end{aligned} \tag{6.3.1}$$

where

$$\begin{aligned}
E_{qi} &= E'_{qi} + (x_{di} - x'_{di})I_{di} \\
P_{ei} &= E''_{qi}I_{qi} + E''_{di}I_{di} + (x''_{qi} - x''_{di})I_{di}I_{qi}) \\
U_{di} &= x''_{qi}I_{qi} + E''_{di} \\
U_{qi} &= x''_{di}I_{di} + E''_{qi} \\
U_{ti} &= (U_{di}^2 + U_{qi}^2)^{\frac{1}{2}} \\
I_{ti} &= (I_{di}^2 + I_{qi}^2)^{\frac{1}{2}},
\end{aligned}$$

where the definition of variables are same as in section6.2.1.

The above n subsystems are interconnected through the transmission network. The state variables of the transmission network are represented in a $x-y$ coordinate as

$$U_F = Z_F I_F \tag{6.3.2}$$

where

$$U_F = \begin{bmatrix} U_{x1} & U_{y1} & U_{x2} & U_{y2} & \cdots & U_{xn} & U_{yn} \end{bmatrix}^T,$$
$$I_F = \begin{bmatrix} I_{x1} & I_{y1} & I_{x2} & I_{y2} & \cdots & I_{xn} & I_{yn} \end{bmatrix}^T,$$

and Z_F is the impedance matrix of the network.

The transformation between the common $x-y$ coordinate and the $d-q$ coordinate of the ith subsystem is given as

$$T_i = \begin{bmatrix} \cos(\delta_i) & \sin(\delta_i) \\ \sin(\delta_i) & -\cos(\delta_i) \end{bmatrix}.$$

For the ith machine, we have

$$\begin{bmatrix} U_{di} \\ U_{qi} \end{bmatrix} = T_i \begin{bmatrix} U_{xi} \\ U_{yi} \end{bmatrix}, \qquad \begin{bmatrix} I_{di} \\ I_{qi} \end{bmatrix} = T_i \begin{bmatrix} I_{xi} \\ I_{yi} \end{bmatrix}.$$

6.3.2 Decentralized nonlinear adaptive controller for the ith subsystem

Defining the state variables as

$$\begin{aligned} x &= \begin{bmatrix} x_1^T & x_2^T & \cdots & x_i^T & \cdots & x_n^T \end{bmatrix}^T, \\ x_i &= \begin{bmatrix} x_{i1} & x_{i2} & x_{i3} & x_{i4} & x_{i5} & x_{i6} \end{bmatrix}^T \\ &= \begin{bmatrix} \delta_i - \delta_{i0} & \omega_i - \omega_{i0} & E'_{qi} - E'_{qi0} & E''_{qi} - E''_{qi0} & E''_{di} - E''_{di0} & V_{ri} \end{bmatrix}^T \end{aligned}$$

and choosing the output of the ith subsystem as $y_i = h_i(x) = x_{i1}$, we have

$$\begin{aligned}
\frac{d}{dt}y_i &= x_{i2} \\
\frac{d^2}{dt^2}y_i &= \frac{\omega_0}{2H_i}[P_{mi} - P_{ei}] \\
\frac{d^3}{dt^3}y_i &= a_i(x) + b_i(x)u_i \\
a_i(x) &= -\frac{\omega_0 I_{qi}}{2H_i T'_{doi}}(E_{fdi0} - E_{qi}) - \frac{\omega_0}{2H_i}E''_{qi}\frac{d}{dt}I_{qi} \\
&\quad -\frac{\omega_0 I_{qi}}{2H_i T''_{doi}}[-E''_{qi} + E'_{qi} - (x'_{di} - x''_{di})I_{di}] \\
&\quad -\frac{\omega_0}{2H_i}E''_{qi}\frac{d}{dt}I_{qi} - \frac{\omega_0}{2H_i}\frac{d}{dt}[E''_{di}I_{di} + (x''_{qi} - x''_{di})I_{di}I_{qi})], \\
b_i(x) &= -\frac{\omega_0 I_{qi}}{2H_i T'_{doi}}.
\end{aligned}$$

Defining the system perturbation as

$$\Psi(x, u, t)_i = a_i(x) + (b_i(x) - b_{i0})u_i, \tag{6.3.3}$$

then we have

$$\frac{d^3 y_i}{dt^3} = \Psi_i(x, u, t) + b_{i0}u_i \tag{6.3.4}$$

where b_{i0} is a constant, chosen as $b_{i0} < b_i(x)/2$, as $b_i(x)$ is negative and bounded when the synchronous generator operates under a normal operation condition.

As $b_i(x) \neq 0, \quad \forall \delta \neq k\pi, \quad k = 0, 1, 2, \cdots$, the ith subsystem (6.3.1) has relative degree $r_i = 3$. Defining new system states $z_{i1} = y_i$, $z_{i2} = \frac{d}{dt}y_i$, $z_{i3} = \frac{d^2}{dt^2}y_i$, $z_{i4} = \Psi_i(\cdot)$, and then a fourth-order sliding mode observer is applied. Finally, the control law of subsystem (6.3.1) can be obtained as:

$$u_i = (v_i - \hat{z}_{i4})/b_{i0}, \tag{6.3.5}$$

$$v_i = -a_{i1}\hat{z}_{i1} - a_{i2}\hat{z}_{i2} - a_{i3}\hat{z}_{i3}. \tag{6.3.6}$$

As the relative degree of subsystem (6.3.1) is $r = 3$, the internal system dy-

namics is

$$\begin{aligned}
\dot{x}_{i4} &= \frac{1}{T''_{doi}}[-x_{i4} - E''_{qi0} + x_{i3} + E'_{qi0} - (x'_{di} - x''_{di})I_{di}] + \dot{E}'_{qi} \\
\dot{x}_{i5} &= \frac{1}{T''_{qoi}}[-x_{i5} - E''_{di0} - (x'_{qi} - x''_{qi})I_{qi}] \\
\dot{x}_{i6} &= \frac{K_{ai}}{T_{ai}}(U_{refi} - U_{ti}) - \frac{x_{6i}}{T_{ai}}.
\end{aligned} \tag{6.3.7}$$

Noting that when $z_{ij} = 0$, j=1, 2, 3, and $\dot{z}_{j3} = 0$, the zero dynamics of system (6.3.1) is :

$$\begin{aligned}
\dot{x}_{i4} &= -\frac{1}{T''_{doi}}x_{i4} \\
\dot{x}_{i5} &= -\frac{1}{T''_{qoi}}x_{i5} \\
\dot{x}_{i6} &= -\frac{x_{6i}}{T_{ai}}.
\end{aligned}$$

It is exponentially stable.

Remark 6.1 Based on the result of Chapter 4, the constant value of b_{i0} must satisfy the following condition to guarantee that the nonlinear system (6.2.5) can be linearized by the estimated nonlinearity:

$$|1 - b_i(x)/b_{i0}| \leq \mu < 1$$

where μ is a positive constant. As $b_i(x)$ is negative when the generator operates within its normal region, then

$$b_{i0} < \frac{1}{2}b_i(x).$$

Remark 6.2 The DNAC described above has a great merit as only one variable, variation of rotor angle $\delta_i - \delta_{i0}$, is required for implementation of the nonlinear control law. It should be mentioned that the steady state of the rotor angle, δ_{i0}, which will change with the variation of operation conditions, is involved in the control. δ_{i0} can be obtained by an ODSS (observation decoupled state space) method described in [104] when the system operation condition varies. It has been noted that there are some methods available now for measuring the relative rotor angle [142]. Using other easily measurable variables, such as rotor speed or active power, to replace the rotor angle, is also under investigation.

Remark 6.3 Another important objective of the generator excitation control is to regulate generator terminal voltage V_t. Most modern generators are equipped with Automatic Voltage Regulators (AVRs). It is well known that the AVR can inject negative damping into the system, while the power system operates at high power loading with leading power factors, particularly in a long distance tie-line transmission system. The FLC designed in [88, 114] introduces an additional feedback loop to add an AVR in the excitation control system, so as to guarantee the regulation of terminal voltage. However, the nonlinearity injected into the system by adding the AVR has not been considered in the design of the FLC [112].

In this study, an AVR is connected, together with the DNAC, to the excitation system to guarantee the regulation of terminal voltage. As the perturbation, which includes system nonlinearities, is estimated online from the real-time measurements, the DNAC can compensate the unmodelled system nonlinear dynamics caused by the employment of AVR in the system. The structure of the total control system is shown in Figure 6.1.

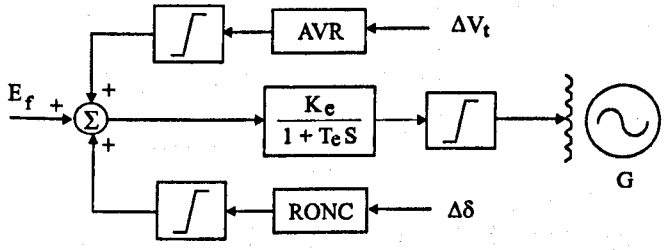

Figure 6.1: The excitation system with DNAC installed

6.4 Simulation results

6.4.1 A three-machine power system with multi-mode oscillations

The designed controller is evaluated on a three-machine power system as shown in Figure 6.2. This three-machine system is widely employed for investigation on damping of multi-mode oscillations[87, 80]. The parameters of the system is given in Appendix B. In this system, multi-mode oscillations can be observed following a large disturbance, a three-phase-grounding short circuit described below, without control provided, as shown in Figure 6.3.

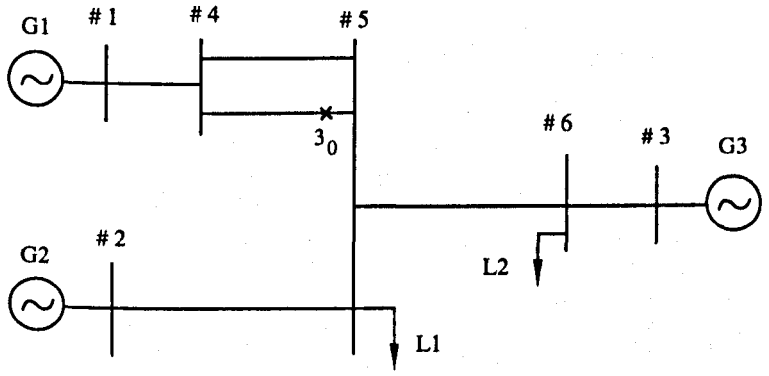

Figure 6.2: The multi-machines power system without infinite bus

All generators are equipped with AVRs, fast-acting exciters and governors. Each generator is simulated by a fifth-order model in the simulation.

This simulation approach demonstrates an example showing that the DNAC can deal with unmodelled system dynamics. The fault is simulated as: a three-phase-to-ground short circuit occurs at the end terminal of line $4-5(2)$ at $t = 0.1\ s$, where (2) denotes the second line between buses 4 and 5. The faulty transmission line is switched off at $t = 0.2\ s$ and switched on again at $t = 0.7\ s$ when the fault is cleared.

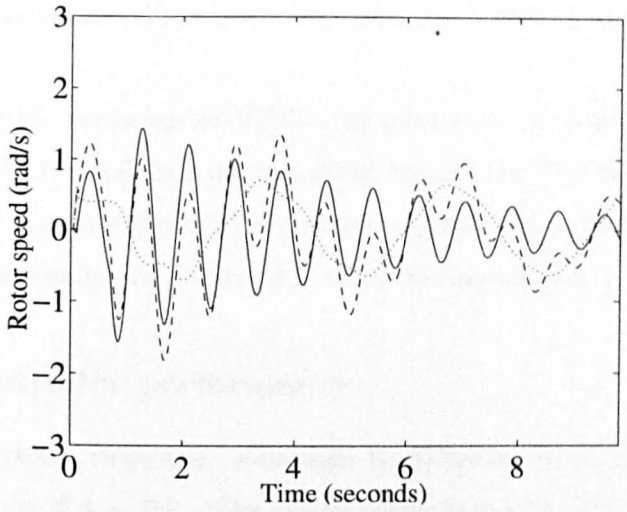

Figure 6.3: Multi-mode oscillations of the multi-machines power system

— $\omega_1 - \omega_2$, – – $\omega_1 - \omega_3$, $\cdots$ $\omega_2 - \omega_3$

The parameters of DNAC are chosen as follows. For observer (3.4.1), $\alpha_{i1} = 200$, $\alpha_{i2} = 1.5 \times 10^4$, $\alpha_{i3} = 5 \times 10^5$ and $\alpha_{i4} = 6.25 \times 10^6$ so as to place all poles of the Luenberger observer at -50; $k_{i1} = 50$, $k_{i2} = 1.5 \times 10^4$, $k_{i3} = 1.5 \times 10^6$, $k_{i4} = 5 \times 10^7$ so as to set the error dynamic on the sliding mode with all poles at $\lambda = -100$. It should be mentioned that the sliding observer is set with high gains to guarantee the quick and accurate track performance when the fault happens. The controller parameters in equation (6.2.28) are chosen as $a_{i1} = 1000$, $a_{i2} = 300$ and $a_{i3} = 30$ so as to place the poles of the linear system at -10. Both DNAC and FLC use the same parameters for the control of the linear system. In equation (6.2.27), $b_{i0} = -0.2$ is chosen for all controllers. Three generator units use the same controller parameters.

The advantages of the FLC in improving the power system stability over other controllers such as PID controller, power system stabilizer(PSS) and linear optimal controller etc., have been discussed in [104, 87]. Therefore in this paper the comparison is focused between the DNAC and FLC. The perfor-

mance of the conventional power system stabilizer (CPSS) is also presented for comparison.

To improve the performance of FLC, the more accurate control law (6.2.22) is used in the FLC simulation instead of the control law (6.2.23). It is also assumed that all system states and parameters required by the FLC are available. The simulation results are presented in the following section.

6.4.2 Controller performance

Case 1: System responses, controlled by DNACs on all generators, are shown in Figures 6.4 $\sim$ 6.7. The system responses with FLCs installed on all generators are shown in the figures. In this case, all kinds of oscillations are well damped out by DNACs or FLCs. From Figures 6.4 $\sim$ 6.7, it can be seen that the DNACs can provide better performance than the FLCs. As the FLC is designed based on a third-order model of generator, there exist unmodelled dynamics, such as high order dynamics of generators, AVRs and governors. These unmodelled dynamics will degrade the response of FLCs. However, as the DNAC uses the real-time estimation of system dynamic modes, it can deal with the unmodelled system dynamics. Therefore, the DNAC can provide consistent satisfactory control performance, when the system suffers from uncertainties, disturbances and variation of operation conditions.

Case 2: System responses, controlled by DNAC on G2 and CPSS on G1 and G3, are shown in Figure 6.8. It is shown that DNAC installed on G2 can improve the damping of the inter-area oscillation between G2 and G3. The DNAC and CPSS installed on different generators can coordinate with each other.

6.4.3 Observer performance

During the period of a large system disturbance, the performance of the observer has been monitored. The estimated errors of states are shown in Figures 6.9 $\sim$ 6.11. The estimated perturbation is illustrated in Figure 6.12. From Figure 6.9$\sim$ 6.11, it can be seen that the the observer can provide accurate estimates of the system states with a fast track rate. There are relatively bigger errors existing in the estimation of x_3. This is because there exists discontinuity in the states at the instant when the faults happen in the power system. In the observer error performance shown in Figures 6.9, 6.10 and 6.11, the estimation error become big at the instant of $t = 0.1\ s, t = 0.2\ s, t = 0.7\ s$, when the fault is simulated, the fault line is disconnected and the transmission line is connected again when the fault is cleared, respectively. The sliding observer, the same as other kinds of nonlinear observer, cannot deal with the discontinuity existed in states very well. However, from the simulation results, the sliding observer can still provide a fast track rate and accurate state estimation for the DNAC despite of the discontinuity.

6.4.4 Robustness to system parameters uncertainties

The robustness of the DNAC and FLC has been evaluated through testing the controllers by changing the inertia constants H and the field time constant T'_{do} of all units. In the FLCs, the values of T'_{do} and H are decreased by 10% from the original values used in the power system simulation. In this case, the system responses to the fault are shown at Figure 6.13. A big difference of the FLC performance has been identified, with and without accurate parameters. By contrast to the FLC, the DNAC performance remains exactly the same, as its design does not require the accurate system parameters.

6.4.5 Controller performance under various operation conditions

The above results are obtained based on a certain operation condition Type I. In order to test the general effectiveness of the proposed DNAC, different operation conditions are simulated. The system responses, controlled by the DNACs on all units, under operation condition type II given in the Appendix, are shown in Figure 6.14. In this case, although units 1 and 2 operate with a leading phase and the system suffers from more severe oscillations when the fault occurs, the DNACs can still provide consistent performance which is much better than that obtained using the FLCs, as illustrated in the figure.

6.5 Conclusion

A decentralized nonlinear adaptive controller has been proposed for excitation control of synchronous generators interconnected in the multi-machine power system. The DNAC employs the estimated states and perturbation to realize the feedback linearizing control of the nonlinear power system. The system states and perturbation can be estimated by a robust sliding mode observer, without requiring the exact knowledge of the power system. The DNAC works as a nonlinear adaptive controller as it is capable of dealing with unmodelled system dynamics, parameter uncertainties and external disturbances. Moreover, the DNAC can be easily implemented than the FLC as only one measurement, relative rotor angle, is required. The simulation results show that the DNAC can damp out the multi-mode oscillations effectively and provide more satisfactory and robust control performance by contrast to that obtained using the FLC.

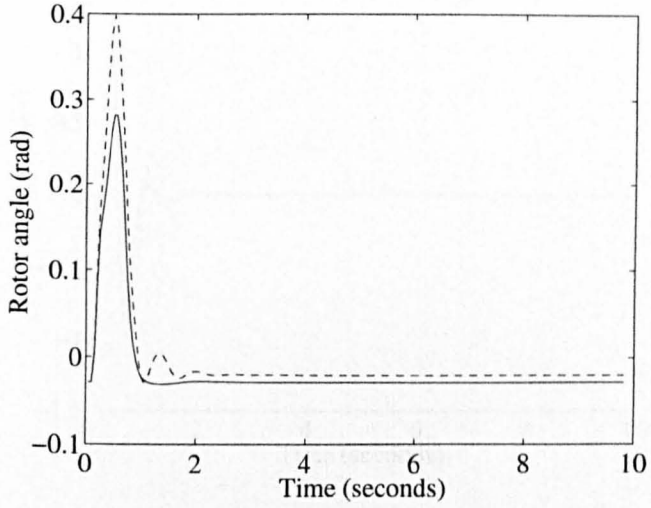

(a) $\delta_1 - \delta_3$

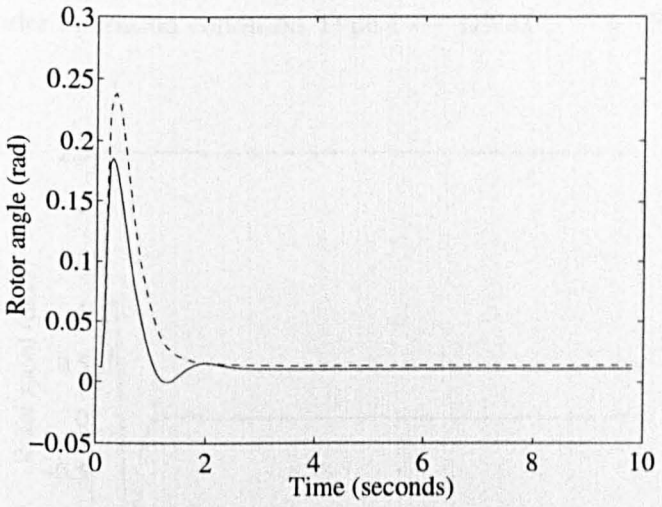

(b) $\delta_2 - \delta_3$

Figure 6.4: Rotor angle responses with DNACs or FLCs on all units under operation condition Type I

— DNAC, – – FLC

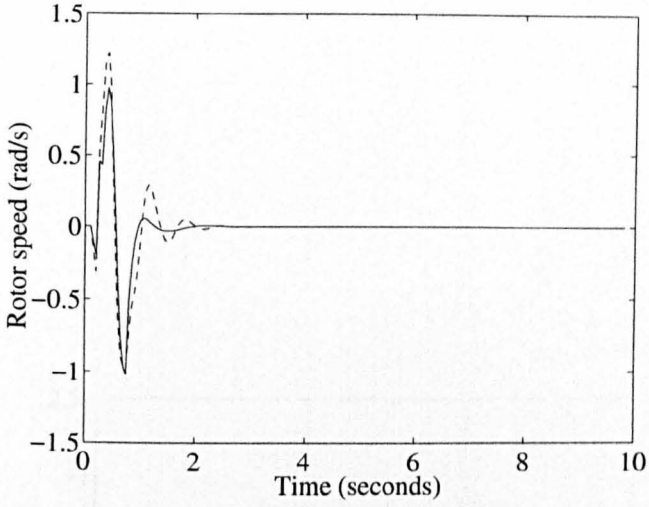

Figure 6.5: $\omega_1 - \omega_2$ with DNACs or FLCs on all units
under operation condition Type I — DNAC, – – FLC

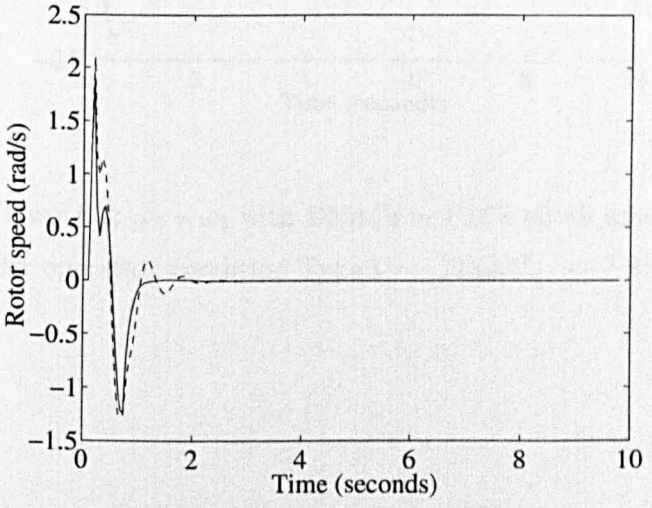

Figure 6.6: $\omega_1 - \omega_3$ with DNACs or FLCs on all units
under operation condition Type I — DNAC, – – FLC

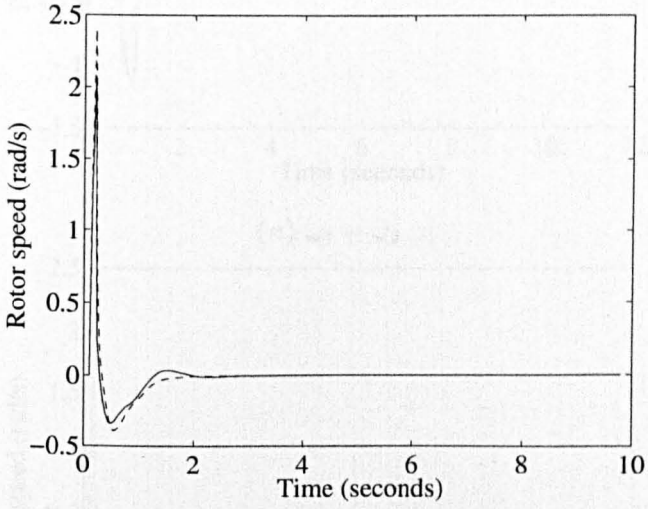

Figure 6.7: $\omega_2 - \omega_3$ with DNACs or FLCs on all units
under operation condition Type I — DNAC, – – FLC

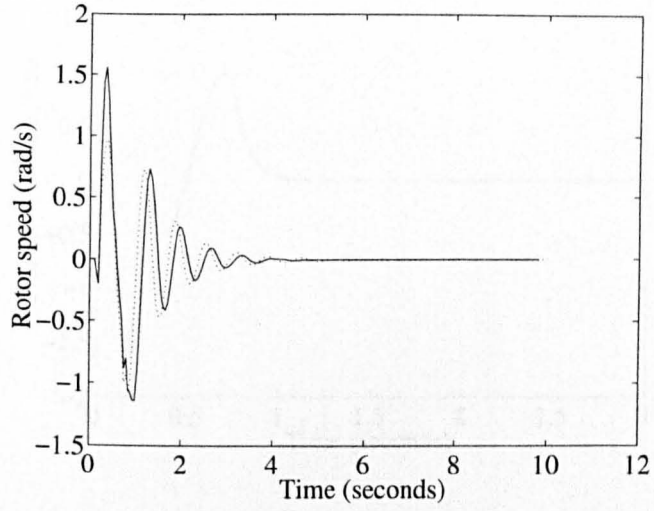

(a) $\omega_1 - \omega_2$

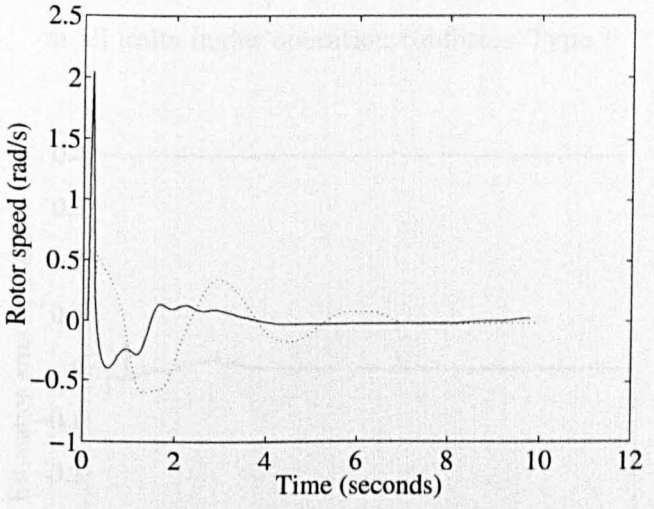

(b) $\omega_2 - \omega_3$

Figure 6.8: Rotor speed responses with DNAC on G2 and CPSS on G1 and G3

under operation condition Type I,— DNAC + CPSS, – – CPSS

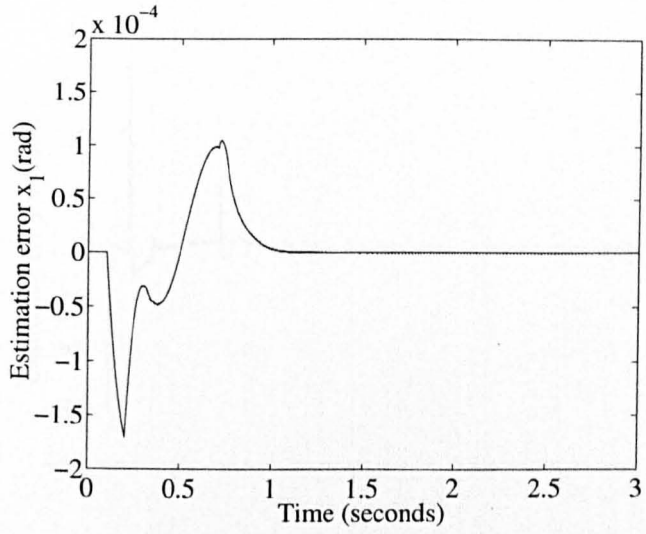

Figure 6.9: Responses of observer estimation error $\tilde{x}_1$ with DNACs on all units under operation condition Type I

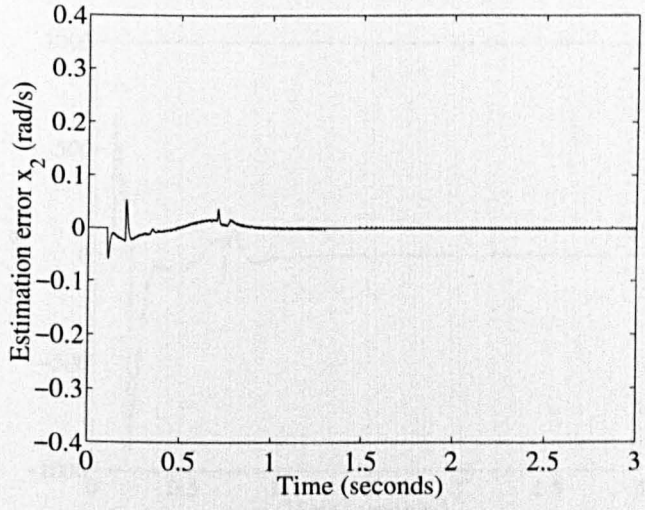

Figure 6.10: Responses of observer estimation error $\tilde{x}_2$ with DNACs on all units under operation condition Type I

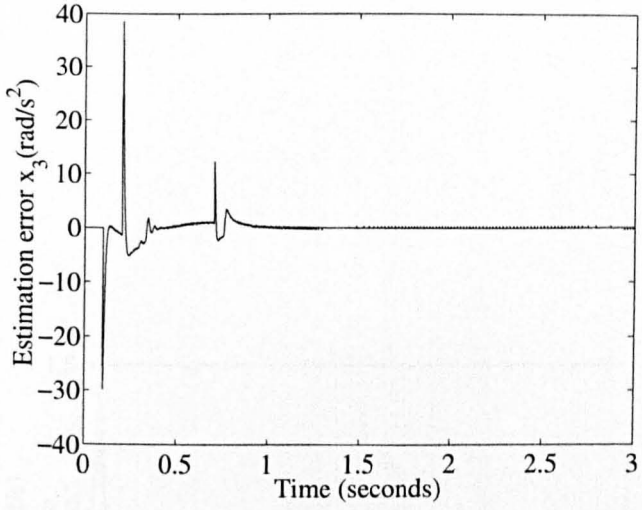

Figure 6.11: Responses of observer estimation error $\tilde{x}_3$ with DNACs on all units under operation condition Type I

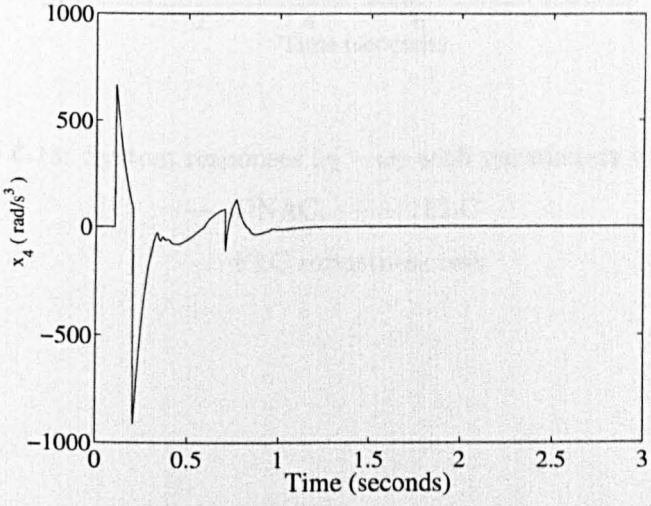

Figure 6.12: The estimated perturbation $\hat{x}_4$

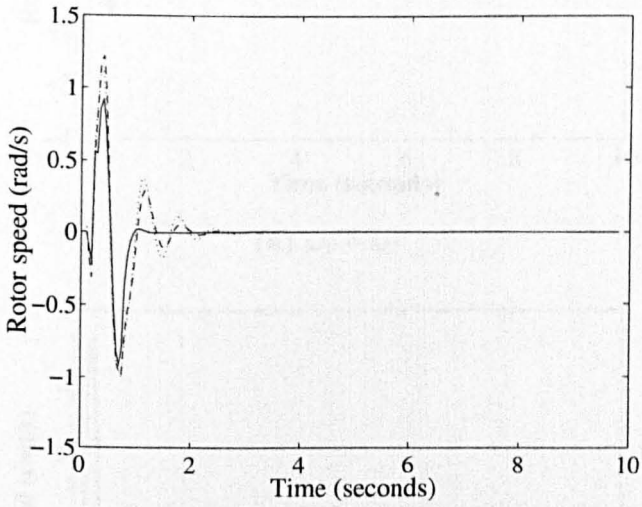

Figure 6.13: System responses $\omega_1 - \omega_2$ with parameters variation

— DNAC, – – FLC

$\cdots$ FLC robustness test

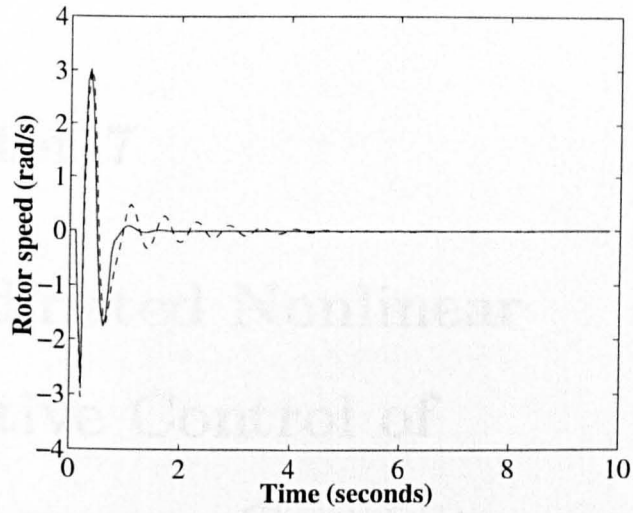

(a) $\omega_1 - \omega_2$

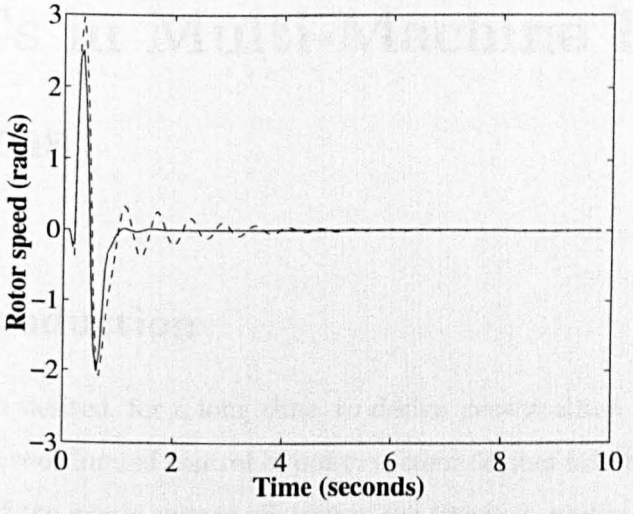

(b) $\omega_1 - \omega_3$

Figure 6.14: System responses with DNACs or FLCs on all units under operation condition Type II, — DNAC, – – FLC

Chapter 7

Coordinated Nonlinear Adaptive Control of Synchronous Generators and TCSCs in Multi-Machine Power Systems

7.1 Introduction

It has been desired, for a long time, to design decentralized adaptive controllers for the coordinated control of power system devices towards an optimal performance of the whole system. However, the previous studies of power system adaptive control were supported by the linear control theory [78]. Although the AI techniques, such as neural networks and learning control [145, 146], have been attempted to resolve the problem, the difficulties arising from system nonlinearities and uncertainties have hampered understanding of nonlinear dynamics interacted between devices and utilizing them for coordinated control

of the power system.

In recent years, Flexible AC Transmission Systems (FACTS) have received an increased research interest for power system control. Numerous research work has been undertaken on the development of Thyristor Controlled Series Capacitor (TCSC) control schemes for power system stability [111]. TCSC, Static Voltage Compensator (SVC), Static VAr CONdenser (STATCON), Static Phase Shifter (SPS) and Power System Stabilizer (PSS) are all fast-acting power system control devices. Although each of them can be used to improve power system operation efficiency and dynamic stability, the coordinated control of these devices has not been investigated intensively.

As a power system is a nonlinear interconnected system, nonlinear control methods have been investigated for power system control [108, 147, 112]. Nonlinear control theory has also been applied to the coordinated control of FACTS devices [105, 148]. However, as these methods reported in the literature require accurate system models and parameters in the controller design process, it is impossible to guarantee their reliable performance when they are implemented in a real multi-machine power system for which the details of system models and parameters are always unavailable.

In this chapter, a coordinated nonlinear adaptive control (CNAC) of synchronous generators and TCSCs in the multi-machine power system is investigated. Analysis begins with de-coupling a nonlinear multi-machine power system into subsystems using Lie differentiation, which provides a basic system structure for the input/output linearization of the subsystems, although the CNAC design does not require explicit mathematical decomposition of the power system. The CNAC design is then undertaken based on the input/output feedback linearizing control of a subsystem by introducing a fictitious state defined to represent the combined effect of system nonlinearities, uncertainties and external disturbances, which are regarded as an external perturbation applied to the nonlinear subsystem. Furthermore, the CNAC can be designed

based on the local measurements without requiring the global system model and mathematical de-coupling. This leads to de-coupling the multi-machine power system into subsystems automatically without ignoring any subsystem interaction. Based on a subsystem, the sliding mode observer is designed to estimate the system states and the fictitious state. The estimated perturbation is then included in the nonlinear feedback control loop to cancel the system nonlinearities and uncertainties, which results in a feedback linearizing control without requiring the knowledge of system nonlinearities and parameters. Consequently, a nonlinear adaptive de-coupled controller, implemented based on local measurements, is obtained.

The CNACs are applied in subsystems respectively for the coordinated control of generators and TCSCs in the multi-machine power system. Simulations studies are undertaken based on a three-machine power system to evaluate the effectiveness of the CNACs. The simulation results are provided to demonstrate the merits of the novel nonlinear adaptive control strategy.

7.2 Power system models

In order to investigate the coordinated control of TCSCs and synchronous generators in the multi-machine power system, the subsystem models in which a TCSC or generator is involved, are described below.

7.2.1 The subsystem including a TCSC

TCSC is an important device in the FACTS family. With the adjustment of the thyristor, it can change its apparent reactance smoothly and rapidly. This characteristic meets the demands of modern power systems that must operate flexibly and react quickly. TCSC is one kind of a capacitive reactance compensator which consists of a series capacitor bank shunted by thyristor

controlled reactor in order to provide a smoothly and rapidly variable series capacitive reactor. As the TCSC controllers, TSSC (Thyristor Switched Series Capacitor) is known as FACTS utilizing thyristor elements. While TSSC controls the capacitive reactance by switching thyristor elements, TCSC is able to compensate it continuously.

The description of power system dynamics is focused on the subsystem which involves a TCSC. An equivalent two-machine system, shown in Figure 7.1, can be used to analyze the performance of TCSC installed on a transmission tie-line in the multi-machine power system. The power transfer characteristics is described as:

$$P(\delta) = \frac{V_1 V_2}{X_L - X_C} \sin(\delta_1 - \delta_2) \tag{7.2.1}$$

where $P(\delta)$ is the power delivered through the transmission line; V_1, V_2 the magnitude of the transmission terminal voltage at buses 1 and 2 respectively; δ_1, δ_2 the phase angle of the two bus voltages respectively; X_L the transmission line reactance and X_C the equivalent reactance of TCSC.

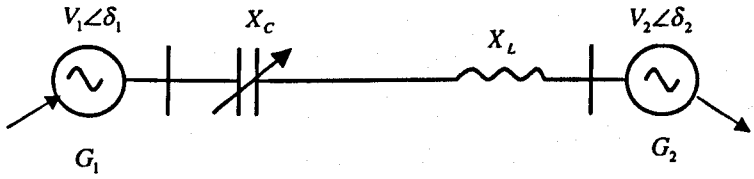

Figure 7.1: The equivalent two-machine power system

The equivalent generator is represented by a classical model. The dynamic model of the two-machine power system is expressed as

$$\begin{aligned} \frac{d}{dt}\Delta\delta &= \Delta\omega \\ \frac{d}{dt}\Delta\omega &= \frac{\omega_s}{H}\left[P_m - \frac{V_1 V_2}{X_L - X_C}\sin(\Delta\delta)\right] \end{aligned} \tag{7.2.2}$$

where $\Delta\delta$ is the deviation between the angle of the two machines from its steady value, with its initial value being $\Delta\delta_0$; $\Delta\omega$ the relative speed between the two machines, with its initial value being $\Delta\omega_0 = 0$; $1/H = 1/H_1 + 1/H_2$; H_1 and H_2 the machine inertia coefficients; P_m the machine mechanical power and ω_s the system normal speed.

7.2.2 The subsystem including a synchronous generator

This subsystem is considered as a single machine to infinite bus system. A simplified third-order model, e.g. E'_q-model, is adopted for the design of the excitation controller of the synchronous generator. The generator dynamics is described as follows:

$$\begin{aligned} \dot{\delta} &= \omega - \omega_0 \\ \dot{\omega} &= \frac{\omega_0}{2H}[P_m - \frac{D}{\omega_0}(\omega - \omega_0) - P_e] \\ \dot{E}'_q &= \frac{1}{T_{do}}(u_2 + E_{f0} - E_q), \end{aligned} \tag{7.2.3}$$

where

$$\begin{aligned} P_e &= E'_q I_q + (X_q - X'_d) I_d I_q \\ E_q &= E'_q + (X_d - X'_d) I_d \\ V_d &= X_q I_q \\ V_q &= E'_q - X'_d I_d, \end{aligned}$$

where δ denotes the rotor angle, in rad; ω the rotor speed, in rad/s; E'_q and E_q the transient voltage and voltage behind the quadrature-axis, respectively; P_m the mechanical power input from the prime mover and assumed to be constant, in $p.u.$; P_e the electrical power output of the generator, in $p.u.$; H the inertia coefficient of rotor, in seconds; T'_{do} the field winding time constant, in seconds; D the damping constant of the generator, in $p.u.$; X_d, X'_d the synchronous and transient impedance in the d-axis; X_q the synchronous impedance in the q-axis;

u_2 the excitation control; I_d and I_q the generator currents in the d-axes and q-axes, respectively; V_d and V_q the generator terminal voltage in the d-axes and q-axes, respectively; and E_{f0} the initial excitation voltage.

7.3 Design of nonlinear adaptive controller for a subsystem

7.3.1 The CNAC of TCSC

The main purpose of TCSC control is to damp the inter-area oscillation of two interconnected power system areas. In practice, local measurements should be used as the controller input signals. In most of the TCSC controllers, the voltage angular difference between two buses connected by a transmission line has been employed as a promising measurement for damping control [149]. In this paper, it is also chosen to mimic the centroid angular difference between the machines in the two areas.

For subsystem 1, equation (7.2.2), defining $x_{11} = \Delta\delta - \Delta\delta_0$, $x_{12} = \Delta\omega$, choosing the voltage angular difference as the output $y_1 = x_{11}$, and denoting the control as $u_1 = 1/(X_L - X_C) - u_{10}$, where $u_{10} = 1/X_L$ is the control initial value, then we can obtain:

$$\begin{aligned} \frac{dy_1}{dt} &= x_{12} \\ \frac{d^2y_1}{d^2t} &= a_1(x) + b_1(x)u_1 = \Psi_1(\cdot) + b_{10}u_1, \end{aligned} \tag{7.3.1}$$

where

$$\Psi_1(\cdot) = a_1(x) + (b_1(x) - b_{10})u_1 \tag{7.3.2}$$

$$a_1(x) = \frac{\omega_s P_m}{H} - \frac{\omega_s V_1 V_2 \sin(x_{11} + \Delta\delta_0)}{H} u_{10} \tag{7.3.3}$$

$$b_1(x) = -\frac{\omega_s V_1 V_2 \sin(x_{11} + \Delta\delta_0)}{H}, \; b_{10} = b_1(0). \tag{7.3.4}$$

It should be mentioned that $b_1(0)$ is a constant and chosen arbitrarily as long as it satisfies condition (4.2.7).

As the relative degree $r_1 = 2$, after defining $z_{11} = y_1$, $z_{12} = \frac{d}{dt}y_1$, $z_{13} = \Psi_1(\cdot)$, a third-order sliding mode observer, in the form of equation (3.4.1), is designed. With the estimated states and fictitious state, the control law of subsystem 1 is:

$$u_1 = (v_1 - \hat{z}_{13})/b_{10}, \tag{7.3.5}$$

$$v_1 = -a_{11}\hat{z}_{11} - a_{12}\hat{z}_{12}. \tag{7.3.6}$$

Denote the compensation rate as $\mu, 0 < \mu < 1$, then $-\mu X_L \leq X_C \leq \mu X_L$. Finally, the limit of control u_1 is: $\frac{-\mu}{1+\mu}\frac{1}{X_L} \leq u_1 \leq \frac{\mu}{1-\mu}\frac{1}{X_L}$.

7.3.2 The CNAC of generator excitation system

For subsystem 2, equation (7.2.3), by choosing the state variables as

$$x_2 = [x_{21} \;\; x_{22} \;\; x_{23}]^T = [\delta - \delta_0 \;\; \omega - \omega_0 \;\; \dot{\omega}]^T$$

and system output as $y_2 = x_{21}$, we can obtain:

$$\begin{aligned} \frac{dy_2}{dt} &= x_{22} \\ \frac{d^2y_2}{d^2t} &= x_{23} \\ \frac{d^3y_2}{d^3t} &= a_2(x) + b_2(x)u_2 = \Psi_2(\cdot) + b_{20}u_2, \end{aligned} \tag{7.3.7}$$

where

$$\Psi_2(\cdot) = a_2(x) + (b_2(x) - b_{20})u_2$$

$$a_2(x) = \frac{-\omega_0}{2H}\left(\frac{D}{\omega_0}\dot{\omega} + E'_q\dot{I}_q + (x_q - x'_d)\frac{d}{dt}(I_dI_q)\right) + \frac{\omega_0 I_q}{2HT'_{do}}E_q \tag{7.3.8}$$

$$b_2(x) = \frac{-\omega_0 I_q}{2HT'_{do}}, \;\; b_{20} = b_2(0), \tag{7.3.9}$$

and $b_2(0)$ is chosen as a constant to satisfy condition (4.2.7).

As $r_2 = 3$, after defining $z_{21} = y_2$, $z_{22} = \frac{d}{dt}y_2$, $z_{23} = \frac{d^2}{d^2t}y_2$, $z_{14} = \Psi_2(\cdot)$, then a fourth-order sliding mode observer is applied. The control law of subsystem 2 can be obtained as:

$$u_2 = (v_2 - \hat{z}_{24})/b_{20}, \tag{7.3.10}$$

$$v_2 = -a_{21}\hat{z}_{21} - a_{22}\hat{z}_{22} - a_{23}\hat{z}_{23}. \tag{7.3.11}$$

7.4 Simulation Study

7.4.1 Test system and CNACs setting

The designed CNAC is evaluated on a three-machine power system as shown in Figure 6.2. In this system, the multi-mode oscillations can be observed following a disturbance. The system responses, after a three-phase-to-ground short circuit occurring at × point, without generator excitation and TCSC control provided, are shown in Figure 6.3. The fault is simulated as: a three-phase-to-ground short circuit occurs at the end terminal of line $4-5(2)$ ((2) denotes the second line between buses 4 and 5) at $t = 0.1$ s. The faulty transmission line is switched off at $t = 0.3$ s and switched on again at $t = 0.7$ s when the fault is cleared. In this case, all generators are equipped with AVRs, fast-acting exciters and governors. Each generator is simulated by a fifth-order model in the simulation, although the simplified model is used for design of the excitation controller. This implies that unmodelled dynamics has been considered in the CNAC design and emulated in the simulation study.

Two sets of parameters are required for the CNAC. One set is associated with the sliding mode observer and the other is for the feedback controller. The parameters of the CNAC for TCSC are given as follows. The determination of the sliding mode observer begins with designing a Luenberger observer, by choosing $\alpha_{11} = 15, \alpha_{12} = 75$ and $\alpha_{13} = 125$ so as to place all the poles at -5. Because the maximum value of $\Delta\omega$ in $p.u.$ will be less than 0.1 after

a serious fault occurs, k_{11} can be chosen to be 5 from equation (3.4.4). In order to ensure the stable and fast convergent error dynamics of the sliding mode observer when fault occurs, the poles in equation (3.4.2) are placed as a relatively high value $\lambda = -50$. Then the other gains of the observer are chosen as $k_{12} = 5 \times 10^2$, $k_{13} = 1.25 \times 10^4$. The CNAC parameters, in equation (7.3.6), are determined as $a_{11} = 100$, $a_{12} = 20$ so as to place the poles of the linear system at -10.

The parameters of the CNAC for generators are given as follows. The parameters of the fourth-order sliding observer are chosen as: $\alpha_{21} = 20$, $\alpha_{22} = 150$, $\alpha_{23} = 500$ and $\alpha_{24} = 625$ so as to place all the poles of the Luenberger observer at -5; $k_{21} = 50$, $k_{22} = 7.5 \times 10^3, k_{23} = 3.75 \times 10^5$, $k_{24} = 6.25 \times 10^6$ so as to set the error dynamic on the sliding mode with all poles at $\lambda = -50$. Because the maximum difference of the generator speed in *p.u.* will be less than 0.1 after a serious fault occurs, $k_{21} = 50$ is large enough to satisfy the existence condition of sliding mode, equation (3.4.4). The CNAC parameters in equation (7.3.11) are determined as $a_{21} = 1 \times 10^3$, $a_{22} = 3 \times 10^2$, $a_{23} = 30$ so as to place the poles of the linear system at -10. In equation (7.3.5), $b_{10} = -0.2$. In equation (7.3.10), $b_{20} = -0.4$. These values are chosen based on equations (7.3.4) and (7.3.9), where $\omega_s = \omega_0 = 1.0$, to satisfy equation (4.2.7).

It should be mentioned that although a number of parameters need to be chosen, they are not sensitive to the CNAC performance. Although the generators involved in the simulation study have different parameters and operation conditions, the CNAC designed for each generator contains the same parameters of the observer and controller. Therefore, with a little experience, these parameters can be easily determined.

The sampling interval of excitation control is $40ms$. Considering the variable impedance response of TCSC has a time delay, the sampling interval for the TCSC controller is chosen as $100ms$. The TCSC is installed at the line $5-6$ and it has compensation rate $\mu = 0.667$.

The advantages of the feedback linearizing controller for improving power system stability have been shown in comparison with the PID controller, PSS and linear optimal controller [87]. However, the feedback linearizing control strategy cannot be applied directly for TCSC as its design involves a complex system model, even in the case where the model is available. As mentioned previously, this paper focuses on designing local controllers for the coordinated control of power system without requiring the knowledge of the power system model, therefore, a PSS is only employed for comparison. In the simulation study, the coordination between the CNAC of TCSC and the CNACs of generators or PSSs equipped on generators is investigated respectively. The PSS's transfer function and parameters are given in the Appendix.

7.4.2 CNAC of TCSC

The system responses with the CNAC equipped on the TCSC installed on line $5-6$ are shown in Figures 7.2 $\sim$ 7.5, compared with the system responses obtained without the CNAC. From the figure, it can be seen that the CNAC can provide satisfactory damping to reduce the inter-area oscillation between generators 2 and 3, in particular the oscillation of voltage angular difference between buses 5 and 6. The dynamic interaction between generators 1 and 2 is not presented here as the TCSC control makes little contribution to the local mode oscillation between generators 1 and 2.

7.4.3 CNACs equipped on all generators

In this case, the CNAC is installed on each generator but not for the TCSC. The system responses are shown in Figures 7.6 $\sim$ 7.9, where the responses of all generators with the PSS installed are provided for comparison. Under this circumstance, all oscillation modes have been damped effectively. It is worthwhile to point out that all the CNACs have the same structure and

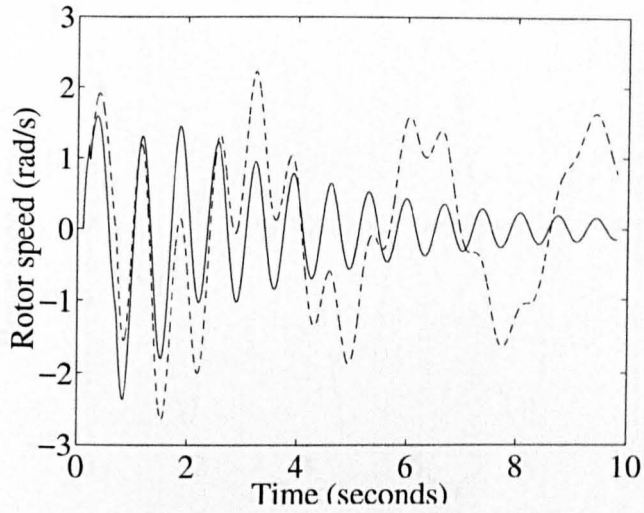

Figure 7.2: $\omega_1 - \omega_3$ responses with an CNAC of TCSC installed on line $5-6$
— CNAC, – – – Without CNAC

parameters.

7.4.4 Coordination between CNAC of TCSC and PSSs equipped on generators

The PSS has been applied for most modern generators. It is necessary to find out whether the CNAC and PSS may cause adverse interaction. Therefore, the interaction and coordination between the CNAC of TCSC and the PSS equipped on all generators are investigated. In this case, the cooperation between the CNAC and the PSSs has been simulated. The system responses are shown in Figures 7.10 $\sim$ 7.13 . From the figure, it can be noted that the CNAC of TCSC can coordinate well with the PSSs of generators to improve the system dynamic performance.

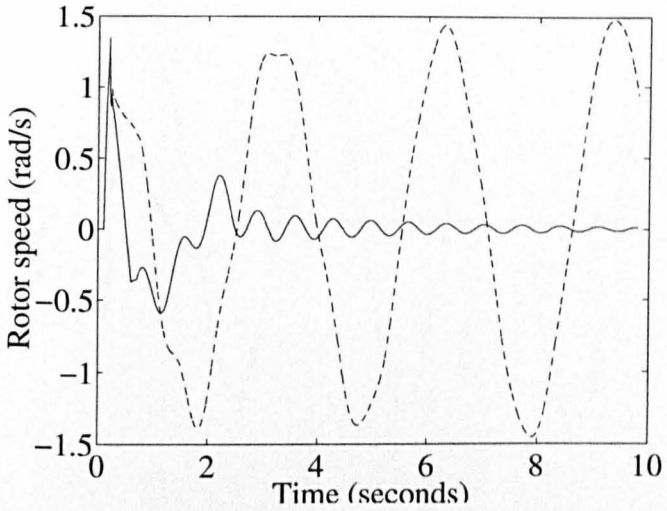

Figure 7.3: $\omega_2 - \omega_3$ responses with an CNAC of TCSC installed on line $5-6$
— CNAC, – – – Without CNAC

7.4.5 Observer performance and perturbation estimation

The performance of the sliding mode observer has been monitored during the period of a large system disturbance, in which the observer functions fully in its nonlinearities. The estimation errors of system states and the estimate of perturbation of generator 2 are shown in Figures 7.14 and 7.15 respectively, where all the generators have the CNAC. It can be seen from the figure that the observer can provide accurate estimates to trace the system states and perturbation rapidly, especially in the case of an abruptly change of states caused by the fault.

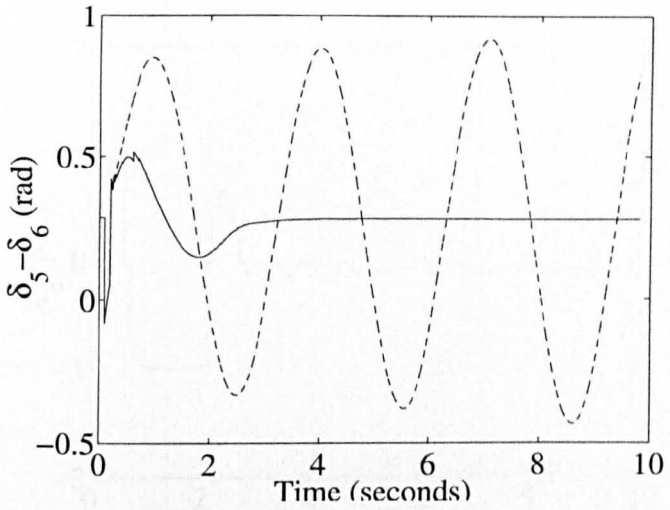

Figure 7.4: $\delta_5 - \delta_6$ responses with an CNAC of TCSC installed on line $5-6$
— CNAC, − − − Without CNAC

7.5 Conclusion

In this chapter, a novel nonlinear adaptive controller has been proposed for the coordinated control of synchronous generators and TCSC devices to improve power system stability. The proposed CNAC is developed, based on a feedback linearizing control strategy and the introduction of a fictitious state, with a robust sliding mode observer designed to estimate the system states and perturbation. Therefore, the CNAC can be designed based on the subsystem structure without requiring the knowledge of system nonlinearities and parameters. The CNAC has a simple form and adaptive nature. It does not ignore any system nonlinear dynamic mode but is able to be installed locally and implemented with a local measurement. The simulation results show that the CNACs can coordinate each other or with PSSs, to provide satisfactory control performance and damp multi-mode oscillations of the power system effectively.

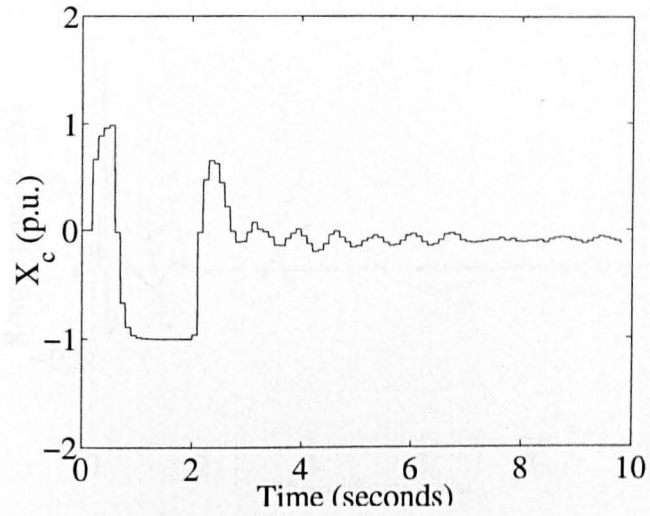

Figure 7.5: X_C responses with an CNAC of TCSC installed on line $5-6$

— CNAC, – – – Without CNAC

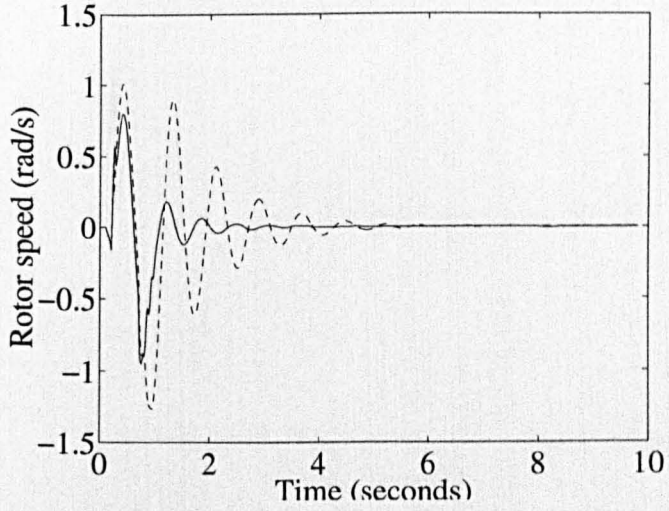

Figure 7.6: $\omega_1 - \omega_2$ responses with the CNAC installed on all generators

— CNAC, – – – PSS

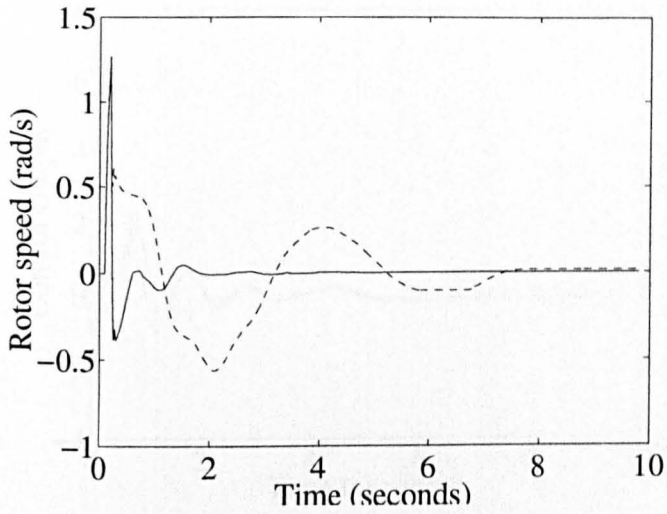

Figure 7.7: $\omega_2 - \omega_3$ responses with the CNAC installed on all generators

— CNAC, – – – PSS

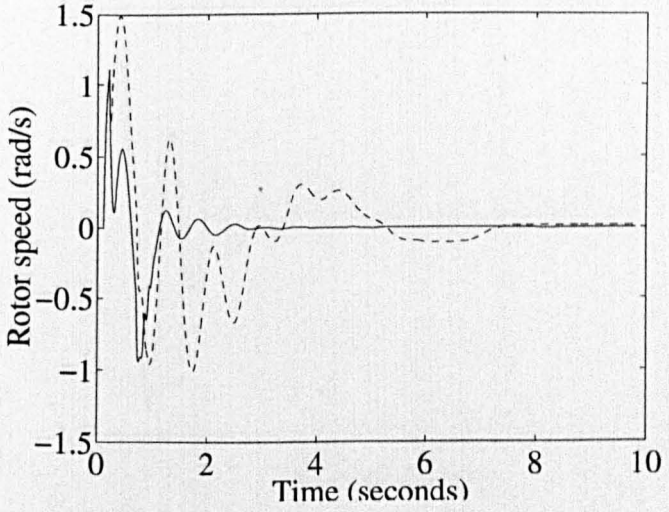

Figure 7.8: $\omega_1 - \omega_3$ responses with the CNAC installed on all generators

— CNAC, – – – PSS

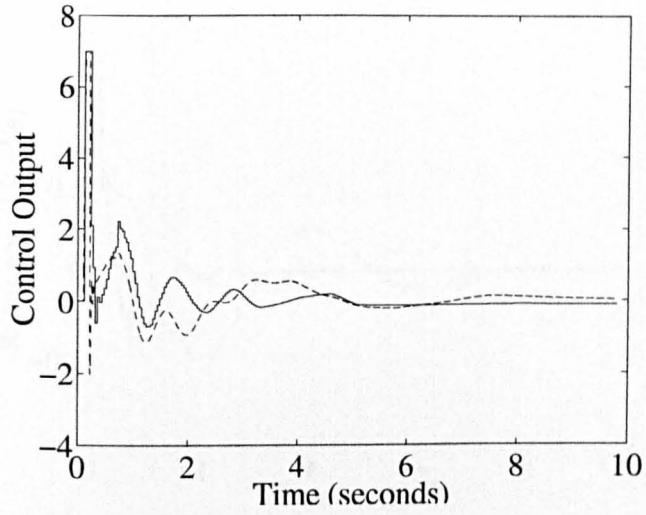

Figure 7.9: Excitation control of generator 2 responses with the CNAC installed on all generators

— CNAC, – – – PSS

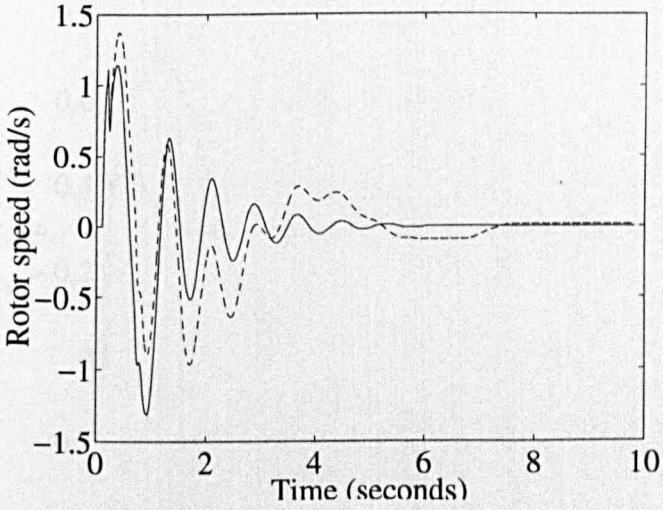

Figure 7.10: $\omega_1 - \omega_3$ responses with an CNAC of TCSC installed on line 5-6 and the PSS equipped on all generators

— CNAC on TCSC and PSS on generators, – – – PSS on generators

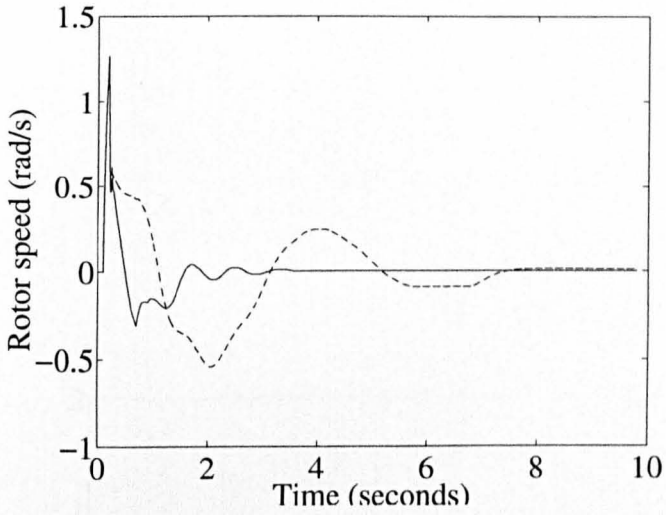

Figure 7.11: $\omega_2 - \omega_3$ responses with an CNAC of TCSC installed on line 5-6 and the PSS equipped on all generators

— CNAC on TCSC and PSS on generators, – – – PSS on generators

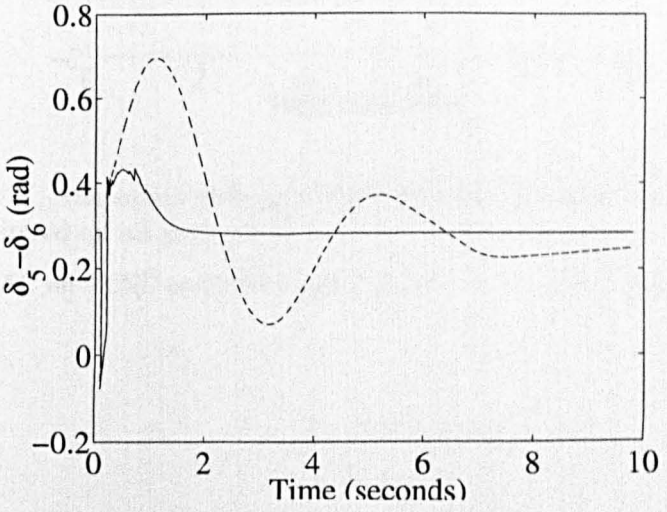

Figure 7.12: $\delta_5 - \delta_6$ responses with an CNAC of TCSC installed on line 5-6 and the PSS equipped on all generators

— CNAC on TCSC and PSS on generators, – – – PSS on generators

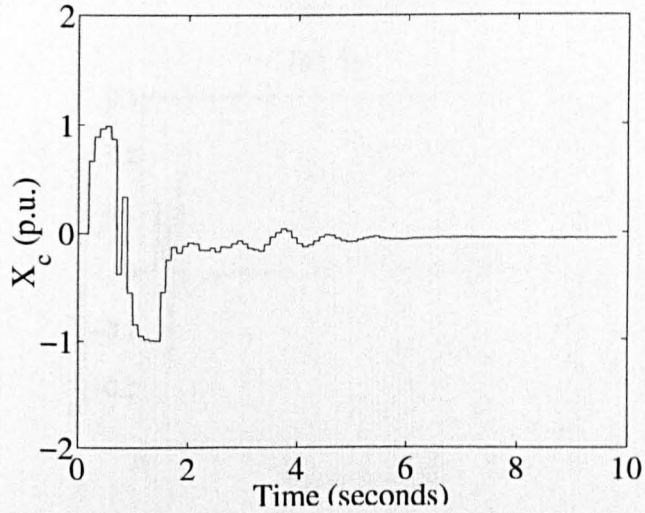

Figure 7.13: X_C responses with an CNAC of TCSC installed on line 5-6 and the PSS equipped on all generators

— CNAC on TCSC and PSS on generators, – – – PSS on generators

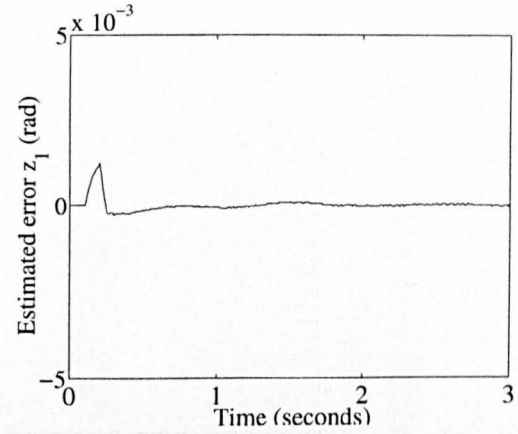

(a) $\tilde{z}_{21}$

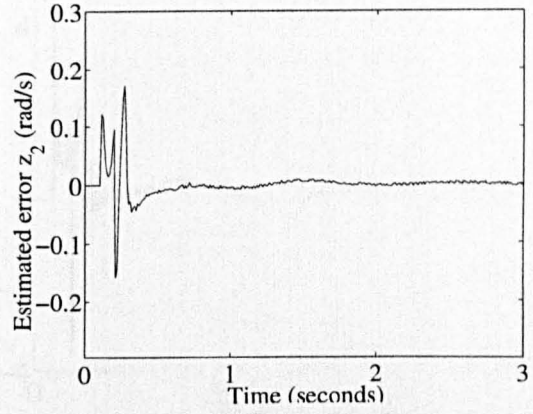

(b) $\tilde{z}_{22}$

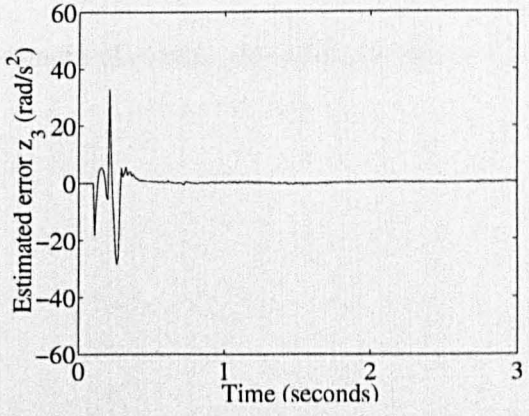

(c) $\tilde{z}_{23}$

Figure 7.14: Estimation errors of states of generator 2

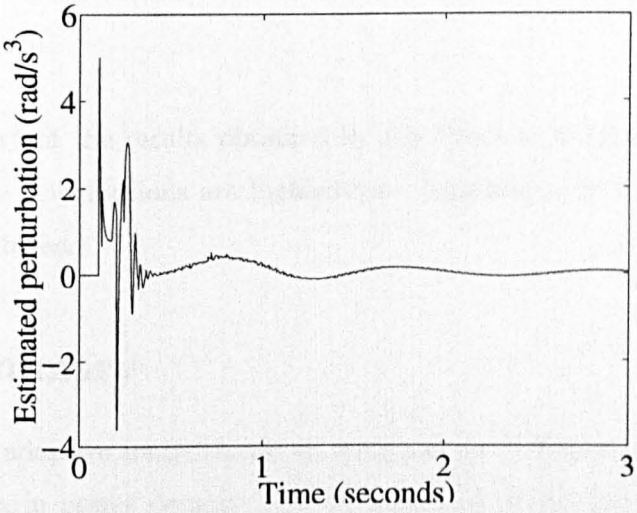

Figure 7.15: Estimate of system perturbation observed from generator 2 — $\hat{z}_{24}$

Chapter 8

Conclusion

A summary of the results obtained in this thesis is given below, and by this means its contributions are highlighted. Suggestions for future research are listed at the end.

8.1 Summary

Nonlinear adaptive control based on state and perturbation estimation and its application in power systems have been studied in this thesis. After the definition of system perturbation to represent the combinatorial effect of the system nonlinearities, uncertainties and external disturbances, two state and perturbation observers are designed and the nonlinear adaptive control schemes are developed. The following results have been presented:

- The real time estimation of system perturbation, which includes nonlinearities, time-varying parameters and external disturbances, is a functional estimation rather than the parameters estimation. A simple nonlinear adaptive control law has been obtained as the accurate system model is not required for the controller design.
- The upper bounds of perturbation are only required in the design of

observer, not the controller loop directly. Moreover, as the upper bound of perturbation is replaced by the smaller bound of its estimation error, an over conservative control input is avoided and the tracking accuracy is improved.

- Nonlinear adaptive control of nonlinear systems via high gain state and perturbation observer, nonlinear adaptive sliding mode control using sliding mode state and perturbation observer and decentralized nonlinear adaptive control of large-scale interconnected systems have been investigated respectively.

- The stability analysis of the closed-loop system including controller and observer for each control scheme has been undertaken and corresponding numeric simulation results of example systems have been given.

- The control of canonical nonlinear system, which can be obtained from fully linearizable nonlinear system, has been mainly dealt with. These control schemes has been also applied to the input/output linearization of minimum phase nonlinear systems.

The proposed control schemes have been applied to design nonlinear adaptive controllers for power systems.

- Nonlinear adaptive control of synchronous generators has been studied. The single machine quasi-infinite bus power system model has been used. A simple adaptive controller based on local measurements and simulation results which is in comparison with a conventional nonlinear state feedback linearization controller have been given.

- Decentralized nonlinear adaptive controller has been designed for the excitation control of synchronous generators interconnected in a multi-machine power systems. The controller has been developed based on a

fully feedback linearizable multi-machine model and a input/output partial linearizable multi-machine model, respectively. The designed controller is robust in performance and is easy to be implemented. Simulation study is carried out based on a three-machine power systems and the results show that the designed controller has better performance and robustness, under variations of power system operation conditions and disturbances, in comparison with a conventional nonlinear state feedback linearization controller.

- Coordinated nonlinear adaptive control for the excitation control of generators and Thyristor Controlled Series Compensators in multi-machine power systems has been studied. The controllers are implemented locally with the design of state and perturbation observer for subsystem. Simulation results show that the locally installed controller can coordinate each other to improve the power system stability.

8.2 Recommendations for further study

We point out several related directions which deserve further investigation as follows.

- Nonlinear adaptive control of non-minimum phase nonlinear system via state and perturbation observer. The nonlinear adaptive control of nonlinear control canonical system and minimum phase nonlinear systems have already been investigated. It is worth extending our results to non-minimum phase nonlinear systems.

- Discrete nonlinear adaptive control via state and perturbation observer. Our research has been developed mainly for continuous systems. It is desired to extend the research into discrete-time systems.

- Nonlinear adaptive control under control constraints. During the design of the nonlinear adaptive control scheme based on the state and perturbation observer, the control output is assumed to be bounded but big enough for the purpose of perturbation cancellation. Although this is also a common problem in feedback linearization techniques, it is needed to investigate how the control constraints will affect the effectiveness of the proposed nonlinear adaptive control.

- Design state and perturbation using the easily measured output is highly desired in power system practice. When the nonlinear adaptive control of synchronous generator is been studied, the rotor angle is taken as the available measurement. However, it is known that the rotor angle can not be measured easily in power systems. Thus the easily obtained generator variables, such as rotor speed or active power, will be considered in further research.

- The nonlinear adaptive control schemes can lead to more applications in power systems, such as the control of induction motor and FACTS controllers, such as STACON and UPFC. As the introduction of FACTS controller increases the difficulties of modelling multi-machine power systems, the proposed control schemes in this thesis are suitable for the delivery of nonlinear adaptive controller for the FACTS devices.

Appendix A

Feedback Linearization Control

A.1 Feedback Linearization Control

In this section, we review the basic results of nonlinear feedback linearization control of a single-input single-output (SISO) nonlinear system. This method employs a transformation of coordinates and feedback control to transform a nonlinear system into a system which dynamic is linear (at least partial). It includes two kinds of approach: input-state linearization, where the full state equation is linearized; and the input-output linearization, where the emphasis is on linearizing the input-output map from input u to output y even if the state equation is only partially linearized.

We consider a single-input single-output affine nonlinear system represented by

$$\dot{x} = f(x) + g(x)u \tag{A.1.1}$$

$$y = h(x) \tag{A.1.2}$$

where $x \in \mathcal{R}^n$ is the state vector, $u \in \mathcal{R}$ the input, $y \in \mathcal{R}$ the output. $f(x)$, $g(x) : \mathcal{R}^n \to \mathcal{R}^n, h : \mathcal{R}^n \to \mathcal{R}$ smooth vector fields on the state space $\mathcal{R}^n$. We will assume $f(x_0) = 0$, $h(x_0) = 0$, i.e., $x_0 \in \mathcal{R}^n$ is an equilibrium point of the unforced system.

The point of departure of the whole analysis of the exact linearization via feedback is the notion of *relative degree* of the system.

Definiton A.1. *Nonlinear system (A.1.1) (A.1.2) is said to have a relative degree r, $r \leq n$, at point x_0 if*

- $\mathcal{L}_g\mathcal{L}_f^k(x)h(x) = 0$, $\forall\ x$ *in a neighbourhood of* x_0 *and* $k \leq r-2$;
- $\mathcal{L}_g\mathcal{L}_f^{r-1}(x)h(x) \neq 0$.

where $x_0 \in \mathcal{R}^n$, $\mathcal{L}_f(\phi(x)) : \mathcal{R}^n \to R$ and $\mathcal{L}_g(\phi(x)) : \mathcal{R}^n \to R$ represent for the Lie derivative of $\phi(x)$ with respect to $f(x)$ and $g(x)$ respectively, and

$$\begin{aligned} \mathcal{L}_f^0(h(x)) &= h(x) \\ \mathcal{L}_f^k(h(x)) &= \left[\frac{\partial}{\partial x}\mathcal{L}_f^{k-1}(h(x))\right] f(x) \\ \mathcal{L}_g\left(\mathcal{L}_f^k(h(x))\right) &= \left[\frac{\partial}{\partial x}\mathcal{L}_f^k(h(x))\right] g(x). \end{aligned}$$

A.1.1 Input-state linearization

System (A.1.1) and (A.1.2) is fully-linearizable if there exists a diffeomorphism $\Psi : U \to R^n$ such that $D = \Psi(U) \in R^n$ and the state transformation $z = \Psi(x)$ transforms the system into the form:

$$\dot{z} = Az + B(\alpha(x) + \beta(x)u) \tag{A.1.3}$$

$$y = Cz \tag{A.1.4}$$

where (A, B) is controllable and $\beta(z)$ is nonsingular $\forall z \in D$. With the system in form (A.1.3) and (A.1.4), we can linearize it exactly by the state feedback control

$$u = (-\alpha(z) + v)/\beta(z) \tag{A.1.5}$$

to obtain the linear system

$$\dot{z} = Az + Bv \tag{A.1.6}$$

$$y = Cz, \tag{A.1.7}$$

where v is the linear system control.

Consider the nonlinear system (A.1.1) and (A.1.2) having the relative degree $r = n$, i.e., exactly equal to the dimension of the state space, at the point x_0. In this case, the change of coordinates is required to construct the normal form is exactly given by

$$\Phi(x) = \begin{pmatrix} \phi_1(x) \\ \phi_2(x) \\ \vdots \\ \phi_n(x) \end{pmatrix} = \begin{pmatrix} h(x) \\ L_f h(x) \\ \vdots \\ L_f^{n-1} h(x) \end{pmatrix} \tag{A.1.8}$$

i.e. by the function $h(x)$ and its first $n-1$ derivatives along $f(x)$. In the new coordinates

$$z_i = \phi_i(x) = L_f^{i-1} h(x), \qquad 1 \leq i \leq n, \tag{A.1.9}$$

the system (A.1.1) will be described in the following form:

$$\begin{cases} \dot{z}_1 &= z_2 \\ &\vdots \\ \dot{z}_{n-1} &= z_n \\ \dot{z}_n &= \alpha(z) + \beta(z)u \end{cases} \tag{A.1.10}$$

where $z = (z_1, ..., z_n)^T$, $\alpha(z) = L_f^n h(x)|_{x=\Psi^{-1}(z)}$, and $\beta(z) = L_g L_f^{n-1} h(x)|_{x=\Psi^{-1}(z)}$. Recall that at the point of $z^0 = \Phi(x_0)$, and thus for all z in a neighborhood of z_0, the function $\beta(z)$ is nonzero. Now, if we choose the state feedback control law (A.1.5) which indeed exists and is well-defined in a neighborhood of z_0. Imposing this feedback control yields a linear and controllable canonical system characterized by equations (A.1.6) and (A.1.7), where A,B and C are

given by

$$A=\begin{bmatrix} 0 & 1 & 0 & \cdots & 0 \\ 0 & 0 & 1 & \cdots & 0 \\ \vdots & & & & \vdots \\ 0 & 0 & 0 & \cdots & 1 \\ 0 & 0 & 0 & \cdots & 0 \end{bmatrix}, \quad B=\begin{bmatrix} 0 \\ 0 \\ \vdots \\ 0 \\ 1 \end{bmatrix}, \quad C=\begin{bmatrix} 1 & 0 & \cdots & 0 & 0 \end{bmatrix} \tag{A.1.11}$$

The problem of finding an output function $\lambda(x)$ such that the relative degree of the system at x_0 is exactly n, namely a function such that

$$L_g\lambda(x) = L_gL_f\lambda(x) = \cdots = L_gL_f^{n-2}\lambda(x) = 0 \qquad \forall x \tag{A.1.12}$$

$$L_gL_f^{n-1}\lambda(x) \neq 0 \tag{A.1.13}$$

is apparently a problem of resolving partial differential equations of the system. It has been proven that above conditions are equivalent to

$$\begin{aligned} ad_f^{i-1}\lambda(x) &= 0, 1 \leq i \leq n-1 \\ ad_f^{n-1}\lambda(x_0) &\neq 0, \end{aligned} \tag{A.1.14}$$

where

$$\begin{aligned} ad_f^0 g(x) &= g(x) \\ ad_f^1 g(x) &= [f,g] \\ &= \frac{\partial g}{\partial x}f(x) - \frac{\partial f}{\partial x}g(x) \\ ad_f^k g(x) &= [f, ad_f^{k-1}g](x), \quad k = 0,\ 1,\ \cdots,\ n-1, \end{aligned} \tag{A.1.15}$$

are called Lie products.

Equation (A.1.14) can be written as:

$$\frac{\partial \lambda(x)}{\partial x}\left[g(x)\ ad_f g(x)\ \cdots\ ad_f^{n-2}g(x)\right] = 0. \tag{A.1.16}$$

If equation (A.1.16) is solvable in a neighborhood of x_0, there exists a function $\lambda(x)$ such that the system (A.1.1) has relative degree n at x_0. The well-known

conditions (necessary and sufficient) for the solution of the state space exact linearization problem are the following.

A.1 Matrix $[g(x_0)\ ad_f^1 g(x_0)\ \cdots\ ad_f^{n-1} g(x_0)]$ has rank n.

A.2 Distribution $D = \text{span}\,[g\ ad_f^1 g\ \cdots\ ad_f^{n-2} g]$ is involutive in a neighbourhood of x_0.

The above feedback linearization is exact input-state linearization. The transformation of a nonlinear system into a linear one involves solving the first-order partial differential equation (A.1.16), which normally is quite difficult.

A.1.2 Input-output linearization

When certain output variables are of interest, as in tracking control problems, the system is described by state and output equations. If system (A.1.1) and (A.1.2) has relative degree n, then it is both input-state and input-output linearizable. In the input/output linearization procedure, output y is differentiated, with respect to time, r times until the control input u appears explicitly. The rth derivative of y with respect to time could be written as

$$\frac{d^r y}{dt^r} = \alpha_r(x) + \beta_r(x)u \tag{A.1.17}$$

where $\alpha_r(x) = L_f^r h(x)$ and $\beta_r(x) = L_g L_f^{r-1} h(x)$. If $\beta(x) \neq 0$, the nonlinear feedback control law

$$u = \beta_r(x)^{-1}\left[-\alpha_r(x) + v\right] \tag{A.1.18}$$

yields a rth-order linear SISO system

$$\frac{d^r y}{dt^r} = v \tag{A.1.19}$$

where $v \in R$ is the control input of the linear system.

As system (A.1.1) and (A.1.2) has relative degree r, $r < n$ at x_0, thus there exist $n - r$ smooth functions $\psi_{r+1}(x), \cdots, \psi_n(x)$ such that

$$\xi \triangleq \begin{bmatrix} z \\ \varphi \end{bmatrix} \triangleq \begin{bmatrix} h(x) \\ \vdots \\ L_f^{r-1}h(x) \\ \psi_{r+1}(x) \\ \vdots \\ \psi_n(x) \end{bmatrix} \triangleq \Psi(x) \tag{A.1.20}$$

is a local diffeomorphism and satisfies

$$L_g\psi_i(x) = 0, \qquad i = r+1, \cdots, n, \tag{A.1.21}$$

and $\Psi(x_0) = 0$.

System (A.1.1) and (A.1.2) can be transferred into the following form

$$\dot{z} = A_r z + B_r[\alpha_r(x) + \beta_r(x)u] \tag{A.1.22}$$

$$\dot{\varphi} = q(z, \varphi) \tag{A.1.23}$$

$$y = C_r z, \tag{A.1.24}$$

where $A_r \in R^{r\times r}$, $B \in R^{r\times 1}$, $C \in R^{1\times r}$ are given by

$$A_r = \begin{bmatrix} 0 & 1 & 0 & \cdots & 0 \\ 0 & 0 & 1 & \cdots & 0 \\ \vdots & & & & \vdots \\ 0 & 0 & 0 & \cdots & 1 \\ 0 & 0 & 0 & \cdots & 0 \end{bmatrix}, \quad B_r = \begin{bmatrix} 0 \\ 0 \\ \vdots \\ 0 \\ 1 \end{bmatrix}, \quad C = \begin{bmatrix} 1 & 0 & \cdots & 0 & 0 \end{bmatrix} \tag{A.1.25}$$

and

$$\begin{aligned} \alpha_r(\xi) &= L_g L_f^{r-1} h(\Psi^{-1}(\xi)) \\ \beta_r(\xi) &= L_f^r h(\Psi^{-1}(\xi)) \\ q_i(\xi) &= L_f \psi_i(\Psi^{-1}(\xi)), \qquad i = r+1, \cdots, n. \end{aligned}$$

If a nonlinear system is minimum-phase, there always exists a smooth state-feedback control to make the whole system locally stable.

Appendix B

Parameters of the three-machine power system

The parameters of the three-machine power system without an infinite bus are given as follows.

The transfer function of the excitation system with an AVR:

$$E_f = K_A(V_{ref} - V_t)/(1 + T_A s)$$

The transfer function of the governor:

$$g = [a + b/(1 + T_g s)]\Delta\omega,$$

The transfer function of the PSS:

$$Z(s) = -\frac{K_Q}{K_A} \cdot \frac{T_Q s}{1 + T_Q s} \cdot \frac{1 + T_1 s}{1 + T_2 s} \Delta\omega$$

Table B.1: Generator parameters in *p.u.*

Parameters	Unit 1	Unit 2	Unit 3
x_d	1.0260	0.1026	0.1026
x_q	0.6580	0.0658	0.0658
x'_d	0.3390	0.0339	0.0339
x''_d	0.2690	0.0269	0.0269
x''_q	0.3350	0.0335	0.0335
T'_{d_0}	0.3670	0.3670	0.3670
T''_{d_0}	0.0314	0.0314	0.0314
T''_{q_0}	0.0623	0.0623	0.0623
H	2.8000	28.000	28.000

Table B.2: Transmission line parameters in *p.u.*

Line No.	Impedance
1-3	$0.015+0.10j$
4-5(1)	$0.075+0.50j$
4-5(2)	$0.1125+0.75j$
2-5	$0.060+0.40j$
5-6	$0.225+1.50j$
3-6	$0.025+0.15j$

Table B.3: Parameters of AVRs, exciters and PSSs in *p.u.*

K_A	T_A	K_Q	T_Q	T_1	T_2
200	0.01	3.00	1.50	0.30	0.06

Table B.4: Parameters of the governors in *p.u.*

T_g	a	b
0.250000	-0.001328	-0.170000

Table B.5: Loads (admittances) in *p.u.*

L_1	L_2
8.6-6.88j	9.8-7.8j

Table B.6: Operating conditions in *p.u.*

Generator	P	Q	V	δ (degree)
Unit 1	0.548	1.915	1.1000	15.0
Unit 2	5.403	1.753	1.0500	16.0
Unit 3	10.758	3.060	1.000	0.0

Appendix C

Notation

Symbols

$\Rightarrow$	implies.
$\rightarrow$	tends to.
$\forall$	for all.
$\in$	belongs to.
$\subset$	subsets of.
$\square$	designation the end of proofs.
max	maximum.
min	minimum.
sup	supremum, the least upper bound.
inf	infimum, the greatest lower bound.
$\mathcal{R}^n$	the n-dimensional Euclidean space.
$B(0,r)$	the ball $\{x \in \mathcal{R}^n \mid \|x\| \leq r\}$.

Vectors and Matrices

$\|a\|$	the absolute value of a scalar a.
$\|x\|_p$	the induced p-norm of vector x, i.e. $\|x\|_p = (\|x_1\|^p + \cdots + \|x_n\|^p)^{1/p}$, $1 \leq p < \infty$; $\|x\|_\infty = \max_i \|x_i\|$.
$\|x\|$	the Euclidean norm of a vector x, i.e. $\|x\| = (x^T x)^{1/2}$.
$\|A\|_p$	the induced p-norm of a matrix A, $\|A\|_p = \sup_{x \neq 0} \frac{\|Ax\|_p}{\|x\|_p}$.
$\|A\|$	the induced 2-norm of matrix, i.e. $\|A\| = \left[\lambda_{\max}(A^T A)\right]^{1/2}$.
$\text{diag}[a_1, \cdots, a_n]$	a diagonal matrix with diagonal elements a_1 to a_n.
block $\text{diag}[A_1, \cdots, A_n]$	a block diagonal matrix with diagonal blocks A_1 to A_n.
$A^T (x^T)$	the transpose of a matrix A (a vector x).
$\lambda_{\max}(P)\,(\lambda_{\min}(P))$	the maximum and (minimum) eigenvalues of a symmetric matrix P.
$P > 0 (P \geq 0)$	a positive definite (semi-definite) matrix P.
$\text{sat}(\cdot)$	the saturation function.
$\text{sgn}(\cdot)$	the signum function.

Abbreviations of control systems

CNAC	Coordinated nonlinear adaptive control.
DNAC	Decentralized nonlinear adaptive control.
DFL	Direct feedback linearization.
FCL	Feedback linearization control.
HGPO	High gain perturbation observer.
HGSPO	High gain state and perturbation observer.
NAC	Nonlinear adaptive control.
SMSO	Sliding mode state observer.
SMPO	Sliding mode perturbation observer.
SMSPO	Sliding mode state and perturbation observer.
SMCPE	Sliding mode control with perturbation estimation.
SMC	Sliding mode control.
TDC	Time delay control.
VSS	Variable structure systems.

Abbreviations in power systems

AC	Alternating current.
FACTS	Flexible alternating current transmission systems.
HVDC	High voltage direct current.
PSS	Power system stabilizer.
p.u.	Per unit
PID	Proportional-integral-differential.
STATCON	Static synchronous condenser.
SVC	Static VAr compensator.
SPS	Static phase shifter.
TCSC	Thyristor-controlled series capacitor.
UPFC	Unified power flow controller.
VAr	Volt-Ampere reactive.

Bibliography

[1] A. Isidori. *Nonlinear control systems.* Springer-Verlag, Berlin, Germany, 1995. Third edition.

[2] A. Isidori. *Nonlinear control systems II.* Springer-Verlag, London, 1999.

[3] J.J.E. Slotine and Weiping Li. *Applied nonlinear control.* Prentice-Hall, Inc., London, 1991.

[4] H. K. Khalil. *Nonlinear systems.* Prentice-Hall, Inc., London, 1996. Second edition.

[5] R. A. Freeman and P. V. Kokotović. *Robust nonlinear control design: state space and Lyapunov techniques.* Birkhäuser, Boston, 1996.

[6] J. Wang. *Practical stabilization of uncertain dynamical systems with application to feedback control of a robotic manipulator.* Ph.d thesis, Coventry University, September 1995.

[7] F. Esfandiari and H. K. Khalil. Output feedback stabilization of fully linearizable systems. *International Journal of Control*, **56**(5):1007–1037, 1992.

[8] J. J. E. Slotine. Sliding controller design for nonlinear systems. *International Journal of Control*, **40**:421–434, 1984.

[9] J. J. E. Slotine and S. S. Sastry. Tracking control of nonlinear systems using sliding surfaces with application to robot manipulators. *International Journal of Control*, **38**:465–492, 1983.

[10] H. Elmali and N. Olgac. Robust output tracking control of nonlinear MIMO systems via sliding mode technique. *Automatica*, **28**(1):145–151, 1992.

[11] S. K. Spurgeon and R. J. Patton. Robust variable structure control of model-reference systems. *IEE Proceedings Part D: Control Theory and Applications*, **137**(6):341–348, Nov. 1990.

[12] X. Y. Lu and S. K. Spurgeon. Output feedback stabilization of SISO nonlinear system via dynamic sliding modes. *International Journal of Control*, **70** (5):735–759, 1998.

[13] X. Y. Lu and S. K. Spurgeon. Output feedback stabilization of MIMO nonlinear systems via dynamic sliding mode. *International Journal of Robust and Nonlinear Control*, **9** (5):275–305, Apr 1999.

[14] Vadim I. Utkin. *Sliding modes in control and optimization.* Springer-Verlag, Berlin, Heidelberg, 1992.

[15] C. Edwards and S. K. Spurgeon. *Sliding mode control: theory and application.* Taylor & Francis, London, 1998.

[16] G. Bartolini, A. Ferrara, and E. Usai. Chattering avoidance by second-order sliding mode control. *IEEE Transactions on Autonmatic Control*, **43** (1):241–246, 1998.

[17] H. Elmali and N. Olgac. Sliding mode control with perturbation estimation (SMCPE): a new approach. *International Journal of Control*, **56**(4):923–941, 1992.

[18] J. T. Moura, H. Elmali, and N. Olgac. Sliding mode control with sliding perturbation observer. *Journal of Dynamic System, Measurement, and Control, Trans. of ASME*, **119**(4):657–665, 1997.

[19] H. Elmali and N. Olgac. Implementation od sliding mode control with perturbation estimation (SMCPE). *IEEE Transactions on Control Systems Technology*, **4**(1):923–941, 1996.

[20] J. T. Moura and N. Olgac. Robust Lyapunov control with perturbation estimation. *IEE Proceedings Part D: Control Theory and Applications*, **145**(3):307–315, 1998.

[21] J. T. Moura, R. G. Roy, and N. Olgac. Sliding mode control with perturbation estimation (SMCPE) and frequency shaped sliding surfaces. *Journal of Dynamic System, Measurement, and Control, Trans. of ASME*, **119**(3):584–588, 1997.

[22] K. Youcef-Toumi. A time delay controller for systems with unknown dynamics. *Journal of Dynamic System, Measurement, and Control, Trans. of ASME*, **112**(1):133–142, 1990.

[23] K. Youcef-Toumi and S. T. Wu. Input/output linearization using time delay control. *Journal of Dynamic System, Measurement, and Control, Trans. of ASME*, **114**(1):10–19, 1992.

[24] K. Youcef-Toumi and S. Reddy. Analysis of linear time invariant systems with time delay. *Journal of Dynamic System, Measurement, and Control, Trans. of ASME*, **114**(4):544–555, 1992.

[25] J. H. Park and Y. M. Kim. Time delay sliding mode control for a servo. *Journal of Dynamic System, Measurement, and Control, Trans. of ASME*, **121**(1):143–148, 1999.

[26] P. H. Chang and J. W. Lee. An observer design for time-delay control and its application to dc servo motor. *Control Engineering Practice*, **2**(2):263–270, 1994.

[27] P. H. Chang and J. W. Lee. A model reference observer for time-delay control and its application to robot trajectory control. *IEEE Transactions on Control Systems Technology*, 4(1):239–256, January 1996.

[28] J. Q. Han. Disturbance auto-rejection controller and its application. *Control and Decision(Chinese)*, **12**(2):12–17, 1997.

[29] J. Q. Han and W. Wang. Nonlinear tracking differentiator. *System Science and Mathematics(Chinese)*, **14**(2):177–183, 1994.

[30] C. Zhang, X.X. Zhou, et al. Co-ordinated disturbances auto-rejection control of TCSC and SVC in power systems. In *Proc. IEEE International Conference on Power System Technology*, pages 338–343, Beijing,China, August 18-21 1998.

[31] An-Chyau Huang and Yue-Shun Kuo. Sliding mode of nonliner systems containing time-varying uncertainties with unknown bounds. *International Journal of Control*, **74**:252–264, 2000.

[32] J. J. E. Slotine and J. A. Coetsee. *Adaptive sliding controller synthesis for* nonlinear systems. *International Journal of Control*, **43**:693–704, 1986.

[33] M. Krstić, I. Kanellakopoulos, and P. V. Kokotović. *Nonlinear and adaptive control design.* John Wiley & Sons, Inc, New York, 1995.

[34] I. Kanellakopoulos, P. V. Kokotović, and A. S. Morse. Systematic design of adaptive controllers for feedback linearizable systems. *IEEE Transactions on Autonmatic Control*, **36**(4):1241–1253, 1991.

[35] M. Krstić, I. Kanellakopoulos, and P. V. Kokotović. Adaptive nonlinear control without overparametrization. *Systems & Control Letters*, **19**:177–185, 1995.

[36] S. S. Sastry and A. Isidori. Adaptive control of linearizable systems. *IEEE Transactions on Autonmatic Control*, **34**:1123–1131, 1989.

[37] J. B. Pomet and L. Praly. Adaptive nonlinear regulation: estimation from the Lyapunov equation. *IEEE Transactions on Autonmatic Control*, **37**:72 740, 1992.

[38] R. Marino and P. Tomei. Global adaptive output-feedback control of nonlinear systems, part i: linear parametrization. *IEEE Transactions on Automatic Control*, **38**:17–32, 1993.

[39] R. Marino and P. Tomei. Global adaptive output-feedback control of nonlinear systems, part ii: nonlinear parametrization. *IEEE Transactions on Automatic Control*, **38**:32–48, 1993.

[40] I. Kanellakopoulos, P. V. Kokotović, and A. S. Morse. Adaptive nonlinear control with incomplete state information. *International Journal of Adaptive Control and Signal Processing*, **6**:367–394, 1992.

[41] A. R. Teel. Adaptive tracking with robust stability. *Proceedings of the 32th IEEE Conference on Decision and Control*, **7**:570–575, December 1993. San Antonio, TX.

[42] H. Khalil. Adaptive output-feedback control of nonlinear systems represented by input-output models. *IEEE Transactions on Autonmatic Control*, **41**(2):177–188, 1996.

[43] B. L. Walcott, M. J. Coreless, and S. H. Żak. Comparative study of nonlinear state observation techniques. *International Journal of Control*, **45**:2109–2132, 1987.

[44] E. A. Misawa and J. K. Hedrick. Nonlinear observers: A state-of-the-art survey. *Transactions of ASME*, **111**:344–352, 1989.

[45] F. E. Thau. Observering the state of nonlinear dynamic systems. *International Journal of Control*, **17**:471–479, 1973.

[46] S. R. Kou, D. L. Elliott, and T. J. Tarn. Exponential observers for nonlinear dynamic systems. *Information and Control*, **29**(3):204–216, 1975.

[47] D. Bestle and M. Zeitz. Canonical form observer design for nonlinear time variable systems. *International Journal of Control*, **38**:419–431, 1983.

[48] W. Baumann and W. Rugh. Feedback control of nonlinear systems by extended linearization. *IEEE Transactions on Autonmatic Control*, **31**(1):40–47, 1986.

[49] H. Khalil. *High gain observers in nonlinear feedback control*, chapter 4 in Part II: Ouput feedback control design. New directions in nonlinear observer design, pages 249–264. Springer, London, 1999. Editor H. Nijmeijer and T.I. Fossen.

[50] A. R. Teel and L. Parly. Global stabilizability and observability imply semiglobal stabilizability by output feedback. *Systems and Control Letters*, **22**:313–325, 1994.

[51] A. N. Atassi and H. K. Khalil. A seperation principle for the stabilization of a class of nonlinear system. *IEEE Transactions on Autonmatic Control*, **44**(9):1672–1687, Sep. 1999.

[52] F. Esfandiari and H. K. Khalil. Semiglobal stabilization f a class of nonlinear systems using output feedback. *IEEE Transactions on Autonmatic Control*, **38**(9):1412–1415, Sep. 1993.

[53] A. R. Teel and L. Parly. Tools for semiglobal stabilization by partial state and output feedback. *SIAM Journal of Control Optimazation*, **33**:1443–1488, 1995.

[54] H. K. Khalil. Robust servomechanism output feedback controllers for a class of feedback linearizable systems. *Automatica*, **30**(10):1587–1599, 1994.

[55] N. A. Mahmoud and H. K. Khalil. Asymptotic regulation of minimum phase nonlinear systems using output feedback. *IEEE Transactions on Autonmatic Control*, **41**(10):1402–1412, 1996.

[56] N. A. Mahmoud and H. K. Khalil. Robust control for a nonlinear servomechanism problem. *International Journal of Control*, **66**(6):779–802, 1997.

[57] A. Isidori. A remark on the problem of semiglobal nonlinear output regulation. *IEEE Transactions on Autonmatic Control*, **42** (12):1734–1738, December 1997.

[58] M. Jankovic. Adaptive nonlinear output feedback tracking with a partial high gain observer and backstepping. *IEEE Transactions on Autonmatic Control*, **42** (1):106–120, January 1997.

[59] S. Oh and H. K. Khalil. Output feedback stabilization using variable structure control. *International Journal of Control*, **62** (4):831–848, 1995.

[60] S. Oh and H. K. Khalil. Nonlinear output-feedback tracking using high-gain observer and variable structure control. *Automatica*, **33**(10):1845–1856, 1997.

[61] H. K. Khalil and E. G. Strangas. Robust speed control of induction motors using position and current measurements. *IEEE Transactions on Autonmatic Control*, **41** (8):1216–1220, August 1996.

[62] İ. İ. Haskara and V. Utkin. On sliding mode observer via equivalent control approach. *International Journal of Control*, **71**(6):1051–1067, 1998.

[63] J. J. E. Slotine, J. K. Hedrick, and E. A. Misawa. On sliding mode observer for nonlinear systems. *Journal of Dynamic System, Measurement, and Control, Trans. of ASME*, **109**:245–252, 1987.

[64] B. L. Walcott and S. H. Żak. State observation of nonlinear uncertain dynamical systems. *IEEE Transactions on Autonmatic Control*, **32**(2):229–234, February 1987.

[65] C. Edwards and S. K. Spurgeon. On the development of discontinuous observer. *International Journal of Control*, **59**(5):1211–1229, 1994.

[66] Y. Xiong and M. Serif. Sliding mode observer for uncertain systems part i: Linear systems case. In *Proceedings of the 39th IEEE Conference on Decision and Control*, pages 316–321, Syndey, Australia, 2000.

[67] Y. Xiong and M. Serif. Sliding mode observer for uncertain systems part ii: Nonlinear systems case. In *Proceedings of the 39th IEEE Conference on Decision and Control*, pages 322–327, Syndey, Australia, 2000.

[68] D.G. Luenberger. An introduction to observers. *IEEE Transactions on Autonmatic Control*, **16**(6), 1971.

[69] B. L. Walcott and S. H. Żak. Observation of dynamical systems in the presence of bounded nonlinearities/uncertainities. In *Proceedings of 25th Conference on Decision and Control*, Athes, Greece, December 1986.

[70] C. Canudas De Wit and J. J. E. Slotine. Sliding observer for robot manipulators. *Automatica*, **27**(5):859–864, 1991.

[71] J. Hernandez and J. P. Barbot. Sliding observer-based feedback control for flexible joints manipulator. *Automatica*, **32**(9):1243–1254, 1996.

[72] B. L. Walcott and S. H. Żak. Combined observer-controller synthesis for uncertain dynamical systems with applications. *IEEE Transactions on Systems, Man, and Cybernetics*, **18** (1):88–104, 1988.

[73] R. Sanchis and H. Nijmeijer. Sliding controller-sliding observer design for nonlinear systems. *European Journal of Control*, **4** (3):208–234, 1998.

[74] P. H. Chang, J. W. Lee, and S.H. Park. Time delay observer: A robust observer for nonlinear plants. *Journal of Dynamic System, Measurement, and Control, Trans. of ASME*, **119**(3):521–527, 1997.

[75] P. Kundur. *Power system stability and control.* McGraw-Hill, New York, 1994.

[76] P. M. Anderson and A. A. Fouad. *Power system control and stability.* IEEE Press, New York, 1994.

[77] E. V. Larsen and D. A. Swann. Applying power system stabilizer: Part 1,2, and 3. *IEEE Trans. on Power Apparatus and Systems*, 4(1):236–241, 1981.

[78] Q.H. Wu and B.W. Hogg. Adaptive controller for a turbogenerator system. *IEE Proceedings Part D: Control Theory and Applications*, **135**(1):35–42, 1988.

[79] Q. H. Wu and B. W. Hogg. Robust self-tuning regulator for a synchronous generator. *IEE Proceedings Part D: Control Theory and Applications*, **135**(6):463–473, 1988.

[80] S. J. Cheng, O. P. Malik, et al. Damping of multi-modal oscillations in power system using a dual-rate adaptive stabiliser. *IEEE Trans. on PWRS*, **3**(1):101–108, 1988.

[81] N. G. Hingorani and L. Gyugyi. *Understanding FACTS: Cocepts and Technology of Flexible AC Transmission Systems.* IEEE Press, New York, 1999.

[82] Q.H. Wu and L. Jiang. Nonlinear control theory and its applications in power systems: a survey. *Automation of Electric Power Systems*, **25**(3):1–10, Feb 2001.

[83] W. Mielczarski and A. M. Zajaczkowski. Nonlinear field voltage control of a synchronous generator using feedback linearization. *Automatica*, **30**(10):1625–1630, 1994.

[84] W. Mielczarski. Observing the state of a synchronous generator, part 1. and part 2. *International Journal of Control*, **45**(10):987–1021, 1987.

[85] Q. Lu and Y.Z. Sun. *Nonlinear control of power systems.* Science Press, China, Beijing, 1993.

[86] Q. Lu and Y. Z. Sun. Nonlinear stabilizing control of multimachine systems. *IEEE Transactions on Power Systems*, **4**(1):236–241, Feb. 1989.

[87] Y. J. Cao, Q. H. Wu, L. Jiang, and S. J. Cheng. Nonlinear control of power system multi-mode oscillations. *International Journal of Electrical Power and Energy Systems*, **20**(1):61–68, 1998.

[88] Y. J. Cao, L. Jiang, et al. A nonlinear variable structure stabiliser for power system stability. *IEEE Transactions on Energy Conversation*, **9**(3):489–496, 1994.

[89] L. Gao, L. Chen, et al. A nonlinear control design for power systems. *Automatica*, **28**(3):975–979, August 1992.

[90] Y. Wang, L. Xie, et al. Robust nonlinear controller design for transient stability enhancement of power system. In *31th IEEE Conference of Decision and Control*, pages 1123–1128, Tucson, 1992.

[91] Y. Wang, D. J. Hill, et al. Transient stabilization of power systems with an adaptive control law. *Automatica*, **30**(6):1409–1413, 1994.

[92] D. G. Taloy. Nonlinear control of electric machiones : An overview. *IEEE Control System Magzine*, **14**(6):41–51, December 1994.

[93] M. Bodson and J. Chiasson. Differential geometric methods for control of electrical motors. *Int. J. Robust Nonlinear Control*, **8**:923–954, 1998.

[94] M. Nambu and Y. Ohsawa. Development of an advanced power system stabilizer using a strict linearization approach. *IEEE Transactions on Power Systems*, **11**:813–818, 1996.

[95] F. K. Mak. Design of nonlinear generator exciters using differential geometric control theories. In *Proceedings of the 31st Conference on Decision and Control*, Tucson, Arizona, December 1992.

[96] T. Lahdhiri and A. T. Alouani. Nonlinear excitation control of a synchronous generator with implicit terminal voltage regulation. *Electrilcal Power Systems Research*, **36**(2):101–112, 1996.

[97] X. C. Li, Z. S. Yan, et al. Anti-disturbance design of the nonlinear excitation regulator. *Proceedings of the Chinese Scociety for Electrical Engineering*, **19**(9), 1999.

[98] Riccardo Marino. An example of a nonlinear regulator. *IEEE Transactions on Autonmatic Control*, **29**(3):276–279, March 1984.

[99] S. M. Savaresi. Exact feedback linearisation of fifth-order model synchronous generators. *IEE Proceedings Part D: Control Theory and Applications*, **146**(1):53–57, Jan. 1999.

[100] A.F. OKOU, O. AKHRIF, et al. Nonlinear control of non-minimum phase systems: application to the voltage and speed regulation of power systems. In *Proceedings of the 1999 IEEE International Conference on Control Applications*, pages 609–615, Kohala Coast-Island of Hawai'i, Hawai'i, USA, August 22-27 1999.

[101] O. AKHRIF, F.A. OKOU, et al. Application of a multivariable feedback linearization scheme for rotor scheme for rotor angle stability and voltage regulation of power systems. *IEEE Transactions on Power Systems*, **14**(2):620–628, May 1999. PSNC60.

[102] Q. Lu, Y.Z. Sun, et al. Nonlinear optimal excitation control for multimachine systems. In *IFAC Symposium of Power Systems Modelling and Control Applications*, pages 27–32, Oxford, UK, 1989.

[103] Q. Lu, Y. Z. Sun, et al. Decentralized nonlinear optimal excitation control. *IEEE Transactions on Power Systems*, **11**(4):1957–1962, Nov. 1996.

[104] J. W. Chapman, M. D. Illic, et al. Stabilizing a multimachine power system via decentralized feedback linearizing exciation control. *IEEE Transactions on Power Systems*, **8**(3):830–839, August 1993.

[105] Y. Y. Wang and D. J. Hill. Robust nonlinear coordinated control of power systems. *Automatica*, **64**(4):611–618, 1996.

[106] Y.Z. Sun and Z.P. Yang. Enhancement of power system stability using nonlinear control strategy of asvg. *Automation of Electric Power Systems*, **20**(11):17–22, Nov 1996.

[107] S. Kaprielian and K. Clements. Feedback stabilization for an ac/dc power system model. In *Proceedings of the 29th Conference on Decision & Control*, pages 3367–3372, Honolulu, Hawaii, USA, December 1990.

[108] Y. L. Tan and Y. Y. Wang. Design of series and shunt FACTS controller using adaptive nonlinear coordinated design techniques. *IEEE Transactions on Power Systems*, **12**(3):1374–1379, August 1997.

[109] Y. L. Tan and Y. Y. Wang. Transient stabilization using adaptive excitation and dynamic brake control. *Control Engineering Practice*, **5**(3):337–346, 1997.

[110] Y. L. Tan and Y. Y. Wang. Augmentation of transient stability using a super conducting coil and adaptive nonlinear control. *IEEE Transactions on Power Systems*, **13**(2):361–366, 1998.

[111] X. X. Zhou and J. Liang. Overview of control schemes for TCSC to enhance the stability of power systems. *IEE Proceedings Part C: Generation, TransmissionF and Distribution*, **146**(2):125–130, 1999.

[112] V. Rajkumar and R. R. Mohler. Nonlinear control methods for power systems: a comparison. *IEEE Transactions on Control Systems Technology*, **3**(2):231–237, June 1995.

[113] J. W. Chapman and M. D. Illic. Some robustness results for feedback linearizing control of generator excitation. In *Proceedings of 31th IEEE Conference on Decision and Control*, pages 1149–1153, Tucson, 1992.

[114] Sun C., Zhao Z., et al. Design of nonlinear robust excitation control for multi-machine power systems. *IEE Proceedings Part C: Generation, TransmissionF and Distribution*, **143**(3):253–257, May 1996.

[115] V. G. D. C. Samarasinghe and N. C. Pahalawaththa. Design of a robust variable structure controller for improving power system dynamic stability. *International Journal of Electrical Power and Energy Systems*, **18**(8):519–525, Nov. 1996.

[116] Y. Y. Wang, G. G. Xiao, and D. J. Hill. Robust decentralized nonlinear controller design for multimachine power systems. *Automatica*, **33**(9):1725–1733, 1997.

[117] S. Jain and F. Khorrami. Robust decentralized control of power system utilizing only swing angle measurement. *International Journal of Control*, **66**(4):581–601, 1997.

[118] G.J. Li and T. T. Lie. Decentralised nonlinear h_∞ control for stability enhancement in power systems. *IEE Proceedings Part D: Control Theory and Applications*, **146**(1):2419–2424, 1999.

[119] T. Lahdhiri and A. T. Alouani. Design of nonlinear excitation controller for a synchronous generator using the concept of exact stochastic feedback linearization. In *Proceedings of the American Control Conference*, pages 1963–1967, Albuquerque, New Mexico, June 1997.

[120] Y. Wang, R. R. Mohler, et al. Variable structure FACTS controllers for power system transient stability. *IEEE Transactions on Power Systems*, **7**(1):307–313, 1992.

[121] Y. Wang, R. R. Mohler, et al. Variable-structure braking-resistor control in a multi-machine power system. *IEEE Transactions on Power Systems*, **9**(3):1157–1562, 1994.

[122] G. V. Subbarao and Ashok Iyer. Nonlinear excitation and governor control using variable structures. *International Journal of Control*, **57**(6):1325–1342, 1993.

[123] F. Jiang, S.S. Choi, et al. Power system stability enhancement using static phase shifter. *IEEE Transactions on Power Systems*, **12**(1):207–214, Feb. 1997.

[124] Nelles D.. Machowski J. A static var compensator control strategy to maximize power system damping. *Electrilcal Machine and Power Systems*, **24**(5):477–495, 1996.

[125] J. Machowski, Bialek J.W., et al. Excitation control system for use with synchronous generators. *IEE Proceedings Part C: Generation, TransmissionF and Distribution*, **145**(5):537–546, 1998.

[126] H. Cai, Z. Qu, D Gan, and J.F. Dorsey. A robust power system stabilizer design based on Lyapunov's approach. In *Proceedings of the American*

Control Conference, pages 1958–1962, Albuquerque, New Mexico, June 1997.

[127] Liu G.X., Lin X.S., et al. Study of excitation control under transient conditions for multimachine power systems based on energy function. *Proceedings of the Chinese Scociety for Electrical Engineering*, **17**(4):264-268, 1997.

[128] H. Jiang, H. Cai, et al. Toward a globally robust decentralized control for large-scale power systems. *IEEE Transactions on Control Systems Technology*, **5**(3):309–319, May 1997.

[129] L. Jiang, Q.H. Wu, et al. Observer-based nonlinear control of synchronous generator with perturbation estimation. *International Journal of Electrical Power and Energy Systems*, September 2000. Accepted.

[130] L. Jiang, Q.H. Wu, J. Wang, et al. Robust observer-based nonlinear control of multi-machine power systems. *IEE Proceedings Part C: Generation, TransmissionF and Distribution*, April 2001. Accepted.

[131] L. Jiang and Q.H. Wu. Decentralized nonlinear control of multi machine power system via states and perturbation observer. *Automation of Electric Power Systems*, **25**(3):26–31, Feb 2001.

[132] L. Jiang, Q.H. Wu, et al. Nonlinear coordinated control of multi-machine power systems. In *Proceeding of IEEE PES Summer Meeting 200*, Seattle, US, July 2000.

[133] Q.H. Wu and L. Jiang. Non-linear adaptive control of multi-machine power systems. *Transcation of Control and Measurement*, Nov. 2000. Accepted.

[134] L. H. Xie S. L. Xie. Decentralized global disturbance attentation for a class of large scale uncertain nonlinear systems. *International Journal of Systems Science*, **31**(10):1285–1297, 2000.

[135] Z. P. Jiang. Decentralized and adaptive nonlinear tracking of large-scale systems via output feedback. *IEEE Transactions on Autonmatic Control*, **45**(11):2122–2128, 2000.

[136] P. A. Ioannou. Decentralized adaptive control of interconnected systems. *IEEE Transactions on Autonmatic Control*, **31**(4):291–298, 1986.

[137] D T. Gavel and D. D. Siljak. Decentralized adaptive control:structural conditions for stability. *IEEE Transactions on Autonmatic Control*, **34**(3):413–426, 1989.

[138] Y. H. Chen. Decentralized robust control for large-scale uncertain sysytems: A design based on the bound of uncertainty. *Journal of Dynamic System, Measurement, and Control, Trans. of ASME*, **114**(1):1–9, March 1992.

[139] L. Shi and S. K. Singh. Decentralized adaptive controller design for large-scale systems with higher order interconnections. *IEEE Transactions on Autonmatic Control*, **37**(8):1106–1118, 1992.

[140] C. Wen. Decentrlaized adaptive regulation. *IEEE Transactions on Autonmatic Control*, **39**(10):2163–2166, 1994.

[141] Feipeng Da. Decentralized slinding mode adaptive controller design based on fuzzy neural networks for interconnected uncertain nonlinear systems. *IEEE Transactions on Neural Networks*, **11**(6):1471–1480, 2000.

[142] F. P. de Mello. Measurement of synchronous machine rotor angle from analysis of zero sequence harmonic components of machine terminal voltage. *IEEE Transactions on Power Delivery*, **9**(1):1770–1775, 1994.

[143] F. Khorrimi S. Jain and B. Fardanesh. Adaptive nonlinear excitation control of power system with unknow interconctions. *IEEE Transactions on Control Systems Technology*, **2**(4):436–446, December 1994.

[144] Y.Y. Wang, D.J. Hill, and G. Guo. Robust decentralized control for multimachine power systems. *IEEE Transactions on Circuits and SystemsPart 1*, **45**(3):271–279, March 1998. PSNC58.

[145] Q.H. Wu, B.W. Hogg, et al. A neural network regulator for turbogenerators. *IEEE Transactions on Neural Networks*, **3**(1):95–100, 1992.

[146] Q.H. Wu. Learning coordinated control of power systems using interconnected learning automata. *International Journal of Electrical Power and Energy Systems*, **17**(2):91–99, 1995.

[147] L.C. Wang, A.A. Girgis, et al. Nonlinear controller design for thristor controlled series compensation to enhance power system stability. In *Proc. of Stockholm Power Tech. International Symp on Electrical Power Enginerring*, pages 109–114, Feb 1995.

[148] S.K. Tso, J. Liang, et al. Coordination of TCSC and SVC for improvement of power system performance with nn-based parameter adaptation. *International Journal of Electrical Power and Energy Systems*, **21**(4):235–244, 1999.

[149] E.V. Larsen, J.J. Sanchez-Gasca, et al. Concepts for design of FACTS controllers to damp power swings. *IEEE Transactions on Power Systems*, **10**(2):948–956, 1995.